

# A 300,000 year record of cold-water coral mound build-up at the East Melilla Coral Province (SE Alboran Sea, western Mediterranean)

Robin Fentimen<sup>1\*</sup>, Eline Feenstra<sup>1</sup>, Andres Rüggeberg<sup>1</sup>, Efraim Hall<sup>1</sup>, Valentin Rime<sup>1</sup>, Torsten Vennemann<sup>2</sup>, Irka Hajdas<sup>3</sup>, Antonietta Rosso<sup>4</sup>, David Van Rooij<sup>5</sup>, Thierry Adatte<sup>2</sup>, Hendrik Vogel<sup>6</sup>, Norbert Frank<sup>7</sup>, Anneleen Foubert<sup>1</sup>

<sup>1</sup> Department of Geosciences, University of Fribourg, Fribourg, CH-1700, Switzerland

<sup>2</sup> Institute of Earth Surface Dynamics, University of Lausanne, Lausanne, CH-1015, Switzerland

<sup>3</sup> Laboratory of Ion Beam Physics, ETH Zürich, Zürich, CH-8093, Switzerland

<sup>4</sup> Department of Biological, Geological and Environmental Sciences, University of Catania, Catania, 95128, Italy

<sup>5</sup> Department of Geology, Ghent University, Ghent, 9000, Belgium

<sup>6</sup> Institute of Geological Sciences and Oeschger Centre for Climate Change Research, University of Bern, Bern, CH-3012, Switzerland

<sup>7</sup> Institute of Environmental Physics, University of Heidelberg, Heidelberg, D-69120, Germany

\* Present address: [Réerves Naturelles de France – Antenne Littorale, Terre Plein de l'Ecluse, 50400, Granville, France](#) [ENS de Lyon, 15 parvis René Descartes, BP 7000, 69342 Lyon Cedex 07, France](#)

Correspondence to: Robin Fentimen ([robin.fentimen@ens-lyon.fr](mailto:robin.fentimen@ens-lyon.fr))

**Keywords.** Cold-water corals, Mounds, Benthic foraminifera, Bryozoans, Palaeoclimate, Holocene, Pleistocene, Levantine Intermediate Water

Formatted: Font: Not Bold

**Abstract.** This study provides a detailed reconstruction of cold-water coral mound build-up within the East Melilla Coral Province (Southeast Alboran Sea), more precisely at the northern part of Brittlestar Ridge I, over the last 300 kyr. The multiproxy investigation of core MD13-3462G reveals that mound build-up took place during both interglacial and glacial periods, at average aggradation rates ranging between 1 and 10 cm.kyr<sup>-1</sup>. These observations imply that corals never thrived but rather developed under stressful environmental conditions. Maximum aggradation rates of 18 cm.kyr<sup>-1</sup> are recorded during the last glacial period, hence providing first evidence of coral mound development during this time period in the western Mediterranean. The planktonic (*Globigerina bulloides*) and benthic (*Lobatula lobatula*)  $\delta^{18}\text{O}$  records from core MD13-3462G show typical interglacial-glacial variations during the last two interglacial-glacial cycles. This is in contrast with  $\delta^{18}\text{O}$  records generally recovered from coral mounds and highlights that the northern part of Brittlestar Ridge I experienced reduced albeit relatively continuous accretion. High abundances of infaunal benthic foraminifera (*Bulimina marginata*, *Bulimina striata* and *Uvigerina mediterranea*) suggest that weak seafloor oxygenation associated to important terrestrial organic matter input characterized interglacial periods, whilst the dominance of large epibenthic species (*Discanomalina coronata* and *Lobatula lobatula*) and Miliolids is probably linked to stronger Levantine Intermediate Water circulation and fresher organic matter input during glacial periods. In addition, the CT-quantification of macrofaunal remains shows that the bryozoan *Buskeq dichotoma* is present throughout the entire 300 kyr of mound build-up history, at the exception of MIS 5, and is possibly a key contributor to mound development during glacial periods. The comparison of our

Formatted: Font: Italic

Formatted: Font: Italic

Formatted: Font: Italic

Formatted: Font: Italic

Formatted: Font: Italic

Formatted: Font: Italic

Formatted: Font: Italic

Formatted: Font: Italic

40 observations to other long-term coral mound records demonstrates that western and central Mediterranean coral  
41 mounds do not show concurrent build-up over interglacial-glacial cycles, implying that their development may be  
42 driven by regional and local environmental forcing.

43 ~~Based on benthic foraminiferal assemblages, macrofaunal quantification, grain size analysis, sediment geochemistry,~~  
44 ~~and foraminiferal stable isotope compositions, a reconstruction of environmental conditions having prevailed in the~~  
45 ~~region is proposed. The variations in planktonic and benthic  $\delta^{18}\text{O}$  values indicate that cold water coral mound build-~~  
46 ~~up follows and records global climate variability. In contrast to northeast Atlantic counterparts, coral mound build up~~  
47 ~~in the southeast Alboran Sea occurs during glacial as well as during interglacial periods and at very low aggradation~~  
48 ~~rates (between 1 and 10  $\text{cm.kyr}^{-1}$ ). Environmental conditions during glacial periods, particularly during the Last~~  
49 ~~Glacial Maximum, appear to better suit the ecological requirements of the erect cheilostome bryozoan *Buskea*~~  
50 ~~*dichotoma*. We propose that *Buskea dichotoma* has an important role in the build up of cold water coral mounds at~~  
51 ~~the East Melilla Coral Province during glacial periods. Benthic foraminiferal assemblages suggest that important~~  
52 ~~terrestrial input favoured cold water coral proliferation during interglacial periods. The existence of strong Alboran~~  
53 ~~Gyres during interglacial periods, promoting mixing between surface and intermediate water masses and bottom~~  
54 ~~water turbulence, was possibly beneficial for cold water coral development. Conversely, benthic foraminiferal~~  
55 ~~assemblages indicate that the seafloor received less organic matter during glacial periods. Overall, the arid~~  
56 ~~continental conditions combined to more stratified water masses resulted in limited coral proliferation during glacial~~  
57 ~~times.~~

## 58 1. Introduction

59 Cold-water coral (CWC) reefs are diverse marine ecosystems that are widespread in the world's ocean common on  
60 Earth (Freiwald et al., 2004; Roberts et al., 2009). The most important reef building CWC species in the Atlantic  
61 Ocean and Mediterranean Sea are the scleractinian species *Desmophyllum pertusum* (formerly known as *Lophelia*  
62 *pertusa*, see Addamo et al., 2016) and *Madrepora oculata* (Roberts et al., 2009). These predominantly suspension-  
63 feeding organisms depend on enhanced hydrodynamic regimes that provide food to their polyps (White et al., 2005;  
64 Mienis et al., 2007; Carlier et al., 2009; Davies et al., 2009; Roberts et al., 2009; Hanz et al., 2019). The role of  
65 played by internal waves (i.e., waves that occur at the interface between two water masses of different densities) in  
66 on the proliferation of CWCs is vital, since these oscillations increase turbulence, and hence nutrient  
67 supply, and accumulate particulate organic matter due to their sharp density gradient (White et al., 2005; Davies et  
68 al., 2009; Pomar et al., 2012; Wang et al., 2019). Physico-chemical properties of the ambient water (e.g., salinity,  
69 temperature, dissolved oxygen concentrations, pH, density) also affect CWC growth (Freiwald et al., 2004; Dullo et  
70 al., 2008; Davies and Guinotte, 2011; Hanz et al., 2019). If favourable conditions are maintained over longer periods,  
71 successive reef generations may build CWC mounds through the interaction between coral growth and sediment  
72 accumulation (Wilson, 1979; Roberts et al., 2006; Foubert and Henriot, 2009; Roberts et al., 2009; Hebbeln et al.,  
73 2016). Consequently, CWC mounds can reach considerable heights of over 300 m and spread for kilometres in width

Formatted: Indent: First line: 0 cm

74 and length at their base (De Mol et al., 2002; Kenyon et al., 2003; Huvenne et al., 2005). Mound development may  
75 span from thousands to millions of years and attain important mound aggradation rates (MAR), e.g.,  $\pm 290\text{--}400$   
76  $\text{cm.ky}^{-1}$  in the ~~Poreupine Seabight~~East Melilla Coral Province (EMCP); (Frank et al., 2009; López Correa et al.,  
77 2012; Fink et al., 2013; Stalder et al., 2015; Wienberg et al., 2018). As such, and in spite of mound formation being  
78 generally discontinuous, CWC mounds are valuable environmental and climate archives, ~~although mound formation~~  
79 ~~is generally discontinuous~~ (Rüggeberg et al., 2007; Roberts et al., 2009). Moreover, the sensitivity of CWCs to  
80 climate change is useful to monitor variations in environmental conditions (e.g., water mass variability, surface  
81 productivity, bottom current velocity; Rüggeberg et al., 2007; Huvenne et al., 2009; Hebbeln et al., 2016; Wienberg  
82 et al., 2018; 2020).

Formatted: Indent: First line: 1,27 cm

83  
84  
85  
86 The long-term development of CWC mounds was first studied in the ~~Northeast-NE~~ Atlantic Ocean, where it ~~is~~  
87 ~~driven was shown by to follow~~ large-scale changes in oceanographic conditions (e.g., De Mol et al., 2002; Dorschel  
88 et al., 2005; Frank et al., 2011; Wienberg et al., 2018; 2020). Coral ~~mounds~~ along the Irish margin ~~grow form~~  
89 during interglacial and interstadial times, whilst they decline during glacial periods (Dorschel et al., 2005; Kano et  
90 al., 2007; Rüggeberg et al., 2007; Eisele et al., 2008). The same distribution pattern has been observed for CWC  
91 mounds situated in the NW Atlantic Ocean (Matos et al., 2015; 2017). In these two regions, CWC development is  
92 tightly knit to the formation of internal waves and increased turbulence at the limit between water masses~~Cold-water~~  
93 ~~coral mound development along the Irish margin depends on the strength of southern sourced water masses like the~~  
94 ~~Mediterranean Outflow Water (MOW) or the Eastern North Atlantic Water (ENAW) and the formation of internal~~  
95 ~~waves~~ (White, 2007; Mohn et al., 2014; Raddatz et al., 2014; Matos et al., 2015; 2017; Hebbeln et al., 2016;  
96 Wienberg et al., 2020). ~~The strong influence of the MOW during interglacial and interstadial times and the~~  
97 ~~resulting enhanced turbulence induced by internal waves provides the correct balance between nutrient and sediment~~  
98 ~~supply (Mohn et al., 2014; Raddatz et al., 2014). In contrast, during glacial times, weak MOW flow lowers nutrient~~  
99 ~~supply and increases sediment smothering, causing coral retreat (Dorschel et al., 2005; Rüggeberg et al., 2007; Mohn~~  
100 ~~et al., 2014). In the NW Atlantic Ocean, CWC mounds also form during interglacial periods, when stronger~~  
101 ~~hydrodynamic regimes and better oxygenated waters dominate the region (Matos et al., 2015; 2017). At lower~~  
102 latitudes in the East Atlantic, off the coast of Mauritania and in the Gulf of Cádiz, coral mounds form essentially  
103 during glacial times (Wienberg et al., 2009; Eisele et al., 2011), ~~although they also developed at lower aggradation~~  
104 ~~rates during the last interglacial (Marine Isotope Stage 5; Wienberg et al., 2018).~~

Formatted: Indent: First line: 0 cm

105  
106  
107 In the Mediterranean Sea, CWC mound provinces are concentrated in the ~~East~~ Alboran Sea (Fink et al., 2013; 2015;  
108 Lo Iacono et al., 2014; Stalder et al., 2015; 2018; Terhzaz et al., 2018; Hebbeln, 2019; Wang et al., 2019; Fentimen  
109 et al., 2020a; Rachid et al., 2020; Corbera et al., 2021, Sánchez-Guillamón et al., 2022), the Corsica Channel (Remia  
110 and Taviani, 2005; Angeletti et al., 2020), the Strait of Sicily (Martorelli et al., 2011), the northern Ionian Sea  
111 (Carlier et al., 2009; Freiwald et al., 2009) and on the Tunisian Plateau (Camafort et al., 2020; Corbera et al., 2022).

112 Except for the North Cabliers Coral Mound Province, situated in the central part of the eastern Alboran Sea (Fig. 1b),  
113 the northern Ionian Sea mounds (i.e. Santa Maria di Leuca CWC mounds), and the Corsica Channel mounds, the  
114 above mentioned CWC mounds are all at present in a stagnation phase with little or no corals living at their surfaces  
115 (Corbera et al., 2019; Hebbeln, 2019; Angeletti et al., 2020; Sánchez-Guillamón et al., 2022).

116 ~~–The largest CWC mound field in this region is the~~ Melilla Mound Field is the largest CWC province in the Alboran  
117 Sea, covering an area greater than 500 km<sup>2</sup> parallel to the margin (Comas and Pinheiro, 2010; Lo Iacono et al., 2014).  
118 It can be divided into two provinces, the West and East Melilla Coral Provinces (~~WMCP and~~ EMCP), respectively  
119 situated 7 km northwest and 35 km northeast of the Cape Tres Forcas (Lo Iacono et al., 2014; Fig. 1b). Within the  
120 EMCP, the localities of Brittlestar Ridge I (BRI) and Dragon Mound have received the most attention  
121 been extensively studied during the last decade (Fig. 1b and c; Fink et al., 2013; 2015; Stalder et al., 2015; 2018; Terhzaz  
122 et al., 2018; Hebbeln, 2019; Fentimen et al., 2020a, Krengel, 2020; Rachid et al., 2020; Wang et al., 2021). U-series  
123 dating of corals revealed that the formation of Dragon Mound began 450 kyr ago, whereas BRI mounds started  
124 building-up over 538 kyr ago (Krengel, 2020). Mound development at Dragon Mound essentially took place during  
125 the ~~three~~ last interglacial periods (MIS ~~59~~, 7 and ~~59~~) at rates varying between 26 and 83 cm.kyr<sup>-1</sup>, although a number  
126 of glacial coral occurrences were recorded during MIS ~~810~~ and MIS ~~810~~ (Krengel, 2020). Krengel (2020) also  
127 observed interglacial mound build-up phases at BRI, more precisely during MIS ~~97~~ and MIS ~~79~~ at rates between 17  
128 and 25 cm.kyr<sup>-1</sup>. Similar to Dragon Mound, glacial periods at BRI appear to host sporadic phases of coral  
129 development, noticeably during MIS ~~124~~ and MIS ~~412~~ (Krengel, 2020). In contrast to Dragon Mound, the Early  
130 Holocene and Bølling-Allerød interstadial marked a rapid phase of mound aggradation at BRI (75-420 cm.kyr<sup>-1</sup>; Fink  
131 et al., 2013; Stalder et al., 2015; 2018; Fentimen et al., 2020a; Krengel, 2020) and at mounds situated in the West  
132 Melilla Coral Province (12-176 cm.kyr<sup>-1</sup>; Wang et al., 2019).

133  
134  
135 The predominant occurrence of CWCs during interglacial periods noticed by Krengel (2020) in the EMCP is also  
136 observed during the last four interglacial-glacial cycles in the South Cabliers Mound Province (~~Corbera et al., 2021~~),  
137 although mound build-up in the latter is the most important during deglacials and temperate interstadials (Corbera et  
138 al., 2021). In contrast, over the last 400 kyr, the Tunisian Coral Mound Province (~~TCMP~~) situated in the central  
139 Mediterranean experienced its most marked phase of coral development during the last glacial period, whereas  
140 interglacial periods were particularly scarce in coral occurrences (Corbera et al., 2022). ~~Mound aggradation rates in~~  
141 the WMCP and EMCP reach their highest values (75–420 cm.kyr<sup>-1</sup>) during the Early Holocene and Bølling-Allerød  
142 interstadial. ~~These different temporal distributions suggest that mound build-up in the western and central~~  
143 Mediterranean Sea does not follow a uniform pattern. Although the development of coral communities at the EMCP  
144 during the last 30 kyr is well documented and that novel long-term records are emerging from the western and  
145 central Mediterranean Sea (Krengel, 2020; Corbera et al., 2021; 2022), the long-term environmental forcing affecting  
146 the EMCP still remains ~~poorly~~ ~~still~~ ~~little~~ ~~constrained~~ ~~documented~~. The aims of this study are hence: 1) to constrain the  
147 environmental parameters driving CWC mound formation in the EMCP over the last 300 kyr, and 2) to assess the  
148 heterogeneities in long-term CWC mound formation within the western Mediterranean Sea.

Formatted: Indent: First line: 1,27 cm

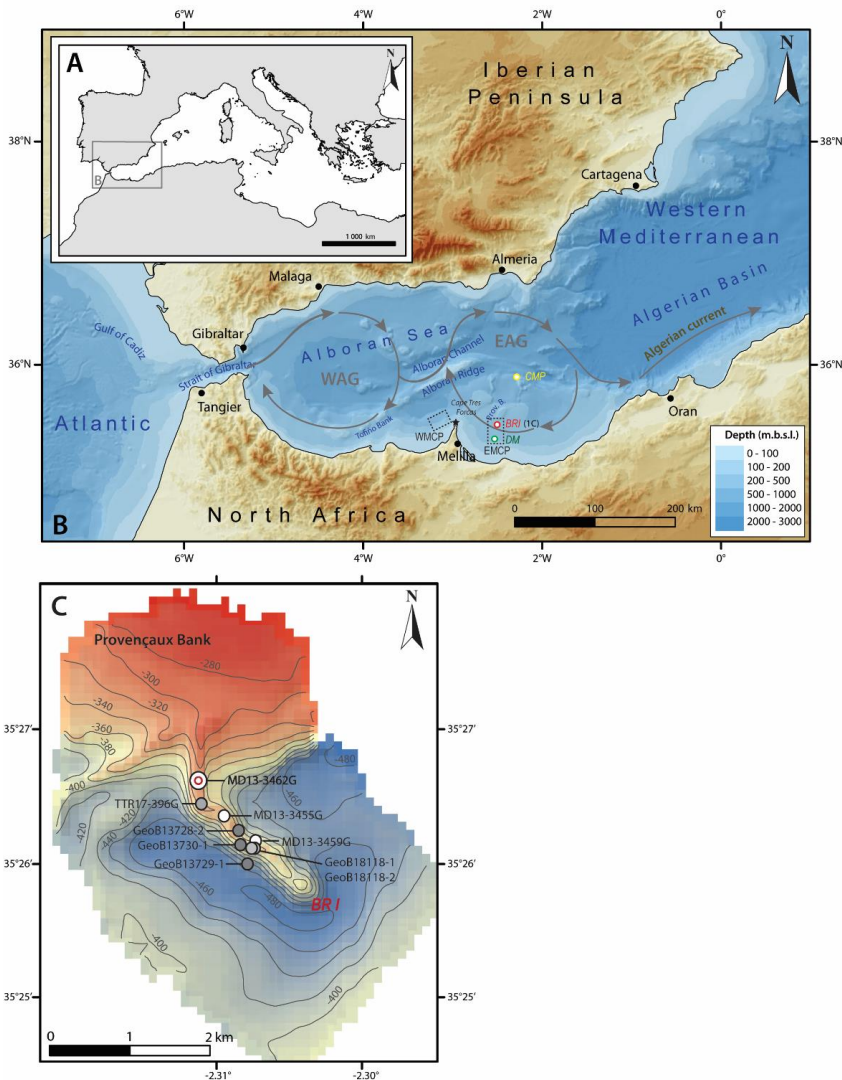
150 ~~In contrast, mound formation halted during the Younger Dryas, demonstrating low mound aggradation rates (30–50~~  
151 ~~cm.ky<sup>-1</sup>; Fink et al., 2013; Stalder et al., 2015; Wang et al., 2019). Based on benthic foraminiferal assemblages,~~  
152 ~~Stalder et al. (2015) suggest that cold/dense well oxygenated bottom water conditions favoured CWC development,~~  
153 ~~whilst Wang et al. (2019) relate the intensified coral proliferation to high surface productivity combined with strong~~  
154 ~~turbulence induced by internal waves.~~

155  
156 ~~Although the development of coral communities at the EMCP during the last 30 ky is well documented, the long-~~  
157 ~~term development and environmental forcing affecting these CWC mounds remain unknown. The aims of this study~~  
158 ~~are: 1) to constrain the influence of climate variability on CWC mound formation in the EMCP over the last 300 ky,~~  
159 ~~and 2) to assess long-term CWC mound formation in the area and compare it to North Atlantic counterparts.~~

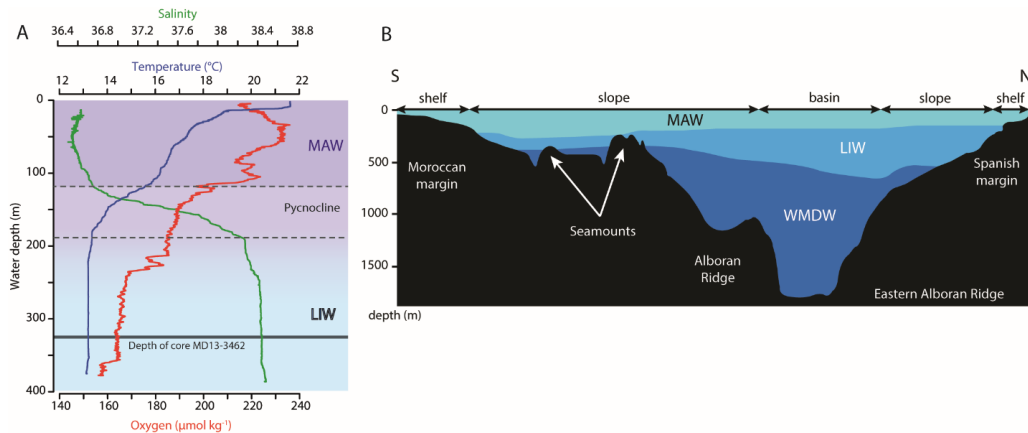
## 160 **2. Study area**

### 161 **2.1 Geological setting**

162 ~~The Alboran domain is structurally complex and its geodynamics are still debated (Duggen et al., 2008). Extension~~  
163 ~~and subsidence occurred during the Early to Middle Miocene (Comas et al., 1999; Faccenna et al., 2004; Do Couto et~~  
164 ~~al., 2016). The Alboran Sea is the westernmost basin of the Mediterranean Sea, and is closely connected to the~~  
165 ~~Atlantic Ocean by the Strait of Gibraltar. It is approximately 400 km long, with a width of 200 km, an average depth~~  
166 ~~of 1300 m and a maximum depth of 1800 m (Olivet et al., 1973; Comas et al., 1999). The Alboran Sea's~~  
167 ~~metamorphic basement is intruded by a number of volcanic plateaus and seamounts formed through the extensional~~  
168 ~~processes that took place between 17 and 8 million years ago (Comas et al., 1999; Duggen et al., 2008). One of these~~  
169 ~~shallow volcanic plateaus, the Banc des Provençaux (ca. 200 m depth), extends in a series of 3 ridges colonized by~~  
170 ~~CWCs, named "Brittlestar ridges" (BRI, BRII, BRIII) (Comas et al., 2009; Fink et al., 2013). They are part of the~~  
171 ~~larger EMCP nestled at depths between 250 and 450 m. The ridges are 3 to 20 km in length and vary in height from~~  
172 ~~50 to 150 mThe ridges are 3 to 20 km in length, whilst the mounds vary in height from 50 to 150 m (Hebbeln et al.,~~  
173 ~~2019). These mounds are characterized by dead coral framework with some living corals at their summits ~~These~~  
174 ~~mounds have mostly dead corals with scarce living corals at their summits and erosional moats at their base,~~  
175 ~~supporting the presence of dynamic currents in the area (Hebbeln et al., 2019) (Fig. 1C).~~~~



176  
 177 **Figure 1.** Location of the study area. (A) General map of the Mediterranean Sea and location of the investigated region (B)  
 178 Bathymetric map of the western Mediterranean Sea based on the GEMCO\_2019 gridded bathymetric data. Yellow, red and green  
 179 dots indicate respectively the locations of the Cabliers Coral Mound Province (CMP), Brittlestar Ridge I (BRI) and Dragon  
 180 Mound (DM). Additional abbreviations: EMCP: East Melilla Coral Province; WMCP: West Melilla Coral Province (red box);  
 181 WAG: Western Alboran Gyre; EAG: Eastern Alboran Gyre. (C) Bathymetry and location of the Bane-des-ProvençauxProvençaux  
 182 Bank and Brittlestar Ridge I (BRI). The white dot indicates the location of the studied core MD13-3462G recovered during cruise  
 183 “GATEWAY” No. 194 on board the research vessel *Marion Dufresne II* (Van Rooij et al, 2013) is indicated together with other  
 184 cores previously acquired and investigated in the area (GeoB13728-2, GeoB13730-1 and GeoB13729-1: Fink et al., 2013;  
 185 TTR17-396G: Stalder et al., 2018; MD13-3455G: Fentimen et al., 2020; GeoB18118-1 and GeoB18118-2: Kregel, 2020).;



186  
187

188 **Figure 2.** (A) CTD profile taken at the east of Brittlestar Ridge I ( $35^{\circ}26_{.087}'N$ ;  $2^{\circ}30_{.100}'W$ ) during cruise “GATEWAY” (No.  
189 194) on board the research vessel *Marion Dufresne II* in June 2013 (Van Rooij et al., 2013). Salinity (PSU), temperature (°C) and  
190 oxygen content ( $\mu\text{mol kg}^{-1}$ ) are indicated. The location of core MD13-3462G in relation to the profile is indicated by the black  
191 line. (B) North-South orientated bottom water profile of the East Alboran Sea modified from Ercilla et al. (2016). Abbreviations:  
192 MAW: Modified Atlantic Water, ~~ShW: Shelf Water~~, LIW: Levantine Intermediate Water, WMDW: Western Mediterranean  
193 Dense Water.

Formatted: Superscript

## 194 2.2 Oceanography

195 Low salinity (ca. 36.5 ~~psu~~ <sup>PSU</sup>), low density Atlantic Water enters the Mediterranean through the Strait of Gibraltar.  
196 This inflowing water mass mixes with Mediterranean water while crossing the Strait of Gibraltar to form the  
197 Modified Atlantic Water (MAW), the dominant surface water mass in the Alboran Sea (La Violette, 1983; Millot,  
198 2009). In addition, evaporation also exceeds river runoff and precipitation; hence MAW becomes saltier and denser  
199 journeying east and finally sinks in the Levantine, Aegean, Adriatic and Liguro-Provençal sub-basins (Millot et al.,  
200 2006). Intermediate waters consist of the highly saline (ca. 38.5 ~~psu~~ <sup>PSU</sup>) and warm (ca. 13.5 °C) Levantine  
201 Intermediate Water (LIW) that forms in the Levantine basin and flows from ~~e~~<sup>e</sup>East to ~~w~~<sup>w</sup>West, entering the western  
202 Mediterranean through the Strait of Sicily, to finally exit through the Strait of Gibraltar (Millot, 2013). Levantine  
203 Intermediate Water contributes to ca. 70 % of the total outflow of Mediterranean Outflow Water (MOW; Millot,  
204 2013) and flows between 200 and 600 m water depth in the Alboran Sea, whilst the core of the LIW is situated at  
205 approximately 400 m depth (Millot, 2009).

206  
207 It is important to note that, as it moves towards the west, the LIW receives contributions from other water masses  
208 and hence, its characteristics gradually change as it gets closer to the Strait of Gibraltar (Millot, 2013)~~It is important~~  
209 ~~to note that the LIW receives contributions from other intermediate water masses before it enters the western~~  
210 ~~Mediterranean and hence has different characteristics to the LIW in the eastern Mediterranean (Millot, 2013).~~  
211 Moreover, intermediate waters appear to differ between the North and South Alboran Sea (Fig. 2). ~~The LIW flows~~



212 ~~essentially along the Spanish margin, whilst Shelf Water (ShW), i.e. a mixture of MAW and Western Mediterranean~~  
213 ~~Deep Water (WMDW), dominates intermediate depths along the Moroccan margin (Ercilla et al., 2016).~~ Brittlestar  
214 Ridge I ~~laysies~~ in the depth range of ~~LIW ShW~~ (Fig. 2). Western Mediterranean Deep Water makes up the deepest  
215 water mass, flowing under ~~the LIW and ShW~~ (Millot and Taupier-Letage, 2005). It forms in the Gulf of Lions and  
216 flows westward to finally exit through the Strait of Gibraltar and contributes to the deeper MOW (Millot et al.,  
217 2006). In the Alboran Sea, WMDW circulates principally along the Moroccan margin (Millot and Taupier-Letage,  
218 2005; ~~Ercilla et al., 2016~~).

219  
220 The surface MAW extends down to approximately 200 m depth (Katz, 1972) and enters the Northwest Alboran Sea  
221 as a jet (1.6 Sv;  $1 \text{ Sv} = 10^6 \text{ m}^3 \text{ s}^{-1}$ ; Lanoix, 1974). This jet triggers the formation of the quasi-permanent anti-cyclonic  
222 Western Alboran Gyre that contributes to mixing between surface MAW and underlying LIW (Heburn and La  
223 Violette, 1990; Lafuente et al., 1998). When the waters of the Western Alboran Gyre reach the African coast, they  
224 separate into two branches: one flows back westward along the coast towards the Strait of Gibraltar while the other  
225 flows towards the eastern part of the basin to form the Eastern Alboran Gyre (La Violette, 1983; Viúdez and Tintoré,  
226 1995). This second non-permanent gyre also contributes to the mixing process between surface and intermediate  
227 water masses. The Banc des Provençaux and Brittlestar Ridge I are situated in the path of the westward circulating  
228 branch of the Eastern Alboran Gyre (Lanoix, 1974; Viúdez and Tintoré, 1995; Fig. 1). The mixing between surface  
229 and intermediate water masses occurs down to ca. 300 m water depth (Heburn and La Violette, 1990). The Strait of  
230 Gibraltar is a shallow (ca. 300 m depth) and narrow (ca. 20 km wide) crossing point for entering lower salinity  
231 MAW and exiting higher salinity MOW (Heburn and La Violette, 1990; Millot, 2009). Thus, the Strait of Gibraltar  
232 plays a key role in controlling water mass exchanges between the semi-enclosed Mediterranean Sea and the Atlantic  
233 Ocean. The importance of the water exchange varies between glacial and interglacial periods as a function of sea  
234 level change. Moreover, the narrow width and depth of the Strait of Gibraltar, together with the geometry of the  
235 Alboran basin and the Coriolis force, ~~affects the formation, mean position and shape of the Alboran gyres (Heburn~~  
236 ~~and La Violette, 1990). Thus, this will in turn affect mixing between surface and intermediate water masses in the~~  
237 ~~Alboran Sea.~~

238  
239  
240  
241 ~~affects the formation, mean position and shape of the Alboran gyres (Heburn and La Violette, 1990). Thus, this will~~  
242 ~~in turn affect mixing between surface and intermediate water masses in the Alboran Sea.~~

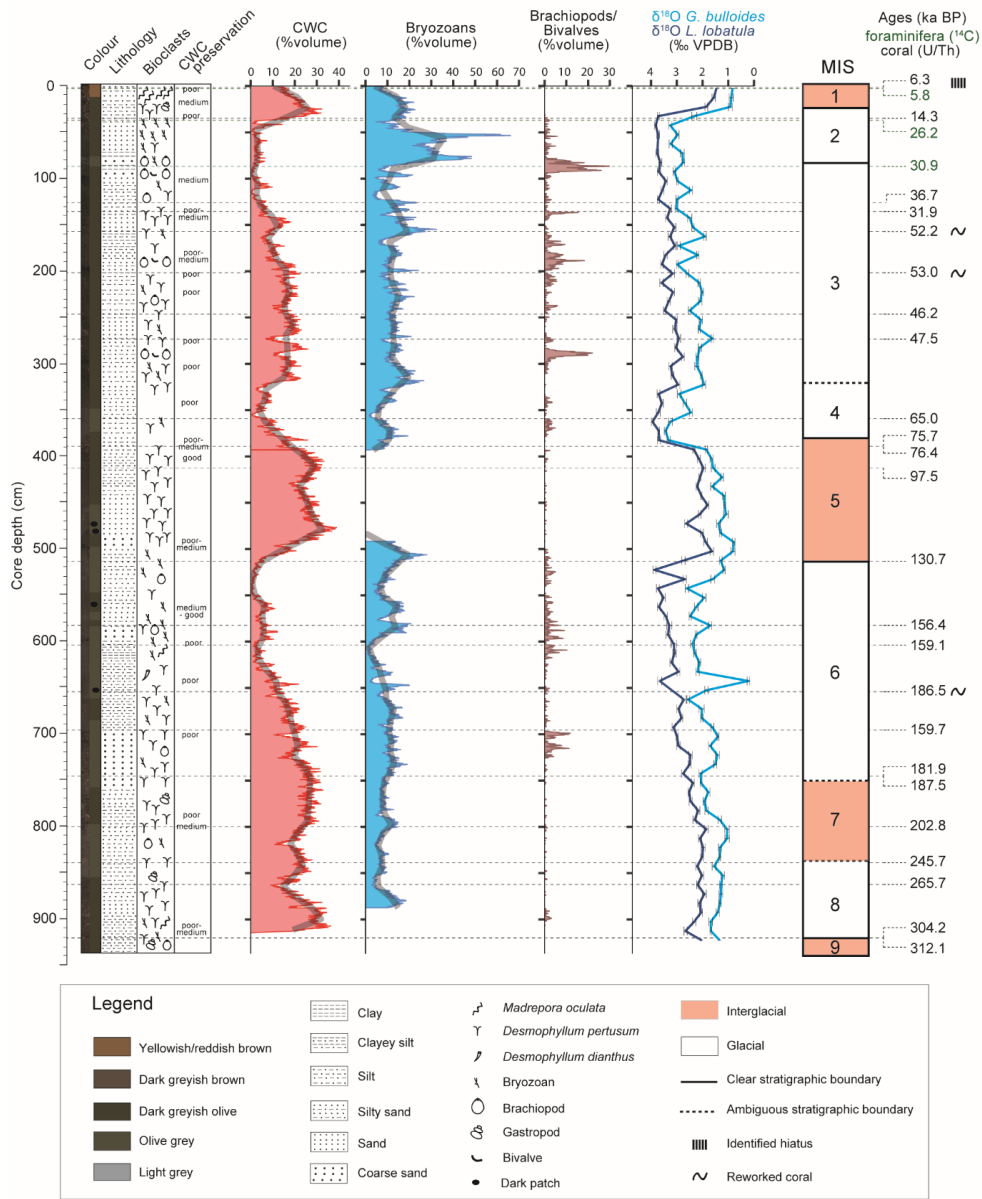
### 243 3. Material and methods

#### 244 3.1 Sample collection

245 This study is based on the multiproxy analysis of gravity core MD13-3462G (35°26.531'N, 2°31.073'W; 327 m  
246 depth; 926 cm long) recovered during the EUROFLEETS cruise MD194 Gateway on board the R/V *Marion-*



247 *Dufresne II* (Van Rooij et al., 2013). Cores were split frozen and sedimentary facies descriptions were made at the  
248 | University of Fribourg prior to sampling. These descriptions include the detailed investigation of texture, grain-size  
249 | and colour of the matrix sediment, together with the identification and assessment of the preservation state of major  
250 | macrofaunal components (Fig. 3). All data was plotted using the ggplot2 package for R (Wickham, 2016; R Core  
251 | Team, \_\_\_\_\_2018).



252

253

254

255

256

**Figure 3.** Core description, stratigraphy and macrofaunal composition of core MD13-3462G. Stratigraphy is based on the planktonic (*G. bulloides*) and benthic (*L. lobatula*)  $\delta^{18}O$  records (‰ VPDB), the Uranium-series ages of coral fragments and the epibenthic foraminiferal radiocarbon ages for the first meter of the core (see Fig. 4).

### 257 3.2 Macrofaunal quantification

258 X-ray Computed Tomography (CT) imaging was carried out on whole-round sections using a Siemens *Somatom*  
259 *Definition AS64* at the Institute of Forensic Sciences at the University of Bern (Switzerland). Core sections were  
260 scanned using an X-ray source operating at 120 kV. The images were reconstructed with a slice thickness of 0.6 mm  
261 taking into account an increment of 0.3 mm, ~~whilst t-~~The pixel resolution of the slices is 0.3 mm. The *Avizo 9.4*  
262 software was used to visualize, segment and quantify the volumes of the main macrofaunal components (coral,  
263 bryozoan and bivalve/brachiopod fragments). Prior to segmentation, images were filtered to remove noise in the  
264 matrix, using a non-local means filter. Brachiopods and bivalves were segmented manually. Corals, matrix, pores  
265 and bryozoans were segmented through the combination of dual thresholding and watershed segmentation. Labelled  
266 fragments smaller than 5 voxels were filtered prior to quantification. The ~~Mmaterial-S~~*Statistics* module was used to  
267 quantify the volume % of faunal fragments per slice and the same volume of interest was selected for each core  
268 section.

Formatted: Font: Italic

### 269 3.3 Geochemical logging

270 Geochemical logging was performed using the *Itrax* high-resolution X-ray fluorescence (XRF) core scanner on split  
271 cores at the Institute of Geological Sciences, University of Bern (Switzerland). Measurements were taken at 5 mm  
272 intervals using an integration time of 20 s at 30 kV and 45 mA. To counter potentially biased measurements linked to  
273 the uneven surface of CWC cores, such as the direct measurement of air or of CWC skeletons, a 3-step post  
274 treatment of the dataset was carried out. First, X-ray fluorescence values with Argon counts higher than 6000,  
275 representing the measurement of air and thereby more porous/cracked media not representative of changes in matrix  
276 sediment composition, were removed from the final dataset. Secondly, each individual measurement point was  
277 compared to high-resolution core images to assess if the measurement was taken on the matrix sediment or not.  
278 Finally, elemental counts were normalized by a conservative (minor) element of the background sediment (~~i.e. -here~~  
279 aluminium). Aluminium can be used effectively to counter variations in coral content (Löwemark et al., 2011).  
280 Normalization of the minor elements with Al is effective when detrital/terrestrial contribution to the sediment is high.  
281 Indeed, aluminium generally behaves conservatively and can hence be used to assess the relative variations of  
282 specific elements in sedimentary records (Calvert and Pedersen, 2007; references therein; Löwemark et al., 2011;  
283 Rodrigo-Gamiz et al., 2011; Martínez-Ruiz et al., 2015)

284  
285 In this study, we use the Log<sub>10</sub> normalized (Gregory et al., 2019) ~~Si/Al and Si/Rb/Al ratios as a proxyies~~ for terrestrial  
286 (fluvial and aeolian) input. ~~Indeed, the Saharan region is the dominant source of aeolian dust in the Mediterranean~~  
287 ~~Sea and is essentially composed of silicates with high quartz content (Guieu and Thomas, 1996; Caquineau et al.,~~  
288 ~~1998; 2002). Moreover, these are rare in Alboran Sea sediments (Masqué et al., 2003), hence the applicability of~~  
289 ~~Si/Al ratio to track variations in terrestrial input~~~~Si/Al has been used to track variations in terrestrial input since the~~  
290 ~~Saharan region, which is the dominant source of aeolian dust in the Mediterranean Sea, is essentially composed of~~  
291 ~~silicates with high quartz content (Guieu and Thomas, 1996; Caquineau et al., 1998; 2002) and that biogenic silica is~~

292 ~~rare in Alboran sediments (Masqué et al., 2003). Rubidium has regularly been utilized as a proxy for terrestrial run-~~  
293 ~~off in the Western Mediterranean because it is often found in aluminosilicate minerals commonly encountered in~~  
294 ~~fluvial material in the region (Calvert and Pedersen, 2007; Croudace and Rothwell, 2015 and references therein;~~  
295 ~~Martinez Ruiz et al., 2015).~~ In combination with information provided by benthic foraminiferal assemblages, Log<sub>10</sub>  
296 normalized ~~the Si/Al and SiRb/Al ratios hence provides a robust and valuable record of terrestrial input~~  
297 ~~indications of terrestrial input.~~

### 298 **3.4 Grain-size analysis and organic geochemistry**

299 Grain-size of the siliciclastic fraction was analysed using the *Malvern Mastersizer 3000* at the Department of  
300 Geology, Ghent University (Belgium). The core was sampled with a small spoon (1 cm<sup>3</sup>) every 5 cm. Large clasts  
301 (>1 cm), such as coral or bryozoan fragments, were sieved out prior to analysis. Samples were placed in 35 % H<sub>2</sub>O<sub>2</sub>  
302 to remove organic matter and boiled until the reaction ended. Following this first step, samples were boiled in 10 %  
303 HCl for 2 minutes to dissolve CaCO<sub>3</sub>. Prior to measurement, samples were placed in 2 % sodium polymetaphosphate  
304 and boiled to assure complete disaggregation. Any remaining particle larger than 2 mm was sieved out before  
305 measurement. Eighty-seven size classes were measured (from 0.01 to 2000 µm). Each sample was measured three  
306 times and results were then averaged. Mean grain-size of the siliciclastic fraction  $\overline{GS}$  (Folk and Ward, 1957) was  
307 calculated on the entire dataset with the *Rysgran* package for R (Gilbert et al., 2015; R Core Team, 2018). The  
308 sortable silt mean size  $\overline{SS}$ , as defined by McCave et al. (1995; i.e., the mean of the 10-63 µm grain size range), was  
309 also calculated following the same procedure. Furthermore, following McCave and Hall (2006), the percentage of  
310 sortable silt (SS%) in the total <63 µm fraction was calculated. This percentage, together with the sortable silt mean  
311 size, was used as an indication of bottom current velocity (McCave and Hall, 2006; Toucanne et al., 2012). It has to  
312 be mentioned that the use of  $\overline{SS}$  as a proxy for bottom current velocity on cores recovered from CWC mounds may  
313 be biased (e.g. Eisele et al., 2011). Indeed, the baffling effect of coral framework can locally reduce bottom current  
314 velocity and favour the deposition of fine sediments (Huvenne et al., 2009; Titschack et al., 2009; Fentimen et al.,  
315 2020b), thus leading to an underestimation of  $\overline{SS}$  during periods with high CWC content. Because of this, only  
316 relative increases in  $\overline{SS}$  are considered in combination with results obtained from other proxies.

317  
318 Total Organic Carbon (TOC, weight%) and Mineral Carbon (MinC, weight%) contents were determined on matrix  
319 sediments every 10 cm using the Rock-Eval6 technique at the laboratory of Sediment Geochemistry at the University  
320 of Lausanne (Fantasia et al., 2019). The RockEval6 technique produces an Oxygen and Hydrogen index, respectively  
321 corresponding to the quantity of CO<sub>2</sub> relative to TOC and the quantity of pyrolyzable organic compounds relative to  
322 TOC (Fantasia et al., 2019). These two indices give an indication about the origin of the organic matter present in the  
323 samples (Van Krevelen, 1993).

### 324 **3.5 Microfaunal and macrofaunal investigations**

325 The core was sampled (sliced) every 10 cm for micropaleontological analysis. Samples were weighed dry, washed  
326 through a 63 µm mesh sieve and dried at 30 °C. Each fraction was then dry sieved through a series of 63, 125 and

327 2000 µm mesh sieves and weighed. A target number of 300 benthic foraminifera were identified from the fraction  
328 larger than 125 µm for each sample. If the residue contained more than 600 specimens, it was split using a dry  
329 | microsplitter. Relative abundances (%percentages) of benthic species were calculated from the total benthic  
330 foraminiferal assemblage. The benthic foraminiferal density was calculated by dividing the total number of  
331 foraminifera of a given sample by the sample fraction's weight. The diversity Shannon index ( $H'$ ) was computed  
332 using the PRIMER6 software (Clarke and Gorley, 2006).

333  
334 Samples prepared for micropaleontological analysis were further used to identify bryozoan species/genera at the  
335 Department of Biological, Geological and Environmental Sciences, University of Catania (Italy) on the 125 µm to 2  
336 | mm and >2 mm sized fractions. Key intervals with high bryozoan content, previously identified by CT imagery,  
337 were selected. Dominant scleractinian corals and main brachiopod and bivalve species were identified at the lowest  
338 | taxonomic level possible on the >2 mm sized fraction at the Department of Geosciences, University of Fribourg  
339 (Switzerland).

### 340 3.6 Radiometric dating

341 Radiocarbon dating was performed on benthic foraminifera from 3 samples from the upper first meter of core MD13-  
342 3462G at the Laboratory of Ion Beam Physics, ETH Zürich, Switzerland (Table 1). The epibenthic foraminifera  
343 species *Discanomalina coronata*, *Lobatula lobatula* and *Cibicides refulgens* were picked in order to obtain between  
344 4 and 10 mg of pure carbonate. The samples were first dissolved in phosphoric acid. The resulting extracted CO<sub>2</sub> was  
345 then converted to graphite and measured by Accelerator Mass Spectrometry (AMS) technique using the MICADAS  
346 dedicated instrument (Synal et al., 2007). Results were corrected for <sup>13</sup>C and calibrated using the Marine13  
347 calibration curve (Reimer et al., 2013) and the software OxCal v4.2.4 (Ramsey, 2017). A reservoir age of 390 ± 80  
348 years was applied to all ages (Siani et al., 2000).

349  
350 Uranium-series dating was carried out on 24 CWC fragments (*D. pertusum* and *M. oculata*) using a multicollector  
351 inductively coupled plasma source mass spectrometer MC-ICPMS (*Thermo Fisher Scientific Neptune<sup>plus</sup>*) coupled  
352 with a dissolver (*Aridus I*) at the Institute of Environmental Physics, Heidelberg University (Table 2). In order to  
353 constrain the chronostratigraphy of the core, well-preserved coral fragments were selected at the upper and lower  
354 boundaries of coral-rich units. These were identified based on visual core descriptions and CT-analysis (macrofaunal  
355 quantification; Fig. 3). Coral fragments were physically cleaned with a *Dremel<sup>®</sup>* drill tool and by sand blasting, and  
356 further chemically cleaned using a weak acid leaching prior to measurements. The detailed sample protocol is  
357 described by Frank et al. (2004), while spectrometry and chemical U and Th extraction and purification followed  
358 | Wefing et al. (2017). Uranium-series coral ages were used to calculate mound aggradation rates ~~mound aggradation~~  
359 ~~rates, MARs~~.

360 **3.7 Oxygen and Carbon stable isotope analysis**

361 Stable oxygen and carbon isotope compositions were measured on 5 to 12 specimens of the planktonic foraminifera  
 362 *Globigerina bulloides* and the benthic foraminifera *Lobatula lobatula* from the size fraction 212-250 µm in order to  
 363 prevent any ontogenic effect on the measurements (Schiebel and Hemleben, 2017). The specimens were first cleaned  
 364 three times with distilled water in an ultrasonic bath for 2 seconds. The measurements were then made using a  
 365 Thermo Fisher Scientific GasBench II connected to a Thermo Finnigan Delta Plus XL isotope ratio mass  
 366 spectrometer at the Stable Isotope Laboratory of the University of Lausanne (Switzerland) according to the method  
 367 adapted from Spötl and Vennemann (2003). Results are reported in the conventional δ-values in permil (‰) relative  
 368 to the Vienna Pee Dee Belemnite (VPDB) standard. Analytical standard deviations (1σ) average 0.04 ‰ for δ<sup>13</sup>C and  
 369 0.06 ‰ for δ<sup>18</sup>O values based on 8 replicate analyses of standards in each sequence of 40 samples.

370

LAB ID	Depth (cm)	<sup>14</sup> C age (BP)	±1σ	2σ lower (cal years BP)	2σ upper (cal years BP)	2σ median (cal years BP)
ETH-87743	2	5777	25	5580	5920	5760
ETH-87744	37	22811	78	25970	26530	26220
ETH-87745	87	27587	124	30730	31160	30950

371

372

373 **Table 1.** Radiocarbon ages of epibenthic foraminifera (species selected: *Lobatula lobatula*, *Cibicides refulgens* and  
 374 *Discanomalina coronata*). Ages are corrected for a reservoir age of 390 ± 80 years (Siani et al., 2000).

375

LAB ID	Depth (cm)	S <sup>(1)</sup>	Age (ka)	±	Age <sup>(2)</sup> (ka)	±	<sup>238</sup> U (µg/g)	±	<sup>232</sup> Th (ng/g)	±	δ <sup>234</sup> U (‰)	±	δ <sup>234</sup> U <sub>i</sub> <sup>(3)</sup> (‰)	±
IUP- 8500	3	M	6.34	0.029	6.32	0.030	4.3377	0.00037	0.4311	0.00140	147.22	0.66	149.88	0.67
IUP- 8501	36	D	14.31	0.047	14.30	0.049	3.4367	0.00012	0.3254	0.00084	145.33	0.64	151.33	0.67
IUP- 10994	126	D	37.16	0.085	36.70	0.25	3.8667	0.00013	7.166	0.01328	121.99	0.51	135.30	0.57
IUP- 10995	136	D	35.53	0.10	31.9	1.3	3.4727	0.00015	36.120 <sup>(5)</sup>	0.06103	126.57	0.46	138.49	0.73
IUP- 8503	158	D	52.57	0.19	52.24	0.22	3.7330	0.00013	4.8320	0.01200	123.72	0.83	143.41	0.96
IUP- 9310	201	D	53.07	0.12	53.04	0.13	2.6348	0.00008	0.3418	0.00059	126.01	0.45	146.39	0.53
IUP- 10996	248	D	46.33	0.12	46.20	0.13	3.5899	0.00012	1.8802	0.0029	122.48	0.60	139.53	0.69
IUP- 10997	272	D	47.57	0.11	47.49	0.12	3.6971	0.00013	1.1538	0.0022	121.93	0.47	139.42	0.54
IUP- 10998	360	M	65.39	0.17	64.96	0.28	3.5499	0.00014	6.0720	0.0084	114.78	0.46	137.87	0.56
IUP- 8504	390	D	76.44	0.29	76.43	0.29	3.6896	0.00011	0.1328	0.00039	115.92	0.67	143.86	0.84
IUP- 9183 <sup>a</sup>	390	D	75.66	0.20	75.65	0.17	3.7004	0.00016	0.1763	0.00046	117.75	0.49	145.83	0.61
IUP- 9312	412	D	97.58	0.23	97.54	0.24	3.6265	0.00012	0.4572	0.00069	112.50	0.61	148.21	0.81
IUP- 9313	507	D	130.7	0.45	130.7	0.46	3.4073	0.00015	0.3844	0.00072	105.96	0.85	153.30	1.25
IUP- 10999	583	D	156.48	0.74	156.38	0.74	3.4985	0.00014	1.3288	0.0024	91.46	0.53	142.19	0.87
IUP- 10100	604	D	159.17	0.69	159.13	0.69	3.5045	0.00013	0.6366	0.0011	92.98	0.55	145.69	0.90
IUP- 10101	654	D	186.50	0.87	186.48	0.87	3.7106	0.00013	0.3339	0.00063	84.77	0.44	143.48	0.81

IUP- 10102	697	<i>M</i>	159.76	0.52	159.65	0.52	4.3503	0.00017	1.9141	0.0027	87.58	0.38	137.42	0.62
IUP- 8505	748	<i>D</i>	194.8	1.40	187.5	4.2	3.5659	0.00220	102.38 <sup>(5)</sup>	0.27000	95.01	0.84	161.40 <sup>(4)</sup>	2.40
IUP- 9184	756	<i>D</i>	181.9	0.79	181.9	0.78	2.8694	0.00013	0.6018	0.00099	102.72	0.79	171.74 <sup>(4)</sup>	1.40
IUP- 10103	801	<i>D</i>	203.07	0.98	202.84	0.98	2.8444	0.00010	2.6095	0.0036	85.04	0.55	150.74	1.05
IUP- 10104	840	<i>D</i>	245.7	1.50	245.70	1.5	3.0611	0.00011	0.2657	0.00048	78.14	0.41	156.32	1.03
IUP- 9314	862	<i>D</i>	265.7	2.10	265.7	2.4	3.4662	0.00018	0.6693	0.00150	70.40	1.10	149.10	2.60
IUP- 8507	921	<i>D</i>	304.2	4.80	304.2	4.9	3.0370	0.00012	0.1176	0.00044	63.32	0.68	149.60	2.60
IUP- 9185 <sup>b</sup>	921	<i>D</i>	312.1	3.40	312.1	3.0	3.3567	0.00016	0.2789	0.00061	58.58	0.77	141.50	2.20

376

377 **Table 2.** Uranium-series isotope measurements (U/Th) carried out on 24 coral fragments. All errors are  $2\sigma$  of the mean analytical  
378 uncertainty. Ratios determined using a Th-U spike calibrated to a secular equilibrium reference material (HU-1 at the IUP).  
379 Uncorrected, closed-system age calculated using the decay constants of Jaffey et al. (1971) for  $^{238}\text{U}$  and Cheng et al. (2000) for  
380  $^{230}\text{Th}$  and  $^{234}\text{U}$ . Ages are reported relative to the date of analysis, from year 2017 (IUP-8500 to IUP-8507) and year 2018 (other  
381 samples), and do not include uncertainties associated with decay constants. <sup>(1)</sup> Coral species: *M: Madrepora oculata*; *D:*  
382 *Desmophylum pertusum*. <sup>(2)</sup> Ages corrected for the contribution of initial  $^{230}\text{Th}$  based on an estimated seawater ( $^{230}\text{Th}/^{232}\text{Th}$ )  
383 activity ratio of  $8 \pm 4$ . <sup>(3)</sup> Typical  $\delta^{234}\text{U}_i$  reconstructed from corals for the past 30 kyr range between 135 and 155 (Chen et al.,  
384 2016). <sup>(4)</sup> Compared to the present-day seawater value of  $146.8 \pm 0.1 \%$ , possibly indicative of U-series open system behaviour. <sup>(5)</sup>  
385 Samples containing strong residual amounts of non-carbonate contamination leading to high  $^{232}\text{Th}$  concentrations and thus age  
386 corrections. <sup>a</sup> Replicate of IUP-8504; <sup>b</sup> replicate of IUP-8507.

## 387 4. Results

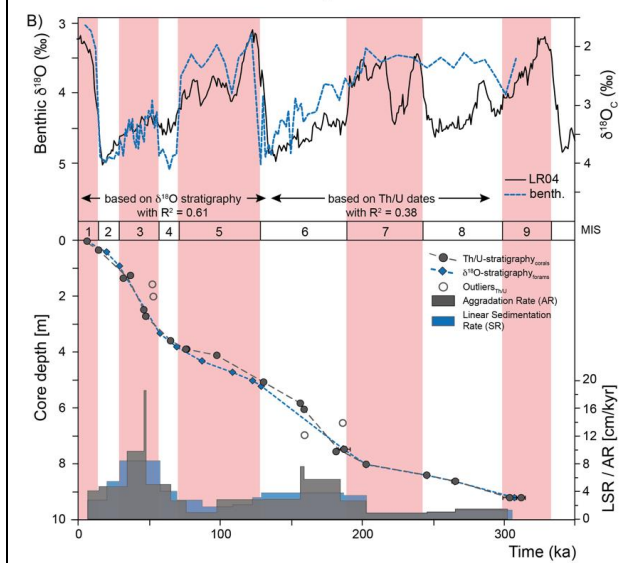
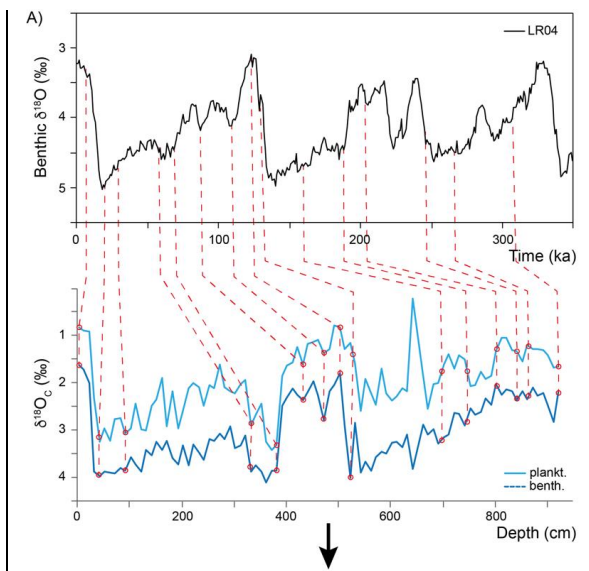
### 388 4.1 Chronostratigraphy

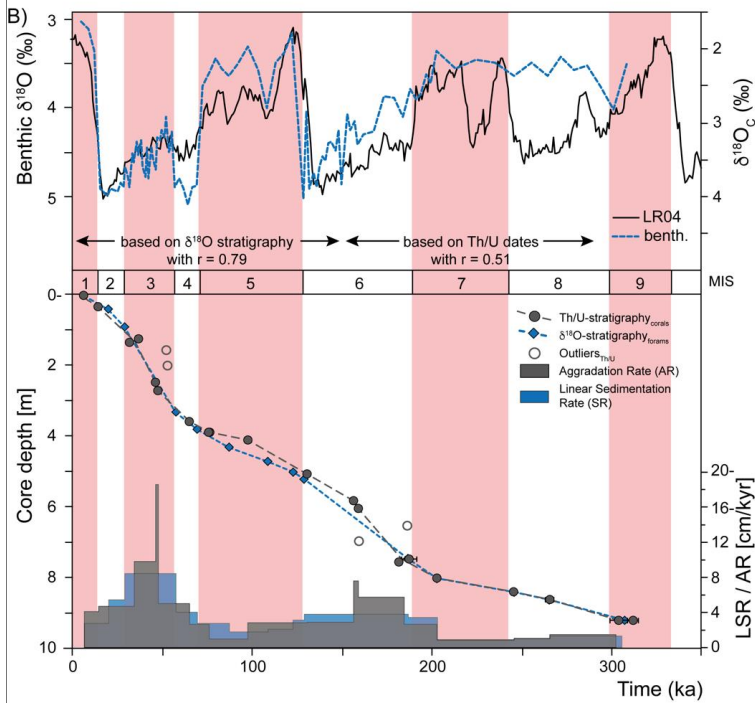
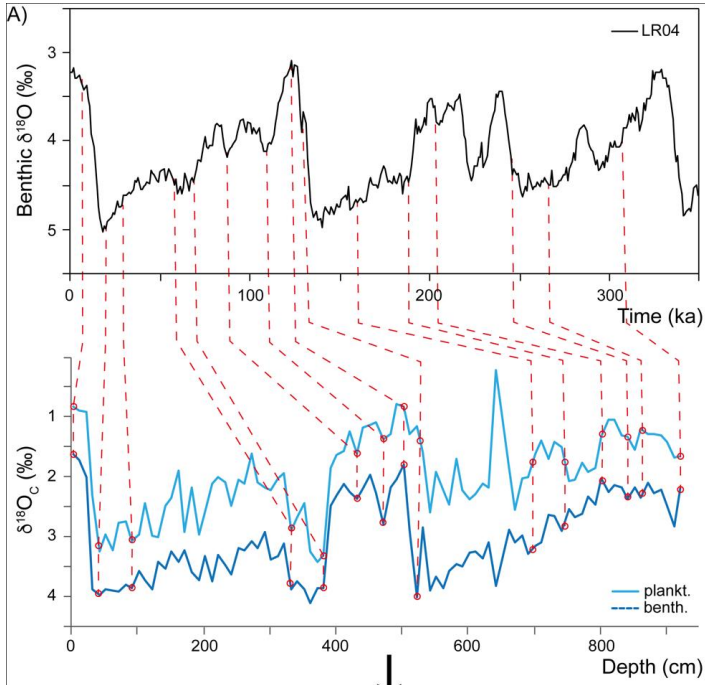
389 The chronostratigraphy of core MD13-3462G is based on the combination of the coral ages (U-series dating), the  
390 planktonic and benthic stable oxygen isotope records, and the foraminiferal radiocarbon ages for the top first meter  
391 of the core (Figs. 3 and 4). The U-series coral ages indicate that core MD13-3462G extends approximately from 300  
392 ka BP (Marine Isotope Stage 9) to the Holocene (Figs 3 and 4, Table 2). Coral ages have been widely used to define  
393 the chronology of cores recovered from coral mounds. This approach provides satisfying results although age  
394 reversals down-core have to be taken into account (e.g., Rüggeberg et al., 2007; Frank et al., 2009; Matos et al.,  
395 2017). Indeed, reefs are fragile structures and can collapse, topple and fragment through the action of bioerosion,  
396 strong bottom currents, and gravity-driven processes, resulting in transport and redeposition of coral fragments  
397 (Beuck et al., 2005; Dorschel et al., 2007; White, 2007). In contrast, constructing a continuous age model based on  
398 stable isotope records is generally considered untrustworthy for cores collected from coral mounds since  
399 sedimentation is intermittent (e.g., Dorschel et al., 2005). However, coral ages at the upper and lower boundaries of  
400 coral build-up phases in core MD13-3462G (e.g., at 390 and 507 cm depth) correspond to changes in the stable  
401 oxygen isotope records (Fig. 3), which in turn match the changes between Marine Isotope Stages (MIS; Lisiecki and  
402 Raymo, 2005). As such, the stable oxygen isotope records can, in the case of core MD13-3462G and in conjunction  
403 with coral ages, indicate important stratigraphic boundaries (Fig. 4). This is particularly relevant during times when  
404 CWCs did not grow and hence cannot serve to construct a timeframe. Stable oxygen isotope records were hence



405 correlated to the reference LR04-stack (Lisiecki & Raymo, 2005) for the  $\delta^{18}\text{O}$ -stratigraphy (see Fig. 4a). Tie points  
406 were visually identified and a best correlation coefficient determined using Lineage in the software package  
407 AnalySeries v. 2.0.8 (Paillard et al., 1996; Table 3). A clear subdivision into glacial–interglacial stages and substages  
408 was possible for Marine Isotope Stages (MIS) 1 to 6 with a Pearson’s correlation coefficient of  $r = 0.79$  ( $p < 0.001$ )  
409  $R^2 = 0.61$ , being in good agreement with the CWC U-series age dates (see Fig. 4b). However, the correlation became  
410 difficult below 65520 cm core depth (> 150 ka) due to the resolution of sampling (= 10 cm), the lower sedimentation  
411 rate and possible hiatuses and reworking units flattening the curve. Therefore, U-series ages were used to correlate  
412 the lower

Formatted: Highlight





415 **Figure 4.** (A) Correlation pointers (see Table 3) between LR04 benthic  $\delta^{18}\text{O}$  stack of Lisiecki and Raymo (2005) and the benthic  
 416 (*L. lobatula*) and planktonic (*G. bulloides*)  $\delta^{18}\text{O}$  record of MD13-3462G. (B) The  $\delta^{18}\text{O}$  stratigraphy has good correlation for the  
 417 younger part (MIS 1–5, 0–150 ka,  $r = 0.79$ ,  $p < 0.001$ ,  $R^2 = 0.64$ ), but the lower part (>MIS-6/150 ka), which is based on the U-  
 418 series CWC dates, has a weak correlation ( $R^2 = 0.38$ ,  $r = 0.51$ ,  $p < 0.009$ ). The comparison between the U-series- and  $\delta^{18}\text{O}$ -  
 419 stratigraphy-based age-depth correlations indicates good coherence. The resulting  $\delta^{18}\text{O}$ -stratigraphy-based Linear Sedimentation  
 420 Rate (LSR) may serve as an indication for changes in the sedimentary regime, but shows similar values/trends as the CWC-age-  
 421 based Aggradation Rate (AR), with higher rates during MIS 3, MIS 6 and late MIS 7. Marine Isotope Stages (MIS) follow  
 422 boundaries defined by the LR04-stack (Lisiecki and Raymo, 2005).

Formatted: Highlight

423  
424

Depth (cm) of core MD13-3462G	Time (ka) of LR04 stack	LSR (cm/ka)	
4	6.3	2.8	Top marker
42	20.0	5.5	MIS 2 peak
91	29.0	8.5	MIS 2/3
333	57.5	4.1	MIS 3/4
381	69.5	2.8	MIS 4/5
431	87.2	1.8	MIS 5.2 peak
472	108.9	2.2	MIS 5.4 peak
501	122.8	3.2	MIS 5.5 peak
522	129.1	3.9	MIS 5/6
697	159.7	3.5	Th/U date
802	203.1	0.9	Th/U date
841	245.8	1.1	Th/U date, MIS 7/8
862	265.6	1.4	Th/U date
920	307.5		Bottom marker, MIS 8/9

425  
 426 **Table 3.** Correlation pointers between sediment depth and time based on the benthic  $\delta^{18}\text{O}$  record of core MD13-3462G and the  
 427 benthic LR04 stack of Lisiecki and Raymo (2005) for main Marine Isotope Stage (MIS) boundaries. The Pearson's correlation  
 428 coefficient ( $r$ ) between the two records is 0.65 ( $p < 0.001$ ,  $R^2 = 0.76$ ). Due to possibly unidentified hiatuses the Linear Sedimentation  
 429 Rate (LSR) should not be considered as absolute but may serve as a guidance to indicate changes in the sedimentary regime.

Formatted: Highlight

430

431 ~~the curve. Therefore, U-series ages were used to correlate the lower~~ ~~hiatuses and reworking units flattening the~~  
432 ~~curve. Therefore, U-series ages were used to correlate the lower~~ part of the core, resulting in a Pearson's correlation  
433 coefficient of  $r = 0.51$  ( $p < 0.009$ ),  $R^2 = 0.38$  (total  $R^2 = 0.43$ ). The foraminiferal  $\delta^{18}\text{O}$  records still follow the LR04-  
434 stack until late MIS 7, but the signal remains at relatively light  $\delta^{18}\text{O}$  values for the bottom ~100 cm of MD13-3462G  
435 covering a timespan of around 100 kyr (Fig. 4b).

Formatted: Highlight

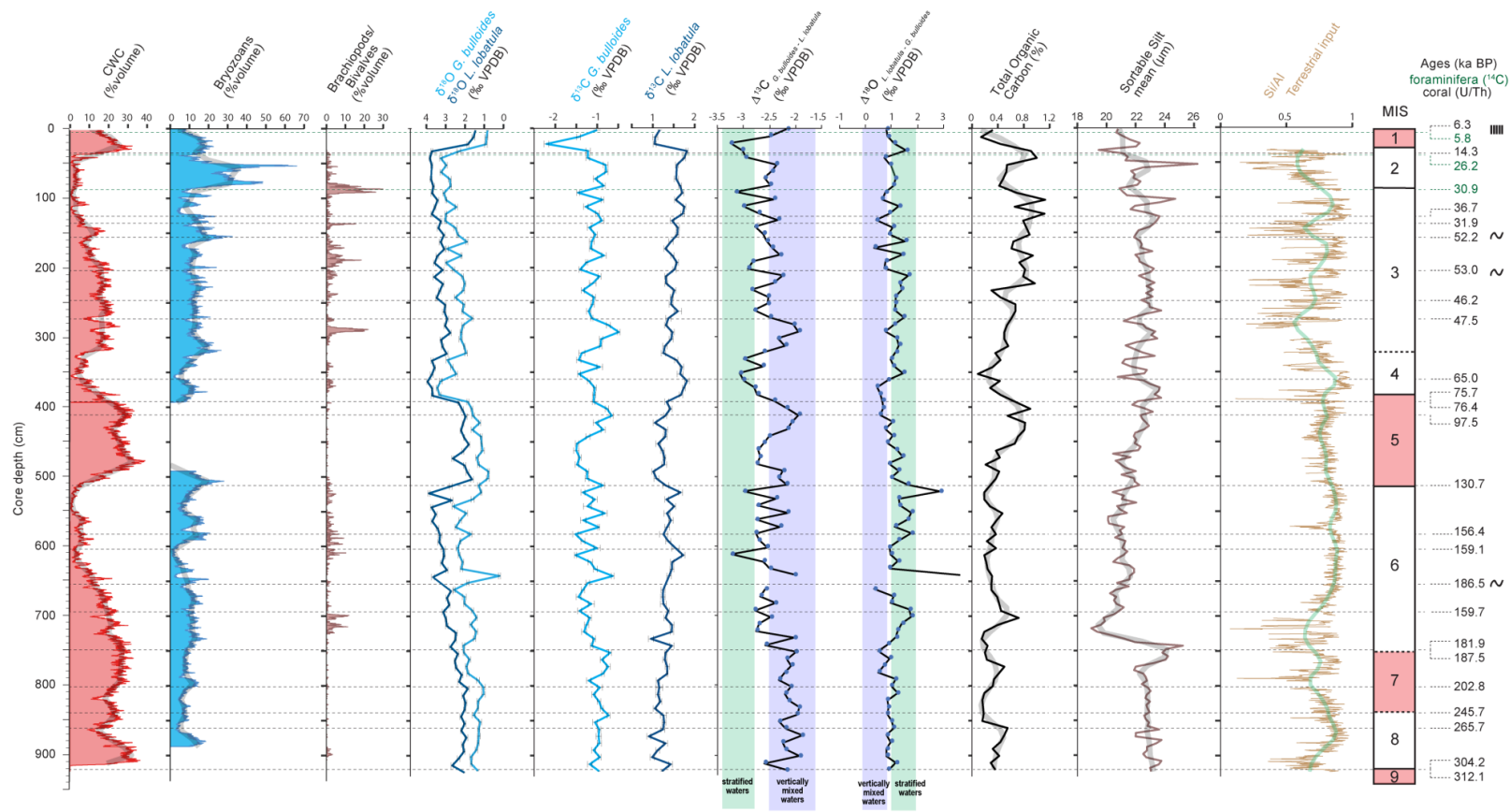
436  
437 The stratigraphic boundaries from the base of the core to ca. 650 cm depth were defined based on the U-series coral  
438 ages, as planktonic stable oxygen isotope compositions show little variation. The boundaries of MIS 8 are the most  
439 poorly defined. Due to difficulties to define precisely the stratigraphy of this section of the core, it will not be  
440 considered in detail during this study. In contrast, the planktonic and benthic  $\delta^{18}\text{O}$  values and the coral ages do  
441 constrain the stratigraphic boundaries from MIS 6 to MIS 1 (Fig. 4). Contrary to sediment records from CWC  
442 mounds of the North Atlantic, where no clear glacial or interglacial  $\delta^{18}\text{O}$  values are reported (e.g., Dorschel et al.,  
443 2005; Rüggeberg et al., 2007; Eisele et al., 2008; Mienis et al., 2009), core MD13-3462G presents typical interglacial  
444 and glacial  $\delta^{18}\text{O}$  values of the Alborán Sea for both, planktonic (< 1 ‰ and ~3 ‰, resp.) and benthic (~1.5 ‰ and  
445 ~4‰, resp.) foraminifera (e.g., Cacho et al., 1999; Cacho et al., 2006; Stalder et al., 2015). Therefore, low planktonic  
446 and benthic  $\delta^{18}\text{O}$  values correspond to interglacial periods, whilst high planktonic and benthic  $\delta^{18}\text{O}$  values  
447 correspond to the two last glacial periods (Figs. 3 and 4).

#### 449 4.2 Sediment characterization

450 The sediment in core MD13-3462G consists mostly of macrofaunal remains (essentially corals and bryozoans)  
451 ~~embedded in~~ ~~surrounded by~~ a clay- to silt-sized carbonate/siliciclastic matrix. No important variation in the matrix  
452 sediment is observed throughout the core. Total organic carbon content in the sediment varies between 0.16 and 1.13  
453 wt% (Fig. 5). The highest TOC value is measured during late MIS 3 (1.13 wt%), whilst the lowest is recorded during  
454 MIS 8 (0.16 wt%; Fig. 5). The most important shifts to higher TOC values are observed during MIS 5, MIS 3 and at  
455 the transition between MIS 2 and MIS 1 (Fig. 5). The sediment samples are further characterized by low Hydrogen  
456 index values (< 300 mg HC/g TOC; Fig. 6), indicating that the organic matter is oxidized and ~~essentially~~ ~~of~~  
457 ~~essentially~~ terrestrial origin (Espitalié et al., 1985).

458  
459  
460 The mean sortable silt grain size of the siliciclastic fraction ( $\overline{SS}$ ) varies between ca. 19 and ca. 26  $\mu\text{m}$  (Fig. 5).  
461 Overall, a decrease in  $\overline{SS}$  ~~is~~ marks the passage from interglacial to glacial periods. This is particularly noticeable at  
462 the transition from MIS 7 to MIS 6, ~~when were~~  $\overline{SS}$  decreases abruptly from approximately 25 to 19  $\mu\text{m}$  (Fig. 5).  
463 Conversely, an increasing trend is observed from ca. 550 to ca. 375 cm depth, corresponding to the passage from the  
464 later phases of MIS 6 to the end of MIS 5 (Fig. 5). ~~The percentage of sortable silt (SS%) increases with  $\overline{SS}$  (Fig. 7).~~  
465 ~~As discussed by McCave and Hall (2006) and McCave et al. (2017), the straight line relationship (slope of ca. 0.125~~

466 |  ~~$\mu\text{m}/\%$  and an intercept at 0% of ca. 17.5  $\mu\text{m}$ ) between  $\overline{SS}$  and  $SS\%$  is indicative of a sorting process induced by~~  
467 | ~~bottom currents (Fig. 7).~~



Formatted Table

Formatted: Section start:  
Width: 27,94 cm, Height:

468

469 **Figure 5.** Planktonic (*G. bulloides*) and benthic (*L. lobatula*)  $\delta^{13}\text{C}$  records,  $\Delta^{13}\text{C}$  ( $\delta^{13}\text{C } G. bulloides - \delta^{13}\text{C } L. lobatula$ ) and  $\Delta^{18}\text{O}$  ( $\delta^{18}\text{O } L. lobatula - \delta^{18}\text{O } G. bulloides$ ) records,  
 470 Total Organic Carbon content (%), mean grain size of the sortable silt fraction (the 10-63  $\mu\text{m}$  grain size range, expressed in  $\mu\text{m}$ ; McCave et al., 2006), and the Log<sub>10</sub> titanium-silica  
 471 (STi) and rubidium (Rb)-aluminium (Al)-normalized ratios. Smoothed curves are indicated by the shaded curves. The planktonic (*G. bulloides*) and benthic (*L. lobatula*)  $\delta^{18}\text{O}$   
 472 records (‰ VPDB) are provided as supporting information.

473

474

Formatted: Font: Italic

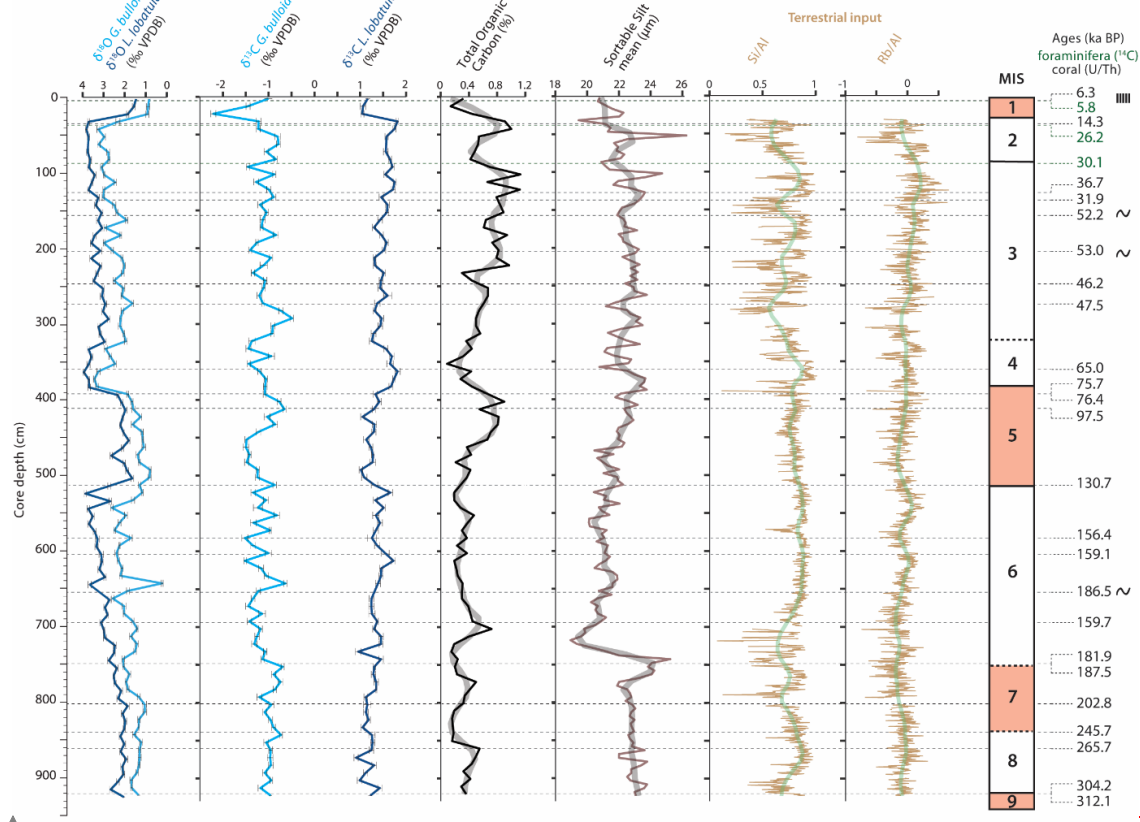
Formatted: Font: Italic

Formatted: Font: Italic

Formatted: Normal;Text

Formatted: Font: Italic





475

476

477

478

479

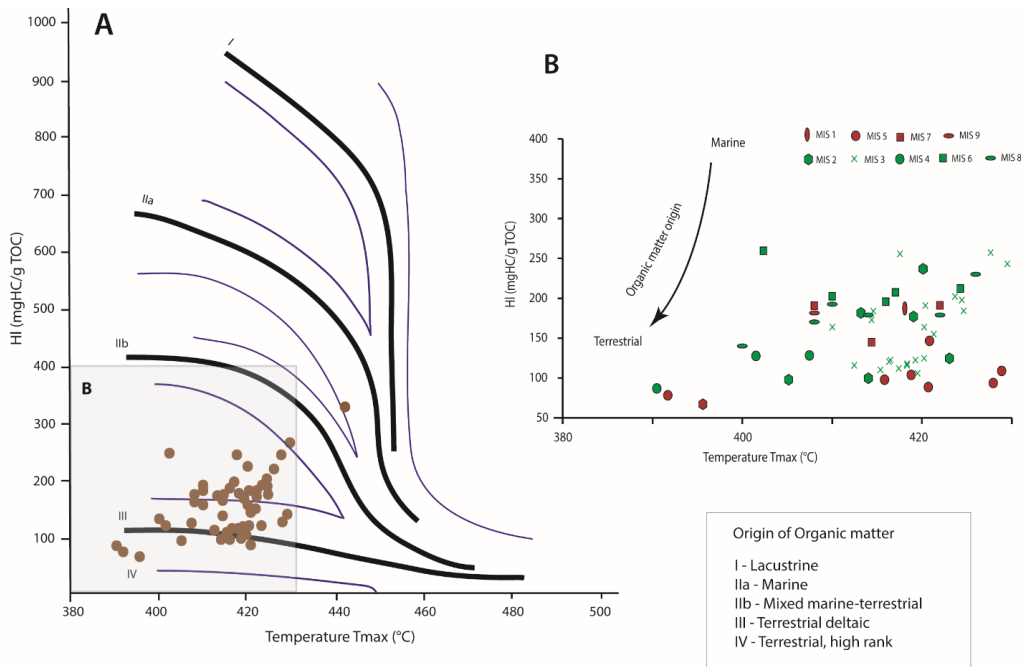
**Figure 5.** Planktonic (*G. bulloides*) and benthic (*L. lobatula*)  $\delta^{13}\text{C}$  records, Total Organic Carbon content (%), mean grain size of the sortable silt fraction (the 10–63  $\mu\text{m}$  grain size range, expressed in  $\mu\text{m}$ ; McCave et al., 2006), and the  $\text{Log}_{10}$  titanium (Ti) and rubidium (Rb) aluminium (Al) normalized ratios. Smoothed curves are indicated by the shaded curves. The planktonic (*G. bulloides*) and benthic (*L. lobatula*)  $\delta^{18}\text{O}$  records (‰ VPDB) are provided as supporting information.

480 **4.3 Stable carbon isotopes and elemental geochemistry**

481 The range of  $\delta^{13}\text{C}$  values of the planktonic *G. bulloides* goes from -2.2 ‰ at 12 cm to -0.5 ‰ at 292 cm, whereas that  
 482 of the benthic *L. lobatula* goes from 0.9 ‰ at 872 cm to 1.8 ‰ at 362 (Fig. 5). *G. bulloides* is between -2.2 ‰ at 12  
 483 cm and -0.5 ‰ at 292 cm, whereas that for the benthic *L. lobatula* is between 0.9 ‰ at 872 cm and 1.8 ‰ at 362 cm  
 484 (Fig. 5). The planktonic  $\delta^{13}\text{C}$  record has a higher variability compared to the benthic  $\delta^{13}\text{C}$  record (Fig. 5). During  
 485 MIS 6, the benthic  $\delta^{13}\text{C}$  is relatively high (ca. 1.5 ‰), whilst the planktonic  $\delta^{13}\text{C}$  record fluctuates between -0.6 ‰  
 486 and -1.5 ‰. A decrease in the planktonic  $\delta^{13}\text{C}$  record (from -0.7 to -1.5 ‰) marks the middle of MIS 5. In contrast,  
 487 the benthic  $\delta^{13}\text{C}$  remains stable and low (ca. 1.2 ‰) throughout MIS 5 (Fig. 5). The passage from MIS 4 to MIS 3 is  
 488 characterized by a shift from the low planktonic  $\delta^{13}\text{C}$  recorded during MIS 4 (-1.5 ‰) to higher planktonic  $\delta^{13}\text{C}$  (-0.5  
 489 ‰). Conversely, benthic  $\delta^{13}\text{C}$  values shift from high (1.8 ‰) to lower values (1.3 ‰). The passage from MIS 2 to  
 490 MIS 1 is marked by a sharp decrease in planktonic and benthic  $\delta^{13}\text{C}$  (from -1.2 ‰ to -2.2 ‰ and from 1.8 ‰ to 1.0  
 491 ‰ respectively). The last two glacial intervals, in particular MIS 4, are overall marked by a more negative stronger  
 492  $\Delta$  difference between benthic and planktonic  $\delta^{13}\text{C}$  values than during interglacial values (Fig. 4).

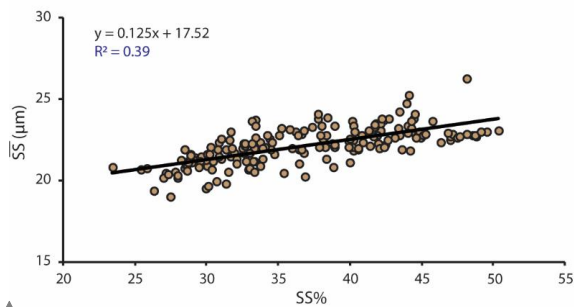
Formatted: Font: Not Bold, Not Italic

Formatted: Font: Not Bold, Not Italic



494  
 495  
 496 **Figure 6.** (A) Hydrogen Index (HI; mgHC/g TOC) vs. Tmax (°C) obtained by RockEval6 pyrolysis. (B) Close-up. The organic  
 497 matter origin becomes more terrestrial with decreasing HI values.  
 498

499  
500  
501



Formatted: Font: Not Bold

502  
503  
504  
505

**Figure 7.** Dispersion plot of the sortable silt mean size (the 10–63  $\mu\text{m}$  grain size range, expressed in  $\mu\text{m}$ )  $\overline{SS}$  vs. the percentage of sortable silt (SS%). The slope of 0.125  $\mu\text{m}$  and intercept at 0 % of 17.52  $\mu\text{m}$  indicates a sorting process induced by bottom currents (McCave et al., 2006).

506

#### 4.4 Elemental geochemistry

507  
508  
509  
510  
511  
512

Variations in Si/Al are more marked during MIS 7 and the last glacial period, in comparison with the more stable values recorded during MIS 6 and MIS 5. The transitions from MIS 7 to MIS 6 and from MIS 5 to MIS 4 are characterized by fluctuating Si/Al values (Fig. 5). The Rb/Al ratios demonstrate overall low values throughout the core. However, higher Rb/Al ratios are reached at the end of MIS 6 and MIS 3 (ca. 100 cm). In the same way as for Si/Al record, Rb/Al ratios demonstrate an important variability during MIS 7 and the last glacial period, in comparison to other periods where the records are comparatively stable (Fig. 5).

513

#### 4.4.5 Macrofauna

514  
515  
516  
517  
518  
519  
520  
521  
522  
523  
524  
525  
526

The major macrofaunal fragments present in the core MD13-3462G are scleractinian corals, bryozoans, brachiopods and bivalves (Figs. 3 and 7). Sea urchins, gastropods, serpulids and gorgonian fragments are more sporadically distributed. Although the dominant coral species in the core is *D. pertusum*, it is replaced in the upper 20 cm by *M. oculata* (Figs. 3 and 7). The dominant coral species in the core is the scleractinian *D. pertusum*. In the upper 20 cm, *D. pertusum* is replaced by *M. oculata* (Fig. 3; Fig. 8). A third and solitary species, *Desmophyllum dianthus*, is scarcely distributed (Fig. 3). Higher CWC content is observed during interglacial periods (22.2 vol% average), whilst lower content characterizes glacial periods (14.5 vol% average) (Fig. 3). However, during MIS 3 coral content shows an unevenly staggered distribution during MIS 3, with a range of values from less than 10 vol% to ca. 27 vol% (Fig. 3). The Aggradation Rate of mound sediments (MARs), determined from the coral ages, indicate higher rates of 5.6 and 18 to 8  $\text{cm.kyr}^{-1}$  during MIS 3 and early MIS 6 being well in coherence with the Linear Sedimentation Rate based on the foraminifera  $\delta^{18}\text{O}$ -stratigraphy of the background sediment (Fig. 4B). In contrast, lower Aggradation rates of mound sediments (MARs) characterize MIS 5 (ca. 2  $\text{cm.kyr}^{-1}$ ) together with MIS 1, 2 and 4 (ca. 4  $\text{cm.kyr}^{-1}$ ) (Fig. 4B).

Formatted: Font: Not Bold, Italic

Formatted: Font: Not Bold, Italic

Formatted: Font: Not Bold, Highlight

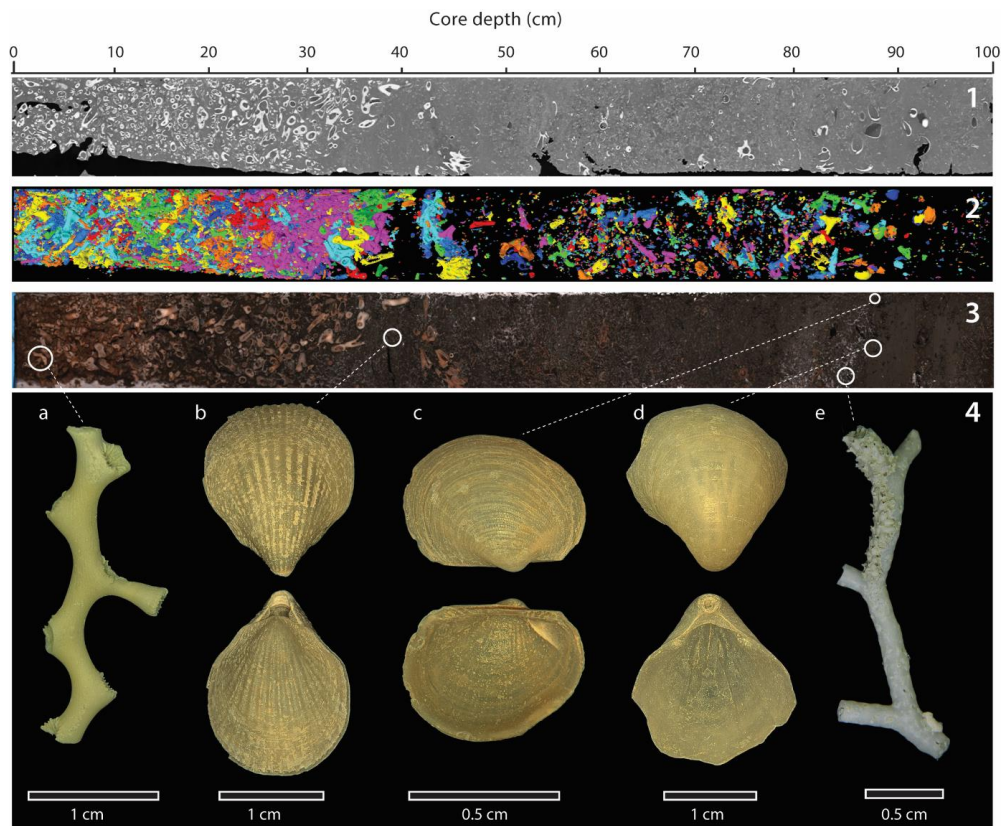
Formatted: Font: Not Bold, Highlight

Formatted: Font: Not Bold, Highlight

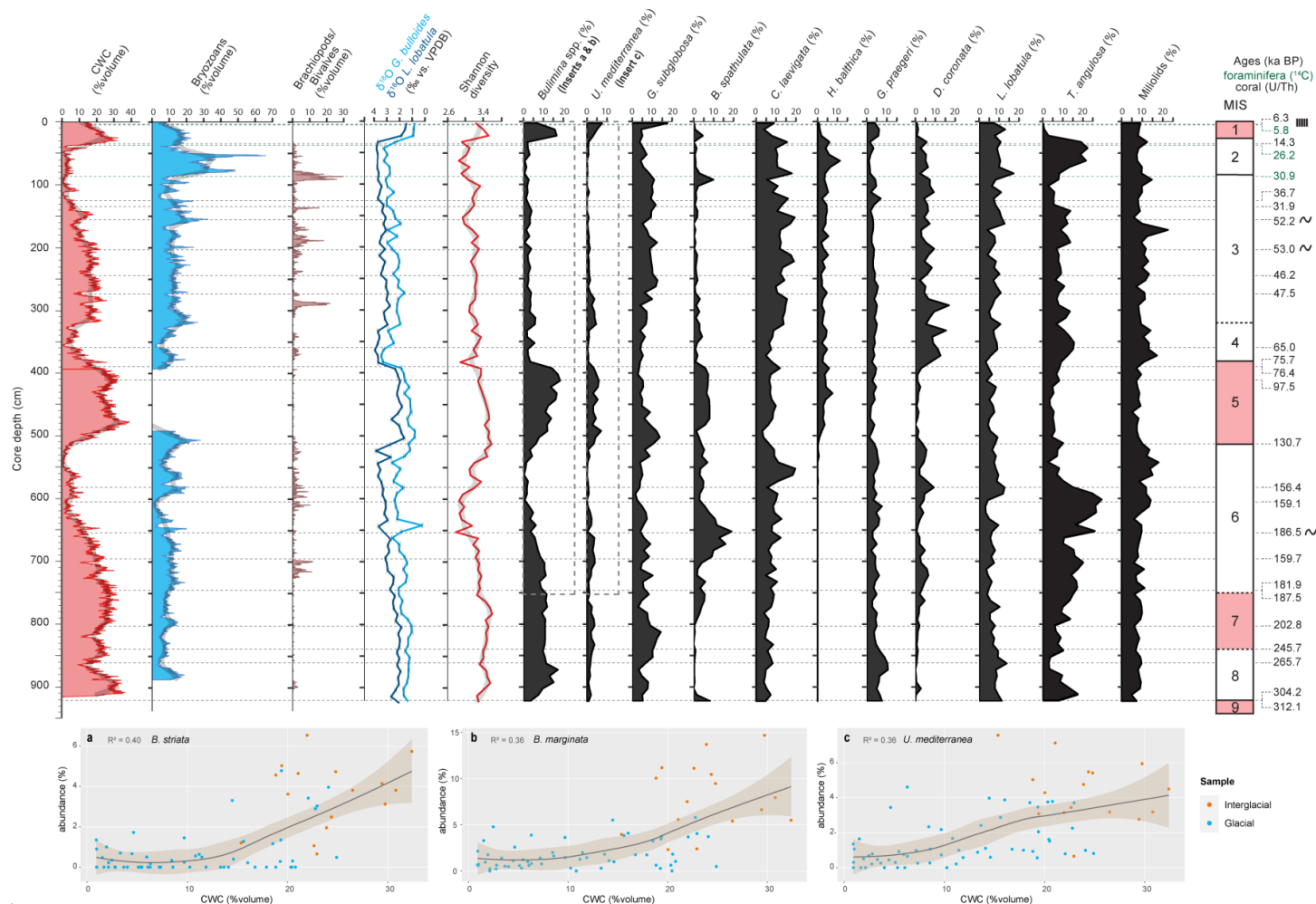
527  
528 In total 23 genera of bryozoans were identified. *Buskea dichotoma* is by far the dominant bryozoan species (Fig. 8).  
529 Accessory species/genera are mainly represented by *Reteporella sparteli*, *Tubuliporina* sp. and *Palmiskenea* sp.  
530 Bryozoan content varies in general between 10 and 20 vol% (Fig. 3). Very high content is, however, observed during  
531 MIS 2, reaching near to 70 vol%. The fragments, although delicate and fragile, are well preserved, large sized and  
532 unworn (Fig. 78). Bryozoans are absent during most of MIS 5. This absence corresponds to the time interval when  
533 coral content is the most important (Fig. 3). Conversely, the maximum abundance of bryozoans during MIS 2  
534 correlates to a minimum in coral content (Fig. 3).

535  
536 Brachiopods are mainly represented by the co-occurrence of the species *Gryphus vitreus* and *Terebratulina retusa*  
537 (Fig. 78). These two brachiopods are regularly associated to the bivalve *Bathyarca pectunculoides* (Fig. 78). These  
538 three invertebrates have been formerly reported from Mediterranean CWC environments. *G. vitreus* and  
539 *T. retusa* are also recorded from Pleistocene CWC deposits from Rhodes, Greece (Bromley, 2005),  
540 whilst *B. pectunculoides* was found at the Santa Maria di Leuca CWC province (Mastrototaro et al., 2010;  
541 Negri and Corselli, 2016). *G. vitreus* was also found associated to “white corals” between 235 and 255 m  
542 depth off the coast of the Hyères Islands, France (Emig and Arnaud, 1988). Although being fragile, the shells are  
543 well preserved (Fig. 78). The brachiopod/bivalves concentrate as layers and demonstrate a non-continuous  
544 distribution (Figs. 3 and 78). They reach their highest abundance during glacial periods, in particular at the end of  
545 MIS 3 (30 vol% at 80 cm). Brachiopods and bivalves are completely absent during the last two interglacial periods  
546 (Fig. 3).

547  
548



549  
 550 | **Figure 78.** Example of a sediment core section showing the main macrofaunal components (section 1, 0-100 cm). (1) X-ray  
 551 | Computed Tomography imagery. (2) Three-dimensional reconstruction of coral fragments performed on X-ray Computed  
 552 | Tomography (CT) images. (3) Split-core high-resolution image. ~~The white circles indicate the location of main macrofaunal~~  
 553 | ~~components.~~ (4) Main macrofaunal components: (a) the scleractinian coral *Madrepora oculata*, (b) the brachiopod *Terebratulina*  
 554 | *retusa*, (c) the bivalve *Bathyarca pectunculoides*, (d) the brachiopod *Gryphus vitreus*, (e) the bryozoan *Buskea dichotoma*.



555 **Figure 8.** Distribution of main benthic foraminifera species (relative abundances) and benthic foraminiferal Shannon diversity. The planktonic (*G. bulloides*) and benthic (*L.*  
 556 *lobatula*)  $\delta^{18}\text{O}$  records (‰, VPDB) are provided as supporting information. Inserts a, b and c: relative abundance of *B. striata*, *B. aculeata*, and *U. mediterranea* relative to vs. CWC  
 557 content (% volume) over the last two interglacial-glacial cycles (dashed grey rectangles). Shaded brown outlines represent the Locally Weighted Regression (Cleveland and Devlin,  
 558 1986).

Formatted: Font: 9 pt, N

Formatted Table

Formatted: Section start:  
 Width: 27,94 cm, Height:

Formatted: Normal;Text

Formatted: Font: Not Ital

Formatted: Font: Not Ital

Formatted: Font: Not Ital

Formatted: Font: Not Ital

Formatted: Font: Not Ital

559

560

**Formatted:** Font: Italic

**Formatted:** Space After:  
spacing: Multiple 1,15 li



561 They reach their highest abundance during glacial periods, in particular at the end of MIS 2 (20 vol% at 80 cm),  
 562 Brachiopods and bivalves are completely absent during the last two interglacial periods (Fig. 3).

Formatted: Section start: New page

563 **4.56 Benthic foraminiferal assemblages**

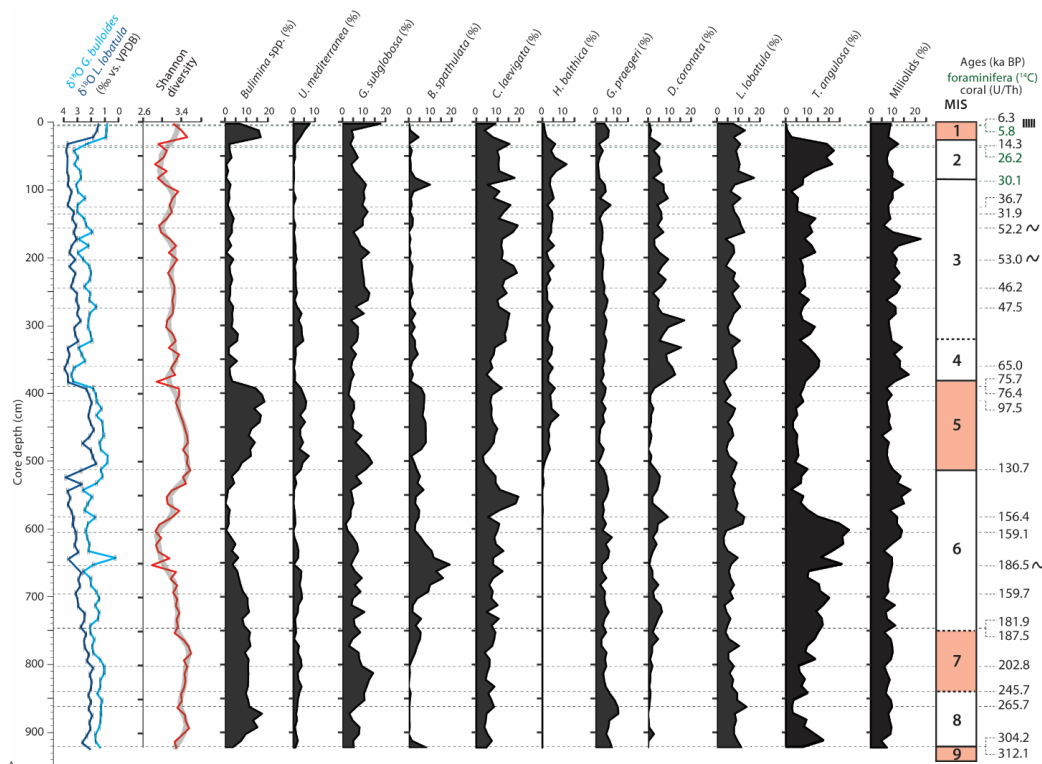
564 Shannon diversity ranges between ca. 2.8 at 652 cm and 3.6 at 782 cm (Fig. 89). High Shannon diversity values  
 565 between 3.4 and 3.6 are recorded during interglacial periods (Fig. 89). The lowest Shannon diversity values (between  
 566 2.8 and 3.0) are associated to glacial periods (Fig. 89). A total number of 166 benthic foraminifera species were  
 567 recognized (see Supplementary material). The most abundant species are *Bolivina spathulata*, *Bulimina marginata*,  
 568 *Bulimina striata*, *Cassidulina laevigata*, *D. iscanomalina coronata*, *Gavelinopsis praegeri*, *Globocassidulina*  
 569 *subglobosa*, *Hyalinea balthica*, *L. lobatula lobatula*, *Miliolinella subrotunda*, *Trifarina angulosa* and *Uvigerina*  
 570 *mediterranea* (Fig. 9).

Formatted: Font: Not Bold, Not Italic

Formatted: Font: Not Bold, Not Italic

571

Formatted: Font: Not Bold

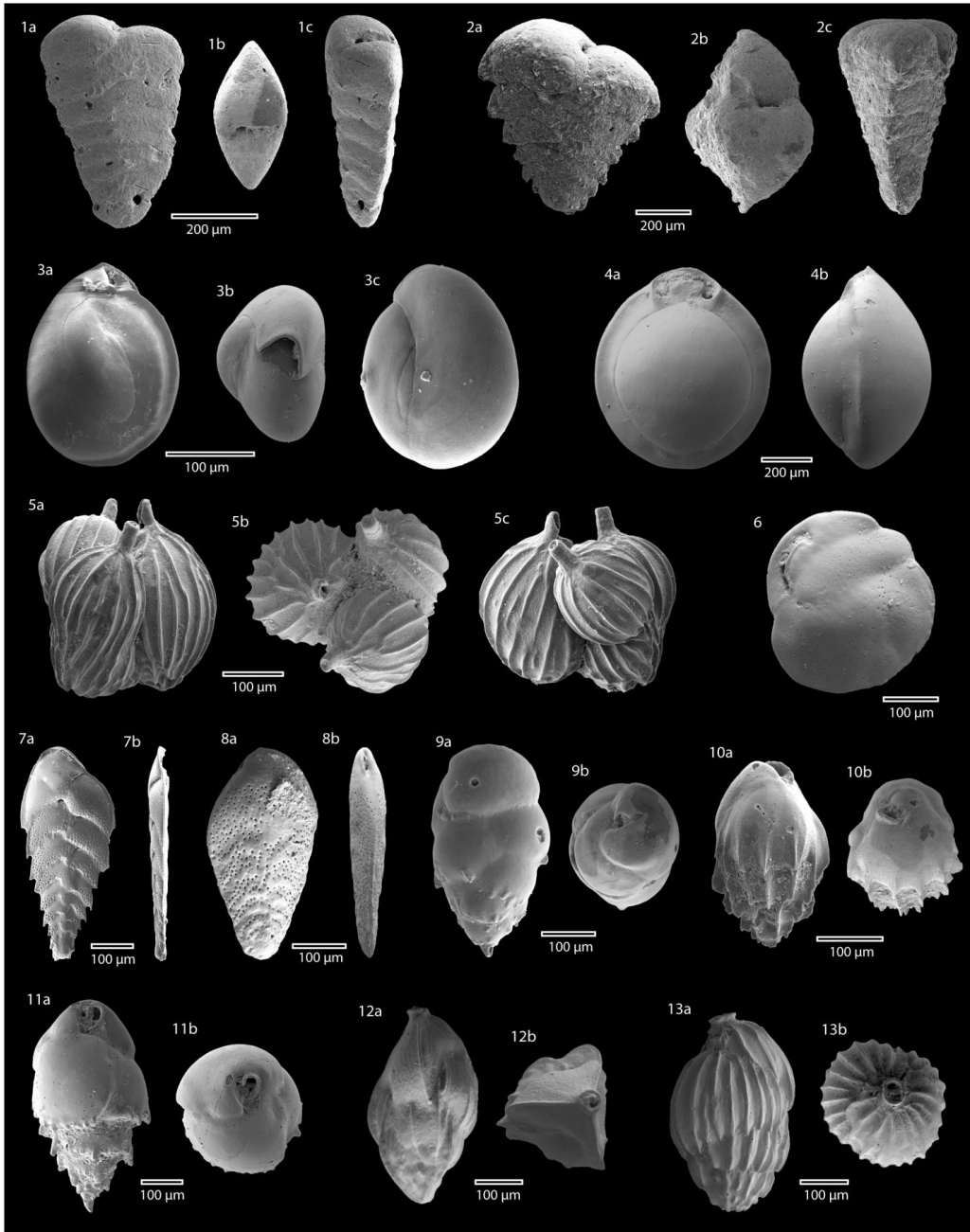


572  
 573  
 574 **Figure 9.** Distribution of main benthic foraminifera (expressed as the percentage of the total number of benthic foraminifera) and  
 575 benthic foraminiferal Shannon diversity (the overlaid grey curve corresponds to the smoothed curve). The planktonic (*G.*  
 576 *bulloides*) and benthic (*L. lobatula*)  $\delta^{18}\text{O}$  records (‰, VPDB) are provided as supporting information.

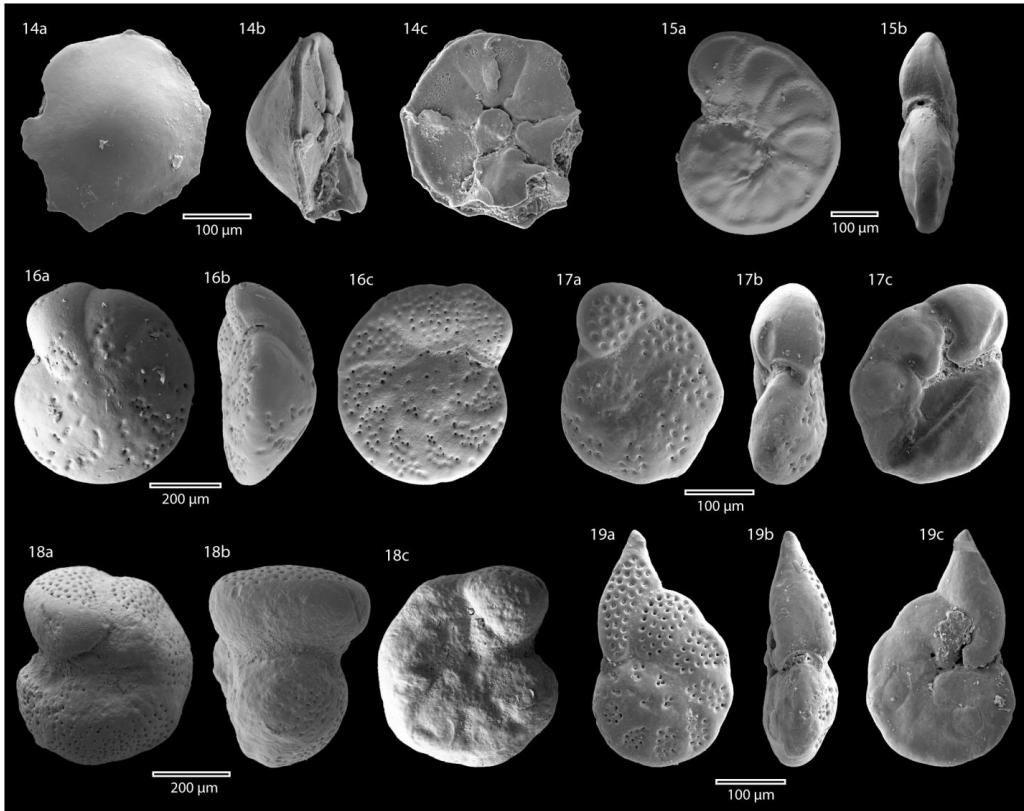
577

578 | The three Buliminid species *Bulimina- aculeata*, *B. marginata* and *B. striata* demonstrate the same distribution  
579 | trends and were thus grouped together as *Bulimina* spp. (Fig. 8). All Miliolids were grouped together for the same  
580 | reason. The species *M. subrotunda* makes up more than half of the total abundance of the Miliolid group with an  
581 | average contribution of ca. 53.4 %. The abundances of all important species are given in Figure 89. The  
582 | opportunistic infaunal *Bulimina* spp. show maximum abundances during interglacial periods (ca. 18 %) and  
583 | minimum abundances during glacial periods (ca. 2 %; Fig. 89). *U. nigerina mediterranea* follows a similar  
584 | distribution to Buliminids, with peak abundances corresponding to interglacial periods (Fig. 89). Relative to  
585 | *Bulimina* spp., *U. mediterranea*, and *G. subglobosa*, the infaunal *T. angulosa* and the epifaunal *D. coronata* are the  
586 | least abundant during the last two interglacials (between ca. 1 and 5 %), whilst they are the most abundant during  
587 | glacial periods, with peak abundances reached during MIS 4 for *D. coronata* (ca. 30 %; Fig. 89). Abundances of  
588 | Miliolids (5-22 %), *L. lobatula* (3-17 %) and *C. laevigata* (3-17 %) are relatively high throughout the entire core  
589 | (Fig. 89); although Miliolids show higher abundances during glacials (ca. 20 %). The highest numbers of *C.*  
590 | *laevigata* are recorded during glacial periods (ca. 20 %), whilst minimum abundances occur during interglacials (3 %  
591 | during MIS 5). The epifaunal *G. praegeri* is homogeneously distributed, in contrast to *H. balthica* that first appears  
592 | in the core at the onset of MIS 5, reaching maximum abundances during MIS 2 (ca. 11 %; Fig. 89). The infaunal *B.*  
593 | *spathulata* is the most abundant during MIS 6 (ca. 20 %) and reaches approximately 10 % during interglacial periods  
594 | (MIS 9, MIS 7 and MIS 5; Fig. 89).

Formatted: Justified, Space After: 0  
pt, Line spacing: 1,5 lines



Formatted Table



Formatted Table

596  
 597 **Figure 9.** Scanning electron microscope (SEM) images of characteristic benthic foraminifera from core MD13-3462G: **1.**  
 598 *Spiroplectammina wrightii* (Silvestri, 1903) a. side view, b. apertural view, c. peripheral view ; **2.** *Spirorutilus carinatus*  
 599 (Cushman, 1921) a. side view, b. apertural view, c. peripheral view ; **3.** *Miliolinella subrotunda* (Montagu, 1803) a. side view 1, b.  
 600 apertural view, c. side view 2 ; **4.** *Pyrgo anomala* (Schlumberger, 1891) a. side view, b. side view ; **5.** *Lagena* sp. (Walker and  
 601 Jacob, 1798) a. side view 1, b. apertural view, c. side view 2 ; **6.** *Cassidulina laevigata* (d'Orbigny, 1826) side view ; **7.** *Bolivina*  
 602 *alata* (Seguenza, 1862) a. lateral view, b. peripheral view ; **8.** *Bolivina spathulata* (Williamson, 1858) a. lateral view, b. peripheral  
 603 view ; **9.** *Bulimina aculeata* (d'Orbigny, 1826) a. lateral view, b. apertural view ; **10.** *Bulimina striata* (d'Orbigny, 1826) a. lateral  
 604 view, b. apertural view ; **11.** *Bulimina marginata* (d'Orbigny, 1826) a. lateral view, b. apertural view ; **12.** *Trifarina angulosa*  
 605 (Williamson, 1858) a. lateral view, b. apertural view ; **13.** *Uvigerina mediterranea* (Hofker, 1932) a. lateral view, b. apertural  
 606 view. **14.** *Gavelinopsis praegeri* (Heron-Allen and Earland, 1913) a. spiral side, b. peripheral view, c. umbilical side ; **15.**  
 607 *Hyalinea balthica* (Schröter, 1783) a. spiral side, b. peripheral view ; **16.** *Lobatula lobatula* (Walker and Jacop, 1798) a. spiral  
 608 side, b. peripheral view, c. umbilical side ; **17.** *Discanomalina vermiculata* (d'Orbigny, 1839) a. spiral side, b. peripheral view, c.  
 609 umbilical side ; **18.** *Discanomalina coronata* (Parker and Jones, 1865) a. spiral side, b. peripheral view, c. umbilical side ; **19.**  
 610 *Discanomalina japonica* (Asano, 1951) a. spiral side, b. peripheral view, c. umbilical side.

Formatted: English (U.S.)

Formatted: English (U.S.)

Formatted: English (U.S.)

Formatted: English (U.S.)

Formatted: English (U.S.)

Formatted: English (U.S.)

Formatted: English (U.S.)

Formatted: English (U.S.)

Formatted: English (U.S.)

613

## 614 5. Discussion

### 615 5.1 Build-up heterogeneity among Mediterranean coral mounds

#### 616 5.1.1 Variability of coral mound build-up within the western Mediterranean

617 Long-term coral mound formation at the location of core MD13-3462G took place during both interglacial and  
 618 glacial periods (Fig. 4B). Highest mound aggradation rates (MARs) of ca. 6 cm.kyr<sup>-1</sup> and 10 cm.kyr<sup>-1</sup> are respectively  
 619 reached during the middle of MIS 6 and MIS 3, with a short peak of 18 cm.kyr<sup>-1</sup> during MIS 3. Mound aggradation  
 620 rates (MARs) do not exceed ca. 4 cm.kyr<sup>-1</sup> during interglacial periods and range generally between 1 and 2 cm.kyr<sup>-1</sup>  
 621 (Fig. 4B). These MAR rates are comparable to inactive reefs in the Porcupine Seabight (<5 cm.kyr<sup>-1</sup>; Frank et al.,  
 622 2011) and are below the 15 cm.kyr<sup>-1</sup> threshold set by Frank et al. (2009) for active CWC reef and mound formation,  
 623 thus suggesting that CWCs did not thrive at the site of core MD13-3462G but rather developed under stressful  
 624 environmental conditions. The planktonic and benthic δ<sup>18</sup>O values recorded for the last two interglacial and glacial  
 625 periods, which demonstrate typical interglacial/glacial variations (Fig. 4; Cacho et al., 1999; Lisiecki and Raymo,  
 626 2005; Cacho et al., 2006), are a clear indication that the studied mound location demonstrates a slow albeit  
 627 continuous build-up history across this time period.

Formatted: Font color: Auto

Formatted: Heading 3

Formatted: Highlight

Formatted: Highlight

Formatted: Highlight

628

629 Mound aggradation rates (MARs) for core MD13-3462G are lower than the rates of 17 and 25 cm.kyr<sup>-1</sup> respectively  
 630 calculated for MIS 9 and 7 in the neighbouring BRI core GeoB18118-2 (Krengel, 2020) and those of 49 and 83  
 631 cm.kyr<sup>-1</sup> respectively calculated for MIS 7 and 5 in core GeoB18116-2 on Dragon Mound (Fig. 1C; Krengel,  
 632 2020). Similar to the very low mound aggradation rates (MARs) observed during MIS 5 in core MD13-3462G (ca. 2  
 633 cm.kyr<sup>-1</sup>, Fig. 4B), Krengel (2020) noticed an absence of coral mound build-up during MIS 5 on BRI. With only 9.24  
 634 m accumulated over the last ca. 300 kyr, against ca. 32 m for the same time period at the site of core GeoB18118-2  
 635 (Krengel, 2020), the overall mound aggradation at the site of core MD13-3462G is particularly low. This threefold  
 636 difference in mound aggradation may suggest that the northern part of BRI (core MD13-3462G) was submitted to  
 637 more mass wasting events and/or erosional processes than the southern area (core GeoB18118-2; Krengel, et al.,  
 638 2020), resulting as such in an overall reduced mound build-up. However, as discussed previously, the benthic and  
 639 planktonic δ<sup>18</sup>O values recorded for the last two interglacial and glacial periods, together with the absence of  
 640 erosional features downcore, allow to dismiss this hypothesis. Krengel (2020) also observed that core GeoB18118-2  
 641 was in stratigraphic order and only showed minor signs of erosional processes. MD13-3462G (this study) and  
 642 GeoB18118-1 (Krengel, 2020) are both situated on the crest of BRI at respectively 327 and 332 m depth at a distance  
 643 of ca. 1.3 km (Fig. 1C). Therefore, the observed differences in timing and rates of long-term mound build-up at BRI  
 644 are likely probably driven by local rather than regional/basin-wide environmental variability. We propose that  
 645 disparities in hydrodynamic regimes could lead to reduced food supply and/or sediment starving/low sediment input  
 646 at the northern part of the ridge where core MD13-3462G was recovered. Supplementary investigations for both

Formatted: Highlight

Formatted: Highlight

647 cores using ~~identical~~ bottom current proxies are however needed to test this hypothesis. A number of studies have  
648 demonstrated that the EMCP and West Melilla Coral Province ~~WMCP~~ experienced a rapid phase of mound build-up  
649 during the Bølling-Allerød interstadial and the early Holocene (Fink et al., 2013; Stalder et al., 2015; 2018; Wang et  
650 al., 2019; Wienberg, 2019; Fentimen et al., 2020a; Kregel, 2020) with mound aggradation rates MARs varying  
651 between 75 and 420 cm.kyr<sup>-1</sup>. Similar mound aggradation rates MARs between 44 and 203 cm.kyr<sup>-1</sup> were calculated  
652 by Corbera et al. (2021) at the CMPabliers Mound Province. However, in contrast with these observations, mound  
653 deposits recovered within core MD13-3462G do not demonstrate such a rapid build-up phase (Fig. 4B). We  
654 hypothesize that this deviation from the Alboran Bølling-Allerød/early Holocene mound build-up trend is further  
655 evidence that the coral communities situated at the northern part of BRI developed under unfavourable  
656 environmental conditions.

Formatted: Highlight

Formatted: Highlight

657  
658 In the South CMPabliers Mound Province, Corbera et al. (2021) identified four mound formation phases covering  
659 the last 4006 kyr, spread between MIS 9, 7, 6 and 5, at rates of respectively 4, 5, 3.5 and 20 cm.kyr<sup>-1</sup>; whereas long-  
660 term mound build-up at the TMCPunisian Coral Mound Province in the central Mediterranean essentially took place  
661 during MIS 2, at rates of ca. 20 cm.kyr<sup>-1</sup> (Corbera et al., 2022). These different mound build-up phases were  
662 separated by periods of mound stagnation (Corbera et al., 2021; 2022). The contrasting observations made at the  
663 CMPabliers Mound Province, Tunisian Coral Mound Province ~~MCP~~, Dragon Mound ~~M~~ and BRI (Kregel, 2020;  
664 Corbera et al., 2021, 2022, this study) suggest that, together with local discrepancies at BRI, timing of long-term  
665 mound build-up in the western and central Mediterranean is not concurrent and does not follow a clear  
666 interglacial/glacial pattern as in the North Atlantic (Dorschel et al., 2005; Rüggeberg et al., 2007; Frank et al., 2009;  
667 2011; Matos et al., 2015; 2017). The temporal distribution of western and central Mediterranean CWC mounds is  
668 rather comparable to mounds situated off the coasts of Angola and Mauritania, ~~with~~ here mound build-up ~~take~~ took  
669 place during both interglacial and glacial periods (Wienberg and Titschack, 2016; Wefing et al., 2017; Wienberg et  
670 al., 2018). Overall, the striking disparity in the timing of mound build-up across the western and central  
671 Mediterranean hints towards strong differences in regional and local environmental forcing.

Formatted: Not Highlight

### 673 5.1.2 Glacial mound build-up: a recurrent Mediterranean trend?

674 Talk about:

Formatted: Normal;Text

675 ~~—The glacial ages compared to the core studied by Kregel (heterogeneity in mound build-up)~~

676 ~~—The role of bryozoans~~

677 ~~—The glacial occurrences in the Tunisian Coral mounds~~

678 ~~—Mention the Gulf of Cadiz mounds~~

680  
681 Core MD13-3462G provides the first record of consistent coral growth during the last glacial period in the EMCP  
682 and more generally in the Alboran Sea (Fig. 3). Previous observations made by Kregel (2020) at BRI and Dragon

Formatted: Font: Not Bold, English (U.S.)

683 Mound evidence very scarce occurrences during MIS 6, with two corals dated at 145.7 and 142.5 ka at BRI and  
684 another individual dated at 171.9 ka at Dragon Mound. The Cabliers Mound Province is also characterized by an  
685 absence of CWCs during the last glacial, despite demonstrating a phase of mound build-up during MIS 6 (Corbera et  
686 al., 2021). Thus, the last glacial occurrence of CWCs in core MD13-3462G stands out, all the more so given that  
687 mound aggradation rates reach their highest values during this time (Fig. 4B). This observation contrasts with the  
688 complete absence of last glacial coral occurrences in the neighbouring core GeoB18118-1 investigated by Krengel  
689 (2020) and demonstrates once again the important heterogeneity in the timing of long-term coral mound build-up  
690 along BRI and more generally in the Alboran Sea.

Formatted: Font: Not Bold, English (U.K.)

692 Last glacial occurrences of CWCs and mound aggradation rates of 18.3-21.6 cm.kyr<sup>-1</sup> have recently been reported at  
693 the Tunisian Coral Mound Province in the central Mediterranean (Corbera et al., 2022). Coral mound formation is  
694 essentially concentrated during MIS 2 (Corbera et al., 2022), unlike at the northern part of BRI (core MD13-3462G)  
695 where the most important mound build-up phase occurred during MIS 3 (Fig. 4B). Corbera et al. (2022) argue that  
696 increased productivity was a main driver behind this MIS 2 mound formation phase. Likewise, coral growth during  
697 the last glacial has been reported from the Gulf of Cádiz and is also suggested to be promoted by increased paleo-  
698 productivity linked to strengthened aeolian dust import (Wienberg et al., 2009). Thus, coral growth during the last  
699 glacial period spans from the Gulf of Cádiz to the western (EMCP) and central (Tunisian Coral Mound Province)  
700 Mediterranean and appears to be a recurrent pattern. The benthic and planktonic foraminiferal  $\delta^{18}\text{O}$  and  $\delta^{13}\text{C}$  values  
701 from core MD13-3462G suggest that environmental conditions were particularly unstable during the last glacial  
702 period, as suggested by previous studies (Cacho et al., 2000; Martrat et al., 2004; Pérez-Folgado et al., 2004; Cacho  
703 et al., 2006; Bout-Roumzeilles et al., 2007). Moreover, high numbers of the infaunal benthic foraminifera *G.*  
704 *subglobosa* and *C. laevigata* (Fig. 8) would infer that MIS 3 was marked by phases of increased productivity  
705 (Schmiedl and Mackensen, 1997; Martins et al., 2006), hence similar to the environmental conditions during the last  
706 glacial at the Tunisian Coral Mound Province and Gulf of Cádiz coral mounds.

Formatted: Font: Not Bold, Superscript

707 In contrast with Atlantic CWC mounds with other long-term Mediterranean coral mound records (Krengel, 2020;  
708 Corbera et al., 2021; 2022), the mound deposits situated at the northern part of BRI (site MD13-3462G) mounds  
709 from the East Melilla Coral Province show a high contribution of the erect cheleistome bryozoan *B. dichotoma* (Fig.  
710 3). High abundance of this species during the Bølling-Allerød has previously been reported from the EMCP, where it  
711 reached approximately 20 % of the total macrofaunal assemblage (Stalder et al., 2015). Fentimen et al. (2020a) also  
712 documented *B. dichotoma* abundances of up to 30 % volume at the end of the last glacial period at BRI (in core  
713 MD13-3455G, see Fig. 1C). At the exception of MIS 5, the mound deposits recovered in core MD13-3462G  
714 demonstrate that *B. dichotoma* was present in numbers throughout the last 300 kyr of mound development and was  
715 particularly abundant during the last glacial (ca. 70 % volume; Fig. 3). Based on mound aggradation rates, MARS and  
716 macrofaunal content, we propose that *B. dichotoma* communities favoured mound formation at the site of core  
717 MD13-3462G BRI, noticeably during glacial periods the last glacial, by capturing fine-grained sediments in a similar  
718 way as CWCs do. As such, mounds at BRI the investigated mound deposits stand out and may be considered as a  
719 mixed *B. dichotoma*/CWC mounds framework, rather than a CWC mounds per se.

Formatted: English (U.S.)

Formatted: Font: Not Bold, Italic

Formatted: Font: Not Bold, Italic

Formatted: Font: Not Bold, Highlight



721  
722 ~~The benthic and planktonic foraminifera  $\delta^{18}\text{O}$  and  $\delta^{13}\text{C}$  values indicate that environmental conditions were~~  
723 ~~particularly unstable during the last glacial period, as suggested by previous studies (Cacho et al., 2000; Martrat et~~  
724 ~~al., 2004; Pérez Folgado et al., 2004; Cacho et al., 2006; Bout Roumazielles et al., 2007). The last glacial shows a~~  
725 ~~strong variability in macrofaunal and benthic foraminiferal assemblages. Maximum coral content is reached during~~  
726 ~~MIS 3 (Fig. 3) and is associated to higher numbers of *G. subglobosa* and *C. laevigata* (Fig. 8). These observations~~  
727 ~~suggest that corals and the benthic foraminiferal community positively responded to short phases of increased~~  
728 ~~surface productivity during MIS 3. This is supported by observations made by Rogerson et al. (2018), who~~  
729 ~~documented more humid conditions during MIS 3 in comparison to the more arid MIS 4 and 2. Humid conditions~~  
730 ~~would hence have promoted coral proliferation through increased fluvial input at BRI, in the same way as during~~  
731 ~~interglacial periods (section 5.2). Nevertheless, the dominance of *G. subglobosa* coupled to the absence of *Bulimina*~~  
732 ~~spp. and *U. mediterranea* suggests that conditions were less eutrophic than during peak interglacial periods and that~~  
733 ~~the organic matter reaching the seafloor may have been less degraded.~~

734

### 735 ~~5.1.3 Oceanographic change after the last two interglacial/glacial periods~~

736 ~~the shift at MIS6/MIS7 as noticed by Krengel (2020) nBWT does not follow SST values after the end of MIS6~~

737

738

Formatted: Font color: Accent 6

Formatted: Normal;Text

### 739 ~~5.2.4 Environmental controls on coral proliferation during the last two interglacial periods-glacial cycles~~

#### 740 ~~5.2.1.1 High food availability associated to humid continental conditions~~

##### 741 ~~Discuss Sapropel events~~

742

743 During interglacial periods, benthic foraminiferal assemblages at BRI are marked by high abundances of the infaunal  
744 *Bulimina* spp., *U. mediterranea* and to a lesser extent *B. spathulata*. Several authors describe *Bulimina* spp. as  
745 characteristic for eutrophic and dysoxic environments (Phleger and Soutar, 1973; Lutze and Coulbourn, 1984;  
746 Jorissen, 1987; Schmiedl et al., 2000). In the Mediterranean Sea, they are dominant in the vicinity of the Po river  
747 delta in the North Adriatic Sea and close to the Rhône River delta (Jorissen, 1987; Mojtahid et al., 2009). The  
748 shallow infaunal *U. mediterranea* and the opportunistic *B. spathulata* are known to demonstrate a positive  
749 correlation with organic matter flux (De Rijk et al., 2000; Schmiedl et al., 2000; Fontanier et al., 2002; 2003; Drinia  
750 and Dermitzakis, 2010). Moreover, *Bulimina* spp. and *U. mediterranea* are reported to be able to feed on fresh but  
751 also more refractory organic matter (De Rijk et al., 2000; Koho et al., 2008; Dessandier et al., 2016). Based on these  
752 observations, the benthic foraminiferal assemblage during interglacials would support a high organic matter export to  
753 the seafloor. The overall higher TOC levels during interglacials confirm that the sediment during these periods was  
754 relatively enriched in organic matter in comparison to glacial periods (Fig. 5). High abundance of the shallow

Formatted: Font: Not Bold, Font color: Accent 6

Formatted: Font color: Accent 6

Formatted: Normal;Text

755 infaunal *G. subglobosa* has been linked to the deposition of fresh phytodetritus on the seafloor after bloom events  
756 (Gooday, 1993; Fariduddin and Loubere, 1997; Suhr et al., 2003; Sun et al., 2006). It is typically found in high  
757 energy (e.g. steep flanks, ridges) and well-oxygenated environments (Mackensen et al., 1995; Milker et al., 2009),  
758 and is a common taxon of the Alboran Platform and of CWC environments (Margreth et al., 2009; Milker et al.,  
759 2009; Spezzaferri et al., 2014). Mackensen et al. (1995) noted that *G. subglobosa* dominated in areas of the South  
760 Atlantic Ocean where the organic carbon flux did not exceed  $1 \text{ g.m}^{-2}.\text{yr}^{-1}$ . In contrast, in the Mediterranean Sea, *B.*  
761 *marginata* is restricted to sites with an organic carbon flux  $>2.5 \text{ g.m}^{-2}.\text{yr}^{-1}$ , whilst *B. aculeata* is associated to a flux  
762 of  $3 \text{ g.m}^{-2}.\text{yr}^{-1}$  (De Rijk et al., 2000). The last two interglacials (MIS 7 and MIS 5) are marked by an increased  
763 abundance of *G. subglobosa* at early stages followed by a general decline. Buliminids follow a converse trend,  
764 particularly during MIS 5, with lower abundances at early stages (Fig. 89). This suggests that conditions during the  
765 later stages of interglacials became increasingly eutrophic and in turn less oxygenated at the sediment/water  
766 interface, as the consumption of organic matter led to oxygen depletion. These more environmentally stressful  
767 conditions resulted in decreased foraminiferal diversity and a proliferation of opportunistic taxa (Fig. 89). Overall  
768 ~~Indeed the~~ lower abundances of Miliolids, which are typically found in well-oxygenated environments (Murray,  
769 2006), further confirm eutrophication coupled to lower oxygenation at the seafloor during interglacials, specifically  
770 towards the end of ~~interglacials such periods~~ (Fig. 89). ~~Yet, the absence of deep infaunal benthic foraminifera (e.g.~~  
771 ~~*Chilostomella* spp. or *Globobulimina* spp.) implies that seafloor oxygenation was never at a minimum, such as~~  
772 ~~during the restricted intervals prior and after sapropel events in the eastern Mediterranean (Jorissen, 1999; Schmiedl~~  
773 ~~et al., 2003).~~

774  
775 Schmiedl et al. (2010) link the high abundance of *U. mediterranea* in the Aegean Sea to humid climatic conditions  
776 and increased river runoff. Increased fluvial input has been widely linked in the eastern Mediterranean to more  
777 humid continental conditions during interglacial times in response to a northern shift of the African monsoon (e.g.,  
778 Gasse, 2000; Gasse and Roberts, 2005; Osborne et al., 2008; Coulthard et al., 2013). In contrast, the Alboran Sea lies  
779 below the maximum Inter-Tropical Convergence Zone northward position and is sheltered by the Atlas Mountain  
780 chain (Rohling et al., 2002; Tuenter et al., 2003; Lavaysse et al., 2009). Modern-day observations show that rainfall  
781 over the northwest Atlas Mountains is generally associated to baroclinic activity over the North Atlantic (Knippertz  
782 et al., 2003; Braun et al., 2019). The south of the Atlas Mountains has one of the highest cyclonic activities in the  
783 Mediterranean borderlands, whilst the largest fraction of cyclones entering the Mediterranean Sea arrives from the  
784 Atlantic (Lionello et al., 2016). Pasquier et al. (2018) noticed that periods of increased input of organic matter from  
785 sediment-laden rivers occur during warm substages of the last 200 kyr. These authors relate these pluvial events to  
786 negative North Atlantic Oscillation-like conditions (Pasquier et al., 2018). The ~~EMCPast Melilla-Coral Province~~  
787 is located 50 km away from the mouth of the Moulouya River which takes its source in the High Atlas Mountains  
788 (Snousi, 2004; Emelyanov and Shimkus, 2012; Tekken and Kropp, 2012). The basin of the Moulouya River covers  
789 approximately  $54,000 \text{ km}^2$ , hence representing the largest river basin in Northwest Africa (Emelyanov and Shimkus,  
790 2012; Tekken and Kropp, 2012). We propose that the influence of warm and moist Atlantic air masses during  
791 interglacial periods promoted warmer and more humid conditions over Northwest Africa and torrential rainfall. This  
792 would have led to a strengthening of the Moulouya River's flow rate, hence triggering episodes of important

793 terrestrial organic matter input at BRI (Fig. 6). These events may have in turn caused eutrophication and oxygen  
794 depletion at the seafloor, compatible with the observed benthic foraminiferal assemblages (Fig. 89).

796 In addition, the variations in the ventilation of the eastern Mediterranean Sea and the formation of LIW may also  
797 drive the observed benthic foraminiferal assemblages and reduced mound aggradation rates during interglacial  
798 periods. Indeed, Stalder et al. (2015) reported at the EMCP a benthic foraminiferal assemblage of similar  
799 composition as the interglacial benthic foraminiferal community within core MD13-3462G. The assemblage  
800 described by Stalder et al. (2015) also demonstrates a high abundance of *B. marginata*, *B. aculeata* and *C. laevigata*.  
801 It coincides with periods of *D. pertusum* absence and the deposition of sapropel S1 in the eastern Mediterranean,  
802 hence suggesting that sapropel-related perturbations to the thermohaline circulation triggered oxygen depletion at the  
803 seafloor. Sapropel events have also been shown to be concurrent with coral demise in the Cabliers Mound Province,  
804 at least since sapropel 7 at the end of MIS 7 (Corbera et al., 2021), and in the southern Adriatic Sea (Taviani et al.,  
805 2019). During sapropel events, water column stratification in the eastern Mediterranean led to a dwindling of LIW  
806 formation and consequently it's reduced circulation in the West Mediterranean Basin (Toucanne et al., 2012; Bahr et  
807 al., 2015; Filippidi et al., 2016). Similar to the Cabliers Mound Province (Corbera et al., 2021) and as suggested by  
808 benthic foraminiferal assemblages, oxygen depletion linked to reduced LIW circulation and important organic matter  
809 input may have resulted in unfavourable and stressful environment conditions for coral growth during interglacial  
810 periods, hence ~~Despite possible dysoxic conditions during interglacial periods~~ explaining the low MARs recorded  
811 within core MD13-3462G – coral mound build-up appears not to have been hampered during interglacial periods  
812 would have hampered coral proliferation, as suggested by the low mound aggradation rates (Fig. 4).

813 ~~However, dysoxic conditions may have been limited to the sediment, thus only affecting foraminiferal communities~~  
814 ~~and not fully preventing colonial corals living above the sediment surface to develop. Such vertical decoupling~~  
815 ~~between sediment and pelagic ecosystems has previously been observed in modern Norwegian CWC reefs~~  
816 ~~(Wehrmann et al., 2009). Such tolerance of CWC reefs to hypoxic conditions has been observed off the coasts of~~  
817 ~~Angola and Namibia (Tamborrino et al., 2019; Hebbeln et al., 2020; Orejas et al., 2021). Overall, high food~~  
818 ~~availability triggered by increased fluvial discharge appears to be a decisive parameter governing coral proliferation~~  
819 ~~at BRI.~~

821 ~~Talk about the influence of sapropels – state that there is no deep infaunal species suggesting an absence of truly~~  
822 ~~sapropel-like conditions.~~

#### 824 **5.21.2 Enhanced surface and intermediate water mass mixing**

825 During interglacial periods, the high sea level and the increased evaporation in the Mediterranean ~~leads~~lead to a more  
826 important inflow of low salinity MAW through the Strait of Gibraltar (Sierro et al., 2005). Thus, surface waters in  
827 the Alboran Sea are, in comparison to glacial periods, warmer and less dense. This is also noticed in the planktonic  
828  $\delta^{18}\text{O}$  record (Fig. 3). The enhanced MAW flow during interglacials triggers stronger Western and Eastern Alboran

Formatted: Font: Not Bold, Italic

Formatted: Font: Not Bold, Italic

Formatted: Font: Not Bold, Italic

Formatted: Font: Not Bold, Italic

Formatted: Font: Not Bold, Font color: Accent 6

Formatted: Normal;Text

Formatted: Normal;Text

829 Gyres, resulting in better mixing and downwelling. Knowing that the Banc des Provençaux and BRI are situated at  
830 relatively shallow water depths and in the path of the westward circulating branch of the Eastern Alboran Gyre  
831 (Lanoix, 1974; Viúdez and Tintoré, 1995; Fig. 10), and that mixing between surface and intermediate water masses  
832 is documented to occur down to ca. 300 m water depth (Heburn and La Violette, 1990), it is conceivable that the  
833 corals living currently at 327 m depth were bathed by, or situated at the limit of mixing between surface and  
834 intermediate water masses during interglacial periods. Wang et al. (2019) suggest that the same phenomenon  
835 occurred during the Bølling–Allerød interstadial and the eEarly Holocene. Higher input of MAW into the Alboran  
836 Sea would lead to an increased contribution of surface waters to ~~intermediate water masses (LIWShW)~~, (Fig. 2 and  
837 10) and a deepening of the pycnocline. This would promote the formation of internal waves and increase turbulence  
838 at the seafloor of BRI, as suggested by the slightly higher  $\overline{SS}$  values ~~during at the end of~~ interglacials (Fig. 5), and  
839 would have favoured coral proliferation by increasing lateral nutrient supply (Fig. 10). A better mixing of surface  
840 and intermediate water masses is suggested by the decreased  $\Delta^{13}C$  and  $\Delta^{18}O$  during the last two interglacial periods  
841 (Fig. 5). We suggest that increased food availability during interglacial periods may have enabled coral communities  
842 to develop despite oxygen-depleted seafloor conditions, in the same way as in the oxygen minimum zones on the  
843 Angolan and Namibian margins (Hanz et al., 2019). These conditions would have however been detrimental for  
844 bryozoan communities.

Formatted: Font: 10 pt

Formatted: Font: 10 pt

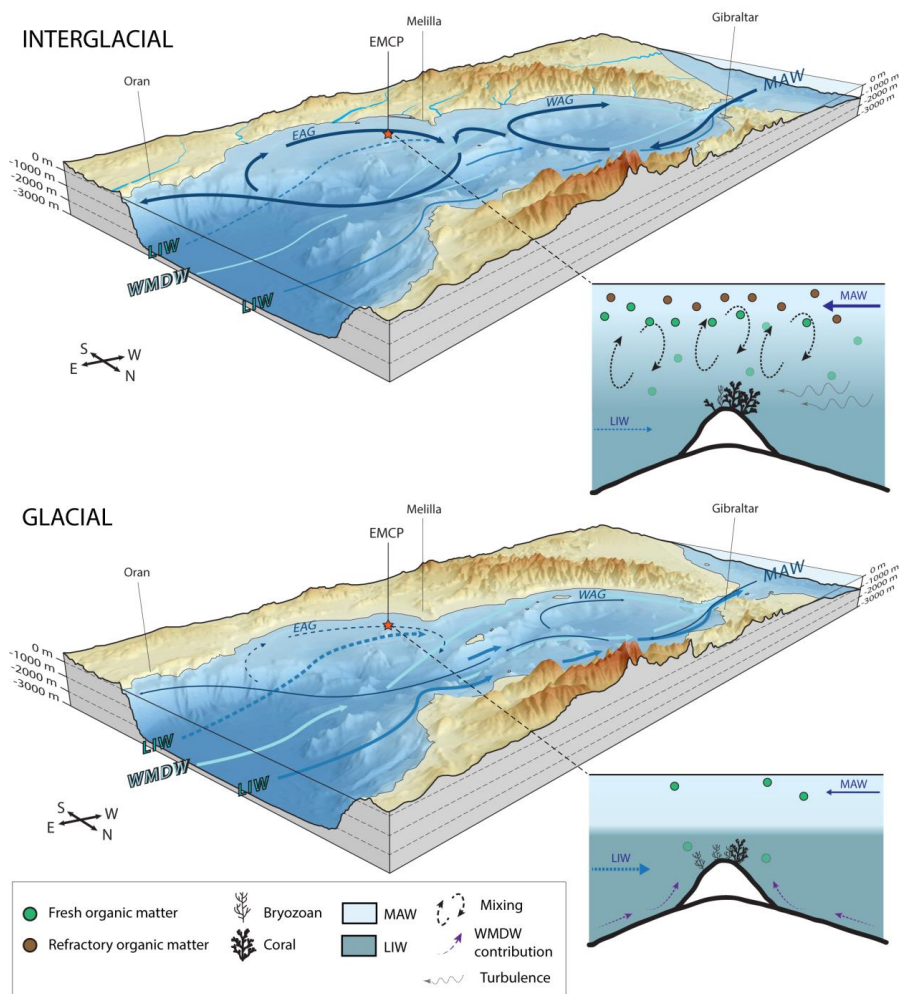
845 ~~The slight offset between planktonic and benthic  $\delta^{13}C$  records towards the end of MIS 7 and MIS 5 (Fig. 5) indicate  
846 that water masses were becoming more stratified towards the end of interglacials and that the contribution of MAW  
847 to intermediate water masses was hence possibly decreasing. Maximum *Bulimina* spp. abundance, minimum *G.*  
848 *subglobosa* abundance, and decreasing benthic foraminiferal diversity may suggest that reduced mixing, in  
849 concomitance with important fluvial discharge (section 5.1.1) led to oxygen depletion at the seafloor at the transition  
850 between interglacial and glacial periods. Severe oxygen depletion may explain the decline of corals at the transition  
851 from interglacial to glacial periods.~~

### 852 5.1.3 Variability of cold water coral mound formation between interglacial periods

Formatted: Normal,Text

853 Highest coral content is reached during MIS 5 and corresponds to a maximum in *Buliminid* abundance. The Al  
854 normalized elemental ratios suggest that terrestrial input was stable during MIS 5 (Fig. 5). These stable conditions  
855 would have favoured a long lasting coral proliferation dominated by the selenactinian *D. pertusum* (Fig. 3). Marine  
856 Isotope Stage 9 and 7 are also dominated by *D. pertusum*. Although MIS 7 is poorly constrained, Al normalized  
857 elemental ratios would indicate that this time period was more unstable than the previous interglacial period (Fig. 5).  
858 The late Holocene is marked by a decrease in coral abundance and a dominance of *M. oculata* over *D. pertusum*. The  
859 coral fragment at the top of core MD13-2462G has an age of 6.3 ka. Fink et al. (2013) obtained ages from surface  
860 coral fragments at BRI that were generally between 2.7 and 3.1 ka, whilst Stalder et al. (2015) reported an age of 5.4  
861 ka for a surface coral fragment sampled at BRI. Similar ages of between 3.5 and 5.8 ka were obtained on surface  
862 coral fragments at the Western Melilla Coral Province (Wang et al. 2019). Dominance of the coral *M. oculata* during  
863 the Late Holocene was also observed at BRI by Stalder et al. (2015), whilst Wienberg (2019) reported that *M.*  
864 *oculata* already became the dominant coral species during the mid Holocene. Previous observations suggest that *M.*  
865 *oculata* is more tolerant to environmental stress than *D. pertusum* (e.g., Wienberg et al., 2009; Stalder et al., 2015).

866 Thus, the dominance of *M. oculata* at the top of the core would indicate that conditions during the late Holocene  
 867 were becoming increasingly unsuitable for coral proliferation, particularly for *D. pertusum*. This is consistent with  
 868 modern day seafloor observations that report a near absence of CWCs at BRI (Hobbelen et al., 2019). These  
 869 combined results point to unfavourable conditions for coral proliferation during the late Holocene, as suggested by  
 870 Fink et al. (2013), Stalder et al. (2015; 2018) and Wang et al. (2019). The recent decline of CWCs at the Eastern and  
 871 Western Melilla Coral



872  
 873  
 874 **Figure 10.** Three dimensional diagrams and schematic models illustrating the differences between interglacial and glacial periods  
 875 and the response of the benthic community at Brittlestar Ridge I. Water masses discussed in the text are illustrated (MAW:  
 876 Modified Atlantic Water, LIW: Levantine Intermediate Water, ~~ShW: Shelf Water~~; WMDW: Western Mediterranean Deep Water)  
 877 as well as the Western Alboran Gyre (WAG) and Eastern Alboran Gyre (EAG). The flow strength of each water mass is depicted

878 by the thickness of the arrows. The red star indicates the location of the East Melilla Coral Province. The position of the EAG and  
879 WAG is based on observations made by Lanoix (1974), La Violette (1983), and Viúdez and Tintoré (1995). Sea level of  
880 interglacial periods corresponds to the current sea level, whilst a 100 m lower sea level stand, following observations made by  
881 Rabineau et al. (2006), illustrates glacial periods. The LIW, ShW and WMDW flows follow the observations made by Ereilla et  
882 al. (2016). They have been simplified and thus do not represent their exact dynamics. The schematic models are not to scale,  
883 although relative depth limits between MAW and LIW have been respected. GEBCO\_2019 gridded bathymetric data was used to  
884 construct the diagrams.

885  
886 ~~Provinces may be linked to the establishment of more arid conditions over North Africa ca. 4 ka ago (Gasse, 2000~~  
887 ~~and references therein; Shanahan et al., 2015). The fluctuations in coral and bryozoan abundances between the~~  
888 ~~different interglacial periods may be caused by the influence of alternating dry and humid conditions.~~

## 889 **5.32 Environmental conditions during the last two glacial periods**

### 890 **5.32.1 Arid continental conditions and reduced bottom currents**

891 At the exception of MIS 8, for which the boundaries are poorly defined, glacial periods are marked by a change in  
892 macrofaunal composition with lower coral and higher bryozoan content in comparison to interglacial periods (Fig.  
893 3). This higher bryozoan content at BRI is in tune with previous observations made at the Great Australian Bight,  
894 where bryozoan proliferation during glacial periods promoted the formation of mounds (James et al., 2000; Holbourn  
895 et al., 2002). ~~Higher bryozoan content during glacials at BRI is in tune with observations made at the Great Australian~~  
896 ~~Bight, where lower temperatures, lower sea level stand, and increased upwelling probably promoted bryozoan~~  
897 ~~proliferation during glacial periods (James et al., 2000; Holbourn et al., 2002).~~ Conversely, higher temperatures and  
898 downwelling during interglacials halted bryozoan extension at the Great Australian Bight (James et al., 2000;  
899 Holbourn et al., 2002). Rigid erect branching bryozoans such as *B. dichotoma* are known to be fragile, and hence to  
900 prefer low energy environments, being unable to withstand strong bottom currents and turbulence (Scholz and  
901 Hillmer, 1995; Bjerager and Surlyk, 2007). Eutrophic environments dominated by infaunal benthic foraminifera (e.g.  
902 *Bulimina* spp.) are unfavourable for erect bryozoans, due to the high concentration of suspended food particles  
903 clogging up their feeding apparatus (Holbourn et al., 2002). Low  $\overline{SS}$  values and reduced TOC content in the sediment  
904 confirm that glacial periods were marked by weaker bottom current velocities and organic matter flux (Fig. 5). The  
905 presence of brachiopod/bivalve layers dominated by the brachiopod *Gryphus G. vitreus* also characterizes the glacial  
906 macrofauna (Fig. 3). This species is found between 160 and 250 m depth along the Mediterranean continental margin  
907 and thrives in areas dominated by moderate bottom currents (Emig and Arnaud, 1988). Thus, this species' co-  
908 occurrence with bryozoans confirms that variations in sea level stand, hydrodynamics and trophic conditions govern  
909 the change in macrofaunal dominance at BRI. Low organic matter flux during glacial periods has been related to  
910 predominantly arid conditions over North Africa, in association with a weak North African monsoon (Gasse, 2000;  
911 Sierro et al., 2005). ~~Such arid conditions led to the complete or severe desiccation of major African lakes during the~~  
912 ~~last glacial, such as Lake Victoria (Talbot and Livingstone, 1989; Johnson, 1996).~~

913  
13

914 The reduced precipitation and retreat of vegetation would have ~~led triggered to~~ a dwindling of terrestrial input during  
915 the last glacial period at BRI, as evidenced by generally lower Si/Al elemental ratio (Fig. 5).

916  
917 Glacial benthic foraminiferal assemblages are characterized by the dominance of large epibenthic suspension feeding  
918 foraminifera, such as *L. lobatula* and *D. coronata*, together with the infaunal *C. laevigata* (Fig. 89). This follows  
919 observations made by Stalder et al. (2018) who noticed increased abundances of *Cibicides* spp., *D. coronata* and *C.*  
920 *laevigata* during glacial periods at BRI. These species share a preference for high quality fresh marine organic matter  
921 (De Rijk et al., 2000; Milker et al., 2009, Stalder et al., 2018). *Lobatula lobatula* and *D. coronata* have been  
922 described to prefer oxygen-rich bottom waters (Linke and Lutze; 1993; Margreth et al., 2009), ~~whilst~~ In the Arctic  
923 basins and Norwegian-Greenland Sea, the dominance of the epibenthic *Cibicides wuellerstorfi* (a relative of *L.*  
924 *lobatula*) reflects a relative low flux of organic matter (Linke and Lutze; 1993) as (This species tolerates vertical flux  
925 rates  $< 2 \text{ g.cm}^{-2}.\text{yr}^{-1}$  (Altenbach, 1989). following Milker et al. (2009), high abundances of *C. laevigata* could be  
926 related to the presence of fine grained material in the western Mediterranean. In the Arctic basins and Norwegian-  
927 Greenland Sea, the dominance of the epibenthic *Cibicides wuellerstorfi* (a relative of *L. lobatula*) reflects a relative  
928 low flux of organic matter (Linke and Lutze; 1993). This species tolerates vertical flux rates  $< 2 \text{ g.cm}^{-2}.\text{yr}^{-1}$   
929 (Altenbach, 1989). The dominance of *L. lobatula*, *D. coronata*, *C. laevigata* and Miliolids would thus indicate that  
930 the seafloor during glacial periods received less but higher quality organic matter and became more oxygenated in  
931 response to the stronger influence of intermediate and deep-water masses (Fig. 10). These observations suggest that  
932 more arid conditions during glacial periods led to a reduced influence of terrestrial input on benthic communities  
933 (Fig. 10). We propose that weaker but comparatively fresher organic matter input favoured-allowed the development  
934 of CWC communities, particularly during the last glacial period, and the bryozoan *B. dichotoma*. This assumption is  
935 supported by experimental observations demonstrating how erect bryozoans feed essentially on diatoms and that  
936 suspension feeding foraminifera use the same food sources (Winston, 1977; 1981; Best and Thorpe, 1994; Goldstein,  
937 1999). ~~Lower nutrient input appears in contrast to have been detrimental for coral proliferation but would not have~~  
938 ~~led to their complete disappearance (Fig. 5 and 10).~~ It can be hypothesized that there may exist a threshold in the  
939 quality and quantity of organic matter determining which of *D. pertusum* or *B. dichotoma* dominates the benthic  
940 environment at BRI.

941  
942 **5.32.2 Increased stratification and deep water overturning**

943 ~~As highlighted previously, the dominant macrofauna and low  $\overline{SS}$  values (Fig. 3 and 5) during glacial intervals at BRI~~  
944 ~~indicate weaker bottom currents.~~ Wang et al. (2019) relate low off mound  $\overline{SS}$  and high benthic foraminiferal  $\delta^{13}\text{C}$   
945 values at BRI during glacials to a dominant influence of MAW coinciding with a low sea level stand. However,  
946 whilst the benthic foraminiferal  $\delta^{13}\text{C}$  values from core MD13-3462G are indeed relatively high during glacial  
947 periods, the planktonic foraminiferal  $\delta^{13}\text{C}$  values do not follow the same trend (Fig. 5). The ~~decoupling between the~~  
948 ~~planktonic and benthic  $\delta^{13}\text{C}$  records overall low  $\Delta^{13}\text{C}$  values~~ during the two last glacial periods, noticeably during  
949 MIS 4, suggests that water mass stratification was greater than during interglacial periods and that the seafloor was

Formatted: Font: Not Bold, Superscript



950 not under the direct influence of surface MAW. During glacial periods, the flow of MAW was reduced due to lower  
951 sea level and the reduced evaporation over the Mediterranean (Sierro et al., 2005). This would have reduced the  
952 contribution of MAW to LIWShW and weakened Western and Eastern Alboran Gyres, which would have in turn led  
953 to less mixing between surface and intermediate water masses, whilst conversely increasing stratification (Fig. 10).

954  
955 Modern observations show that recently formed dense waters do not necessarily reach the deep western  
956 Mediterranean but may, in contrast, be located at intermediate water depths, above 1500 m depth (Sparnocchia et al.,  
957 1995; Millot, 1999; Ercilla et al., 2016). Ercilla et al. (2016) further exposed that WMDW can be identified at depths  
958 shallower than 500 m depth along the Moroccan margin and that it contributes to the overlying LIWShW, whilst  
959 deep water overturning and ventilation peaked during MIS 2 (Cacho et al., 2006; Toucanne et al., 2012). Increased  
960 oxygenation of the seafloor, as evidenced by the benthic foraminiferal assemblage (Fig. 98), may suggest that the  
961 contribution of well-ventilated deep and intermediate water masses at BRI was more important during glacials than  
962 during interglacials (Fig. 10). The physical shape and structure of BRI possibly plays a role in the shoaling of deep  
963 waters during glacial periods. In addition, the overall heavier-higher benthic  $\delta^{13}\text{C}$  values record and the  
964 abundance of fresh organic matter feeding foraminifera (*L. lobatula* and *D. coronata*) during glacial periods could  
965 indicate that these waters were also nutrient-rich. Although stratification between surface and intermediate water  
966 masses was greater during glacials, the stronger flow of well-ventilated WMDW at BRI would explain the higher  
967 oxygen availability at the seafloor. Overall during glacial periods, and in particular during the LGM, enhanced  
968 contribution of food-nutrition-rich and well-ventilated WMDW to overlying LIWShW, coupled to reduced terrestrial  
969 input and turbulence, would have promoted mound aggradation bryozoan proliferation (Fig. 10).

Formatted: Font: Not Bold,  
Superscript

### 970 5.2.3 Fluctuating environmental conditions during the last glacial period

971 ~~The benthic and planktonic foraminifera  $\delta^{18}\text{O}$  and  $\delta^{13}\text{C}$  values indicate that environmental conditions were~~  
972 ~~particularly unstable during the last glacial period, as suggested by previous studies (Cacho et al., 2000; Martrat et~~  
973 ~~al., 2004; Pérez Folgado et al., 2004; Cacho et al., 2006; Bout Roumazielles et al., 2007). The last glacial shows a~~  
974 ~~strong variability in macrofaunal and benthic foraminiferal assemblages. Maximum coral content is reached during~~  
975 ~~MIS 3 (Fig. 3). This increased coral content is associated to higher numbers of *G. subglobosa* and *C. laevigata*,~~  
976 ~~together with phases of higher Rb/Al elemental ratios (Fig. 5 and 9). These observations suggest that corals and the~~  
977 ~~benthic foraminiferal community positively responded to short phases of increased surface productivity related to~~  
978 ~~important continental runoff during MIS 3, as indicated by the high coral aggradation rates (Fig. 4B). This is~~  
979 ~~supported by observations made by Rogerson et al. (2018), who documented more humid conditions during MIS 3 in~~  
980 ~~comparison to the more arid MIS 4 and 2. Humid conditions would hence have promoted coral proliferation through~~  
981 ~~increased fluvial input at BRI, in the same way as during interglacial periods (section 6.1). Nevertheless, the~~  
982 ~~dominance of *G. subglobosa* coupled to the absence of *Bulimina* spp. and *U. mediterranea* suggests that conditions~~  
983 ~~were less eutrophic than during peak interglacial periods and that the organic matter reaching the seafloor may have~~  
984 ~~been less degraded.~~

985



986 5.3 Long term Differences build up heterogeneity between among Southeast Mediterranean Alboran and  
987 North Atlantic coral mound formations

988 5.3.1 Variability of coral mound build up within the western Mediterranean

989 Talk about the shift at MIS6/MIS7 as noticed by Krenzel (2020).

Formatted: Normal;Text

991 5.1.3 Variability of cold water coral mound formation between interglacial periods

992 Highest coral content is reached during MIS 5 and corresponds to a maximum in Buliminid abundance. The Al-  
993 normalized elemental ratios suggest that terrestrial input was stable during MIS 5 (Fig. 5). These stable conditions  
994 would have favoured a long lasting coral proliferation dominated by the scleractinian *D. pertusum* (Fig. 3). Marine  
995 Isotope Stage 9 and 7 are also dominated by *D. pertusum*. Although MIS 7 is poorly constrained, Al normalized  
996 elemental ratios would indicate that this time period was more unstable than the previous interglacial period (Fig. 5).  
997 The late Holocene is marked by a decrease in coral abundance and a dominance of *M. oculata* over *D. pertusum*. The  
998 coral fragment at the top of core MD13\_3462G has an age of 6.3 ka. Fink et al. (2013) obtained ages from surface  
999 coral fragments at BRI that were generally between 2.7 and 3.1 ka, whilst Stalder et al. (2015) reported an age of 5.4  
1000 ka for a surface coral fragment sampled at BRI. Similar ages of between 3.5 and 5.8 ka were obtained on surface  
1001 coral fragments at the Western Melilla Coral Province (Wang et al. 2019). Dominance of the coral *M. oculata* during  
1002 the Late Holocene was also observed at BRI by Stalder et al. (2015), whilst Wienberg (2019) reported that *M.*  
1003 *oculata* already became the dominant coral species during the mid Holocene. Previous observations suggest that *M.*  
1004 *oculata* is more tolerant to environmental stress than *D. pertusum* (e.g., Wienberg et al., 2009; Stalder et al., 2015).  
1005 Thus, the dominance of *M. oculata* at the top of the core would indicate that conditions during the late Holocene  
1006 were becoming increasingly unsuitable for coral proliferation, particularly for *D. pertusum*. This is consistent with  
1007 modern day seafloor observations that report a near absence of CWCs at BRI (Hebbeln et al., 2019). These  
1008 combined results point to unfavourable conditions for coral proliferation during the late Holocene, as suggested by  
1009 Fink et al. (2013), Stalder et al. (2015; 2018) and Wang et al. (2019). The recent decline of CWCs at the Eastern and  
1010 Western Melilla Coral Provinces may be linked to the establishment of more arid conditions over North Africa ca. 4  
1011 ka ago (Gasse, 2000 and references therein; Shanahan et al., 2015). The fluctuations in coral and bryozoan  
1012 abundances between the different interglacial periods may be caused by the influence of alternating dry and humid  
1013 conditions.

Formatted: Normal;Text

1016 5.3.2 Glacial mound build up: a recurrent Mediterranean trend?

1017

1018 ~~The benthic and planktonic foraminifera  $\delta^{18}\text{O}$  and  $\delta^{13}\text{C}$  values indicate that environmental conditions were~~  
1019 ~~particularly unstable during the last glacial period, as suggested by previous studies (Cacho et al., 2000; Martrat et~~  
1020 ~~al., 2004; Pérez-Folgado et al., 2004; Cacho et al., 2006; Bout-Roumazielles et al., 2007). The last glacial shows a~~  
1021 ~~strong variability in macrofaunal and benthic foraminiferal assemblages. Maximum coral content is reached during~~  
1022 ~~MIS 3 (Fig. 3). This increased coral content is associated to higher numbers of *G. subglobosa* and *C. laevigata*,~~  
1023 ~~together with phases of higher Rb/Al elemental ratios (Fig. 5 and 8). These observations suggest that corals and the~~  
1024 ~~benthic foraminiferal community positively responded to short phases of increased surface productivity related to~~  
1025 ~~important continental runoff during MIS 3, as indicated by the high coral aggradation rates (Fig. 4B). This is~~  
1026 ~~supported by observations made by Rogerson et al. (2018), who documented more humid conditions during MIS 3 in~~  
1027 ~~comparison to the more arid MIS 4 and 2. Humid conditions would hence have promoted coral proliferation through~~  
1028 ~~increased fluvial input at BRI, in the same way as during interglacial periods (section 6.1). Nevertheless, the~~  
1029 ~~dominance of *G. subglobosa* coupled to the absence of *Bulimina* spp. and *U. mediterranea* suggests that conditions~~  
1030 ~~were less eutrophic than during peak interglacial periods and that the organic matter reaching the seafloor may have~~  
1031 ~~been less degraded.~~

1032

Formatted: Normal;Text

### 1033 **5.3.3 Comparison to Atlantic counterparts ?**

Formatted: Font color: Accent 3

1034

Formatted: Normal;Text

1035

1036

#### 1037 **5.3.1 Coral proliferation and environmental forcing**

1038 ~~In the Northeast and Northwest Atlantic, corals thrive during interglacial periods whilst their proliferation is halted~~  
1039 ~~during glacial periods (Dorschel et al., 2005; Rüggeberg et al., 2007; Frank et al., 2009; 2011; Matos et al., 2015;~~  
1040 ~~2017). Coral proliferation at BRI does not follow the same pattern. Indeed corals develop during both interglacial~~  
1041 ~~and glacial periods (Fig. 3). The positive response of corals to increased bottom current velocity is important in both~~  
1042 ~~the North Atlantic and Southeast Alboran Sea. This follows the consensus that strong bottom currents are decisive~~  
1043 ~~for the development of corals (e.g. White et al., 2005; Mienis et al., 2007; Roberts et al., 2009). The topography of~~  
1044 ~~Brittlestar Ridge I may favour the formation of Taylor columns and the retention of organic matter, such as observed~~  
1045 ~~in the Rockall Trough (Northeast Atlantic, White, 2007). However, benthic foraminiferal assemblages associated to~~  
1046 ~~phases of coral proliferation in the Northeast Atlantic (Rüggeberg et al., 2007) and in the Southeast Alboran Sea (this~~  
1047 ~~study) differ. Benthic foraminiferal assemblages associated to phases of sustained coral proliferation at Propeller~~  
1048 ~~Mound (Northeast Atlantic) are essentially characterized by large epibenthic foraminifera (*L. lobatula*, *Cibicides*~~  
1049 ~~*refulgens*, *D. coronata*, and *Planulina ariminensis*) and the infaunal *Trifarina bradyi* (Rüggeberg et al., 2007). In~~  
1050 ~~contrast, at BRI, higher abundances of *L. lobatula*, *D. coronata* and *T. angulosa* are associated to glacial periods or~~  
1051 ~~transition phases between interglacial and glacial periods with low coral abundance, while small infaunal~~  
1052 ~~foraminifera dominate phases of coral proliferation (Fig. 89). These contrasting observations suggest differences in~~

1053 food supply and bottom current regimes. Corals in the Northeast Atlantic thrive on fresh marine derived organic  
1054 matter resulting from North Atlantic blooms which are fuelled by upwelling (Dickinson et al., 1980). In contrast,  
1055 corals at BRI are likely supplied by plankton blooms triggered by the input of degraded fluvial organic matter during  
1056 interglacial times, whilst aeolian dust input allows corals to survive during glacial times by triggering local moderate  
1057 nutrient supply to the seafloor. In this regard, coral mounds situated in the Southeast Alboran Sea show more  
1058 similarities to mounds located in the Viosea Knoll area, where the dispersal of terrestrial organic matter by the  
1059 Mississippi River triggers an increase in primary productivity, providing nutrients for coral communities during  
1060 interglacial periods (Mienis et al., 2012). The respective shallow location and proximity of BRI to the continent  
1061 explains the higher influence of continental runoff on coral communities than in the deeper Northeast Atlantic sites.  
1062 As such, water mass rearrangements appear to be of secondary importance, whilst the input of terrestrial organic  
1063 matter would be the primary factor triggering coral proliferation at BRI.

### 1065 5.3.2 Long-term coral mound build-up

1066 Long-term coral mound formation at BRI and in the Poreupine Seabight do not show the same temporal distribution.  
1067 Indeed, mound aggradation in the Poreupine Seabight is restricted to interglacial periods, whilst winnowing and mass  
1068 wasting are considered as precursor events for the re-initiation of coral proliferation during glacial terminations  
1069 (Rüggeberg et al., 2007; Frank et al., 2011). In contrast, benthic foraminiferal assemblages and  $\overline{SS}$  would indicate  
1070 that terminations were not marked by winnowing or erosional events at BRI (Fig. 5 and 89). Thus, the environmental  
1071 mechanisms triggering the reset of coral proliferation at the onset of interglacials at BRI appear to be different from  
1072 the Northeast Atlantic. Long-term coral mound formation at BRI took place during interglacial and glacial periods,  
1073 though at much lower aggradation rates than in the Poreupine Seabight (Fig. 4B; Frank et al., 2011). Highest  
1074 aggradation rates occur during MIS 3 and MIS 6. The maximum rate of ca. 10 cm.ky<sup>-1</sup> is reached during the middle  
1075 of MIS 3 with a short peak to 18 cm.ky<sup>-1</sup>, whilst rates do not exceed ca. 4 cm.ky<sup>-1</sup> during interglacial periods (Fig.  
1076 4B).

1077  
1078 The limited coral mound build-up during both interglacial and glacial periods at BRI can explain the observed  $\delta^{18}O$   
1079 values throughout core MD13-2462G which demonstrate typical interglacial/glacial variations (Fig. 4, Cacho et al.,  
1080 1999; Lisiecki and Raymo, 2005; Cacho et al., 2006). The  $\delta^{18}O$  values recorded for interglacial and glacial periods  
1081 are a clear indication that coral mounds at BRI demonstrate a more continuous build-up history across  
1082 interglacial/glacial periods than their North Atlantic counterparts. Mound aggradation rates in core MD13-3462G are  
1083 comparable to inactive or abandoned reefs in the Poreupine Seabight, i.e. <5 cm.ky<sup>-1</sup> (Frank et al., 2011), thus  
1084 suggesting that CWCs did not thrive at the site of core MD13-3462G but rather developed under stressful  
1085 environmental conditions. Average long-term mound aggradation rates at BRI show more similarities with mounds  
1086 situated along the Mauritanian margin that developed during the last glacial (28-45 cm.ky<sup>-1</sup>) but also during the last  
1087 interglacial period (16 cm.ky<sup>-1</sup>; Wienberg et al., 2018; Wienberg and Titschak, 2015). In contrast with Atlantic CWC  
1088 mounds, mounds from the East Melilla Coral Province show a high contribution of the erect cheleistome bryozoan *B.*

1089 ~~*dichotoma*. Based on mound aggradation rates and macrofaunal content, we propose that *B. dichotoma* communities~~  
1090 ~~favoured mound formation at BRI, noticeably during glacial periods, by capturing fine grained sediments in a similar~~  
1091 ~~way as CWCs do (Fig. 3 and 8). As such, mounds at BRI stand out and may be considered as mixed *B.*~~  
1092 ~~*dichotoma*/CWC mounds, rather than CWC mounds per se.~~

## 1093 Conclusions

1094 The multiproxy study of core MD13-3462G ~~provides information on the long-term build-up of a cold-water coral~~  
1095 ~~mound at Brittlestar Ridge I reveals that mound build-up at the northern part of Brittlestar Ridge I (East Melilla Coral~~  
1096 ~~Province, SE Alboran Sea) took place during both interglacial and glacial periods. A number of key observations can~~  
1097 ~~be underlined: Two important points can be highlighted:~~

1098  
1099 (1) ~~Cold water coral mound build up takes place during both interglacial and glacial periods.~~ Average coral mound  
1100 aggradation rates are particularly low, varying between 1 and 10 cm.kyr<sup>-1</sup>, ~~whilst maximum aggradation rates are~~  
1101 ~~recorded during MIS 3 (18 cm.kyr<sup>-1</sup>).~~ ~~Low mound aggradation rates during interglacial and glacial periods~~  
1102 ~~suggest~~ ~~These rates suggest~~ that corals ~~did not thrive~~ ~~never did thrive~~ in this sector of Brittlestar Ridge I but rather  
1103 developed under stressful environmental ~~conditions.~~ ~~conditions at Brittlestar Ridge I.~~ We propose that weak bottom-  
1104 water oxygenation linked to sapropel-related events and/or increased precipitation over North Africa led to the slow  
1105 development of coral communities during interglacial periods. Intensified circulation of Levantine Intermediate  
1106 Water and the import of fresh organic matter would have provided suitable conditions for bryozoan and coral  
1107 communities during glacial periods.

1108  
1109 (2) Core MD13-3462G provides the first record of consistent coral growth during the last glacial period in the East  
1110 Melilla Coral Province and more generally in the Alboran Sea. This conspicuous observation, in conjunction with  
1111 other records of Mediterranean long-term coral mound build-up, suggests that coral mound development does not  
1112 follow a clear cut interglacial-glacial pattern in the western Mediterranean. Furthermore, regional and local-scale  
1113 environmental variability appears to play a decisive role on mound build-up in the eastern Alboran Sea. ~~During~~  
1114 ~~interglacial periods, coral development is driven by the combination of increased terrestrial input and enhanced~~  
1115 ~~turbulence at the seafloor. The dominant influence of warm and moist Atlantic air masses together with intensified~~  
1116 ~~Western and Eastern Alboran Gyres promoted high food availability at the seafloor during interglacial periods.~~  
1117 ~~In contrast, more arid continental conditions and the upwelling of deep water masses would have characterized~~  
1118 ~~glacial conditions. The bryozoan *Buskea dichotoma* appears to be better suited to these glacial environmental~~  
1119 ~~conditions than the scleractinian *D. pertusum*. Overall, our results demonstrate the paramount importance of~~  
1120 ~~enhanced terrestrial input as a trigger for cold water coral mound build-up in the Southeast Alboran Sea.~~

1121  
1122 (3) The planktonic and benthic  $\delta^{18}\text{O}$  records of cold-water coral mound sediments at Brittlestar Ridge I shows  
1123 typical interglacial ~~glacial~~ variations ~~since early MIS 6~~. This is in contrast with  $\delta^{18}\text{O}$  records ~~observed in sediments~~

Formatted: Font: Not Bold

1124 | ~~from Northeast Atlantic~~generally recovered from coral mound deposits ~~cold-water coral mounds~~ and ~~underlines~~  
1125 | ~~highlights the discrepancies in mound build-up processes between the two regions~~that the northern part of Brittlestar  
1126 | ~~Ridge I experienced reduced albeit continuous~~ -build-up.

1127 |  
1128 | From a wider perspective, the build-up of cold-water coral mound~~s~~s situated at Brittlestar Ridge I during both  
1129 | interglacial and glacial periods stresses how cold-water coral communities are capable of withstanding important  
1130 | environmental changes and to survive and adapt to different climatic conditions. This study further ~~suggests~~ shows  
1131 | that the role of associated species, such as rigid erect bryozoans, may be ~~linked~~ associated to the resilience of coral  
1132 | ecosystems.

#### 1133 **Data availability**

1134 | The datasets used in this study are available at the open-access repository PANGAEA:  
1135 | <https://doi.pangaea.de/10.1594/PANGAEA.915601>.

#### 1136 **Sample availability**

1137 | Archive halves of all core sections investigated for this study are available at the Department of Geosciences,  
1138 | University of Fribourg (Switzerland). The sediment residues and the splits of each sample analysed for benthic  
1139 | foraminiferal assemblages are stored at the Department of Geosciences, University of Fribourg (Switzerland).  
1140 | Bryozoans identified in this study are available at the Palaeontological Museum of the University of Catania (Italy).

#### 1141 **Author contributions**

1142 | RF: writing (original draft), visualization, conceptualization, core sampling, investigation (benthic foraminiferal  
1143 | assemblages, main macrofaunal fragments, particle size analysis, stable isotope measurements assisted by TV and  
1144 | radiocarbon dating assisted by IH). EF: conceptualization, writing (review and editing), XRF investigation (assisted  
1145 | by HV), preparation of samples for Uranium-series dating and RockEval6 pyrolysis. ARü: conceptualization, writing  
1146 | (review and editing), supervision. EH: investigation (CT analysis, macrofaunal quantification). VR: writing (review  
1147 | and editing), visualization. TV: writing (review and editing), investigation (stable isotope measurements), resources.  
1148 | IH: writing (review and editing), investigation (radiocarbon dating), resources. ARo: writing (review and editing),  
1149 | investigation (bryozoan taxonomy). DVR: writing (review and editing), resources. TA: writing (review and editing),  
1150 | investigation (RockEval6 pyrolysis), resources. HV: writing (review and editing), investigation (XRF), resources. NF  
1151 | ~~& TK~~: writing (review and editing), investigation (Uranium-series dating). AF: investigation (core description, CT  
1152 | data analysis, XRF data analysis), conceptualization, writing (review and editing), project administration, funding  
1153 | acquisition, supervision.

1154 **Conflict of interests**

1155 The authors declare that they have no conflict of interest.

1156 **Acknowledgements**

1157 We thank the SNSF (Swiss National Science Foundation) projects ‘Unconventional Carbonate Factories’ and ‘4D-  
1158 Diagenesis@Mound’ (project numbers 200020\_153125 and 200021\_149247) for funding this research. We also are  
1159 grateful for the ship time provided by IPEV on the R/V *Marion Dufresne II* within the framework of the  
1160 EuroFLEETS GATEWAYS project (grant agreement 228344). We further thank Tim Collart for the help he  
1161 provided with the *Rysgran* package for R and Marc Schori for his help with the *ArcGIS* software. We further  
1162 acknowledge the help of Rene Eichstädter and Andrea Schröder-Ritzrau regarding Uranium-series dating and quality  
1163 control. The DFG has provided funding for the Uranium-series dating of corals via the project FR1341/9-1.

1164 **References**

- 1165 Addamo, A.M., Vertino, A., Stolarski, J., García-Jiménez, R., Taviani, M., and Machordom, A.: Merging  
1166 scleractinian genera: the overwhelming genetic similarity between solitary *Desmophyllum* and colonial  
1167 *Lophelia*, *BMC Evol Biol*, 16, 108, 2016.
- 1168 [Angeletti, L., Castellán, G., Montagna, P., Remia, A., Taviani, M. The « Corsica Channel Cold-Water Coral](#)  
1169 [Province” \(Mediterranean Sea\), \*Frontiers in Marine Science\*, 7, 2020.](#)
- 1170 Altenbach, A.V. and Sarnthein, M.: Productivity Record in Benthic Foraminifera, in: Productivity of the Ocean:  
1171 Present and Past, edited by: Berger, W.H., Smetacek, V.S., and Wefer, G., John Wiley & Sons Limited, 255-  
1172 269, 1989.
- 1173 [Bahr, A., Kaboth, S., Jiménez-Espejo, F.J., Sierro, F.J., Voelker, A.H.L., Lourens, L., Röhl, U., Reichart, G.J.,](#)  
1174 [Escutia, C., Hernández-Molina, F.J., Pross, J., Friedrich, O.: Persistent monsoonal forcing of mediterranean](#)  
1175 [outflow water dynamics during the late Pleistocene, \*Geology\*, 43, 951-954, 2015.](#)
- 1176 Best, M.A. and Thorpe, J.P.: Particle size, clearance rate and feeding efficiency in marine Bryozoa, in: Biology and  
1177 Palaeobiology of Bryozoans, edited by: Hayward, P.J., Ryland, J.S., and Taylor, P.D., Olsen and Olsen,  
1178 Fredensborg, Denmark, 9-14, 1994.
- 1179 Beuck, L. and Freiwald, A.: Bioerosion patterns in a deep-water *Lophelia pertusa* (Scleractinia) thicket (Propeller  
1180 Mound, northern Porcupine Seabight), in: Cold-water corals and ecosystems, published by: Freiwald, A. and  
1181 Roberts, J.M., Springer-Verlag, Berlin Heidelberg, 915-936, 2005.
- 1182 Bjerager, M. and Surlyk, F.: Benthic palaeoecology of Danian deep-shelf bryozoan mounds in the Danish Basin,  
1183 *Palaeogeogr Palaeoclimatol*, 250, 184-215, 2007.
- 1184 Bout-Roumazeilles, V., Combourieu Nebout, N., Peyron, O., Cortijo, E., Landais, A., and Masson-Delmotte, V.:  
1185 Connection between South Mediterranean climate and North African atmospheric circulation during the last  
1186 50,000 yr BP North Atlantic cold events, *Quaternary Sci Rev*, 26, 3197-3215, 2007.

**Formatted:** Font: Not Bold, Italian (Switzerland)

**Formatted:** Indent: Left: 0 cm, Hanging: 1,83 ch

**Formatted:** Italian (Switzerland)

1187 Braun, K., Nehme, C., Pickering, R., Rogerson, M., and Scroxton, N.: A window into Africa's past hydroclimates: the  
1188 SISAL\_V1 database contribution, *Quaternary*, 2, 4, 2019.

1189 Bromley, R.G.: Preliminary study of bioerosion in the deep-water coral *Lophelia*, Pleistocene, Rhodes, Greece, in:  
1190 Cold-water Corals and Ecosystems, edited by: Freiwald, A. and Roberts, J.M., Springer-Verlag, Berlin  
1191 Heidelberg, 895-914, 2005.

1192 Cacho, I., Grimalt, J.O., Pelejero, C., Canals, M., Sierro, F.J., Flores, J.A., and Shackleton, N.: Dansgaard-Oeschger  
1193 and Heinrich event imprints in Alboran Sea paleotemperatures, *Paleoceanography*, 14, 698-705, 1999.

1194 Cacho, I., Grimalt, J.O., Sierro, F.J., Shackleton, N.J., and Canals, M.: Evidence for enhanced Mediterranean  
1195 thermohaline circulation during rapid climatic coolings, *Earth Planet Sc Lett*, 183, 417-429, 2000.

1196 Cacho, I., Shackleton, N., Elderfield, H., Sierro, F.J., and Grimalt, J.O.: Glacial rapid variability in deep-water  
1197 temperature and  $\delta^{18}\text{O}$  from the Western Mediterranean Sea, *Quaternary Sci Rev*, 25, 3294-3311, 2006.

1198 Calvert, S.E. and Pedersen, T.F.: Elemental Proxies for Palaeoclimatic and Palaeoceanographic Variability in Marine  
1199 Sediments: Interpretation and Application, in: *Developments in Marine Geology*, edited by Hillaire-Marcel, C.  
1200 and De Vernal, A., Elsevier, 2007.

1201 [Camafort, M., Gracia, E., Ranero, C.R.: Quaternary Seismostratigraphy and Tectonosedimentary Evolution of the](#)  
1202 [North Tunisian Continental Margin, \*Tectonics\*, 39, 2020.](#)

1203 Caquineau, S., Gaudichet, A., Gomes, L., and Legrand, M.: Mineralogy of Saharan dust transported over  
1204 northwestern tropical Atlantic Ocean in relation to source regions, *J Geophys Res-Atmos*, 107, 1-14, 2002.

1205 Caquineau, S., Gaudichet, A., Gomes, L., Magonthier, M-C., Chatenet, B.: Saharan dust: Clay ratio as a relevant  
1206 tracer to assess the origin of soil-derived aerosols. *Geophysical Research Letters*, 25, 983-986, 1998.

1207 Carlier, A., Le Guilloux, E., Olu, K., Sarrazin, J., Mastrototaro, F., Taviani, M., and Clavier, J.: Trophic relationships  
1208 in a deep Mediterranean cold-water coral bank (Santa Maria di Leuca, Ionian Sea). *Mar Ecol Prog Ser*, 397,  
1209 125-137, 2009.

1210 Cheng, H., Adkins, J., Lawrence Edwards, R., and Boyle, E.A.: U-Th dating of deep-sea corals, *Geochim*  
1211 *Cosmochim Ac*, 64, 14, 2401-2416, 2000.

1212 Clarke, K.R. and Gorley, R.N.: PRIMER v6: User Manual/Tutorial (Plymouth Routines in Multivariate Ecological  
1213 Research), PRIMER-E, Plymouth, 2006.

1214 [Cleveland, W.S., Devlin, S.J.: Regression Analysis by Local Fitting, \*Journal of American Statistical Association\*, 83,](#)  
1215 [403, 596-610, 1986.](#)

1216 Comas, M., and Pinheiro, L.M.: The Melilla carbonate mounds: do deep-water coral mounds count on seeping fluids  
1217 in the Alboran Sea? *Rapp. Comm. Int. Mer Médit*, 39, 16, 2010.

1218 Comas, M.C., Pinheiro, L.M., Ivanov, M. and TTR-17 Leg 1 Scientific Party: Deep-water coral mounds in the  
1219 Alboran Sea: the Melilla mounds field revisited, IOC Workshop Report No. 220, Granada (Spain), 2-5 February  
1220 2009, 2009.

1221 Comas, M.C., Platt, J.P., Soto, J.I. and Watts, A.B.: The origin and tectonic history of the Alboran Basin: insights  
1222 from Leg 161 results, *Proceedings of the Ocean Drilling Program 161, Scientific Results*, 1999.

1223 [Corbera, G., Lo Iacono, C., Gràcia, E., Grinyo, J., Pierdomenico, M., Huvenne, V.A.I., Aguilar, R., Gili, J.M.:](#)  
1224 [Ecological characterisation of a Mediterranean cold-water coral reef: Cabliers Coral Mound Province \(Alboran](#)  
1225 [Sea, western Mediterranean\), \*Progress in Oceanography\*, 175, 245-262, 2019.](#)

1226 Corbera, ~~GC.~~, Lo Iacono, C., Standish, D., Anagnostou, E., Titschack, J., Katsamenis, O., Cacho, I., Van Rooij, D.,  
1227 Huvenne, V.A.I., ~~and~~ Foster, G.L.: Glacio-eustatic variations and sapropel events as main controls on the Middle  
1228 Pleistocene-Holocene evolution of the Cabliers Coral Mound Province (W Mediterranean). *Quaternary Science*  
1229 *Reviews*, 253, 106783, 2021.

1230 [Corbera, G., Lo Iacono, C., Standish, C.D., Gràcia, E., Ranero, C., Huvenne, V.A.I., Anagnostou, E., Foster, G.L.:](#)  
1231 [Glacial-aged development of the Tunisian Coral Mound Province controlled by glacio-eustatic oscillations and](#)  
1232 [changes in surface productivity, \*Marine Geology\*, 446, 106772, 2022.](#)

1233 Coulthard, T.J., Ramirez, J.A., Barton, N., Rogerson, M., and Brucher, T.: Were rivers flowing across the Sahara  
1234 during the last interglacial? Implications for human migration through Africa, *PLoS One*, 8, e74834, 2013.

1235 ~~Croudaee, I.W., Rothwell, R.G.: *Micro XRF Studies of Sediment Cores: Applications of a non-destructive tool for*~~  
1236 ~~*the environmental sciences. Developments in Paleoenvironmental Research (Springer)*, 17, 656 pp, 2015.~~

1237 Davies, A.J. and Guinotte, J.M.: Global habitat suitability for framework-forming cold-water corals, *PLoS One* 6,  
1238 e18483, 2011.

1239 Davies, A.J., Duineveld, G., Lavaleye, M., Bergman, M., van Haren, H., and Roberts, J.: Downwelling and deep-  
1240 water bottom currents as food supply mechanisms to the cold-water coral *Lophelia pertusa* (*Scleractinia*) at the  
1241 Mingulay Reef Complex, *Limnol Oceanogr*, 54, 620-629, 2009.

1242 De Mol, B., Van Rensbergen, P., Pillen, S., Van Herreweghe, K., Van Rooij, D., McDonnell, A., Huvenne, V.A.I.,  
1243 Ivanov, M., Swennen, R., and Henriot, J.-P.: Large deep-water coral banks in the Porcupine Basin, southwest of  
1244 Ireland, *Mar Geol*, 188, 193-231, 2002.

1245 De Rijk, S., Jorissen, F., Rohling, E.J., and Troelstra, S.R.: Organic flux control on bathymetric zonation of  
1246 Mediterranean benthic foraminifera, *Mar Micropaleontol*, 40, 151-166, 2000.

1247 Dessandier, P.-A., Bonnin, J., Kim, J.-H., Bichon, S., Deflandre, B., Grémare, A., and Sinninghe Damsté, J.S.:  
1248 Impact of organic matter source and quality on living benthic foraminiferal distribution on a river-dominated  
1249 continental margin: A study of the Portuguese margin, *J. Geophys. Res. Biogeosci.*, 121, 1689-1714, 2016.

1250 ~~Dickinson, R.R., Gurbutt, P.A., and Pillai, V.N.: *Satellite evidence of enhanced upwelling along the European*~~  
1251 ~~*continental slope, *Geology*, 813-819, 1980.*~~

1252 [Do Couto, D., Gorini, C., Jolivet, L., Lobret, N., Augier, R., Gumiaux, C., d'Acremont, E., Ammar, A., Jabour, H.,](#)  
1253 [and Auxietre, J. L.: Tectonic and stratigraphic evolution of the Western Alboran Sea Basin in the last 25 Myrs,](#)  
1254 [\*Tectonophysics\*, 677-678, 280-311, 2016.](#)

1255 Dorschel, B., Hebbeln, D., Foubert, A., White, M., and Wheeler, A.J.: Hydrodynamics and cold-water coral facies  
1256 distribution related to recent sedimentary processes at Galway Mound west of Ireland, *Mar Geol*, 244, 184-195,  
1257 2007.

1258 Dorschel, B., Hebbeln, D., Ruggeberg, A., Dullo, W-C, and Freiwald, A.: Growth and erosion of a cold-water coral  
1259 covered carbonate mound in the Northeast Atlantic during the Late Pleistocene and Holocene, *Earth Planet Sc*  
1260 *Lett*, 233, 33-44, 2005.

Formatted: Font: Not Bold, English (U.K.)

Formatted: Font: Not Bold, English (U.K.)

Formatted: Font: Not Bold, English (U.S.)



1261 Drinia, H. and Dermitzakis, M.D.: The response of benthic foraminifera to palaeoenvironmental disturbance: A  
1262 quantitative approach in turbidite-like successions, *N. Jb. Geol. Paläont. Abh*, 258, 3, 325–338, 2010.

1263 Duggen, S., Hoernle, K., Klügel, A., Geldmacher, J., Thirlwall, M., Hauff, F., Lowry, D., and Oates, N.:  
1264 Geochemical zonation of the Miocene Alborán Basin volcanism (westernmost Mediterranean): geodynamic  
1265 implications, *Contrib Mineral Petr*, 156, 577-593, 2008.

1266 Dullo W-C., Flögel, S. and Rüggeberg, A.: Cold-water coral growth in relation to the hydrography of the Celtic and  
1267 Nordic European continental margin, *Mar Ecol Prog Ser*, 371, 165-176, 2008.

1268 Eisele, M., Frank, N., Wienberg, C., Hebbeln, D., López Correa, M., Douville, E., and Freiwald, A.: Productivity  
1269 controlled cold-water coral growth periods during the last glacial off Mauritania, *Mar Geol*, 280, 143-149, 2011.

1270 Eisele, M., Hebbeln, D., and Wienberg, C.: Growth history of a cold-water coral covered carbonate mound —  
1271 Galway Mound, Porcupine Seabight, NE-Atlantic, *Mar Geol*, 253, 160-169, 2008.

1272 Emelyanov, E.M. and Shimkus, K.M.: *Geochemistry and sedimentology of the Mediterranean Sea*, Springer Science  
1273 and Business Media, 2012.

1274 Emig, C.C. and Arnaud, P.M.: Observations en submersible sur la densité des populations de *Gryphus vitreus*  
1275 (Brachiopode) le long de la marge continentale de Provence (Méditerranée nord-occidentale), *C. R. Acad. Sci.*  
1276 *Paris*, 306, 501-505, 1988.

1277 ~~Ercilla, G., Juan, C., Hernández-Molina, J., Bruno, M., Estrada, F., Alonso, B., Casas, D., Farran, M., Llave, E.,  
1278 García, Vázquez, J.T., D'Acremont, E., Gorini, C., Palomino, D., Valencia, J., El Moumni, B., and Ammar, A.:  
1279 Significance of bottom currents in deep-sea morphodynamics: An example from the Alboran Sea, *Mar Geol*,  
1280 378, 157-170, 2016.~~

1281 Espitalié, J., Deroo, G., and Marquis, F.: La Pyrolyse Rock-Eval et ses applications, *Revue de l'Institut Français du*  
1282 *Pétrole*, 40, 5, 1-34, 1985.

1283 ~~Faceenna, C., Piromallo, C., Crespo Blane, A., Jolivet, L., and Rossetti, F.: Lateral slab deformation and the origin of  
1284 the western Mediterranean arcs, *Tectonics*, 23, 2004.~~

1286 Fantasia, A., Adatte, T., Spangenberg, J.E., Font, E., Duarte, L.V., and Föllmi, K.B.: Global versus local processes  
1287 during the Pliensbachian-Toarcian transition at the Peniche GSSP, Portugal: a multi-proxy record, *Earth-Sci*  
1288 *Rev*, 198, 102932, 2019.

1289 Fariduddin, M. and Loubere, P.: The surface ocean productivity response of deeper water benthic foraminifera in the  
1290 Atlantic Ocean, *Mar Micropaleontol*, 32, 289-310, 1997.

1291 Fentimen, R., Feenstra, E., Rüggeberg, A., Vennemann, T., Hajdas, I., Adatte, T., Van Rooij, D., and Foubert, A.:  
1292 Cold-Water Coral Mound Archive Provides Unique Insights Into Intermediate Water Mass Dynamics in the  
1293 Alboran Sea During the Last Deglaciation, *Frontiers in Marine Science*, 7, 354, 2020a.

1294 Fentimen, R., Lim, A., Rüggeberg, A., Wheeler, A.J., Van Rooij, D., and Foubert, A.: Impact of bottom water  
1295 currents on benthic foraminiferal assemblages in a cold-water coral environment: The Moira Mounds (NE  
1296 Atlantic), *Mar. Micropaleontol*, 154, 101799, 2020b.

Formatted: Font: Not Bold

Formatted: Font: Not Bold

Formatted: Indent: Left: 0 cm,  
Hanging: 1,83 ch

Formatted: English (U.K.)

1297 [Filippidi, A., Triantaphyllou, M. V., De Lange, G.J.: Eastern-Mediterranean ventilation variability during sapropel](#)  
1298 [S1 formation, evaluated at two sites influenced by deep-water formation from Adriatic and Aegean Seas,](#)  
1299 [Quaternary Science Reviews, 144, 95-106, 2016.](#)

1300 Fink, H.G., Wienberg, C., De Pol-Holz, R., and Hebbeln, D.: Spatio-temporal distribution patterns of Mediterranean  
1301 cold-water corals (*Lophelia pertusa* and *Madrepora oculata*) during the past 14,000 years, Deep-Sea Res Pt I,  
1302 103, 37-48, 2015.

1303 Fink, H.G., Wienberg, C., De Pol-Holz, R., Wintersteller, P., and Hebbeln, D.: Cold-water coral growth in the  
1304 Alboran Sea related to high productivity during the Late Pleistocene and Holocene, Mar Geol, 339, 71-82, 2013.

1305 Folk, R.L. and Ward, W.C.: A Study in the Significance of Grain-Size Parameters, J Sediment Petrol, 27, 3-26, 1957.

1306 Fontanier, C., Jorissen, F.J., Chaillou, G., David, C., Anschutz, P., and Lafon, V.: Seasonal and interannual  
1307 variability of benthic foraminiferal faunas at 550m depth in the Bay of Biscay, Deep-Sea Res Pt I, 50, 457-494,  
1308 2003.

1309 Fontanier, C., Jorissen, F.J., Licari, L., Alexandre, A., Anschutz, P., and Carbonel, P.: Live benthic foraminiferal  
1310 faunas from the Bay of Biscay: faunal density, composition, and microhabitats, Deep-Sea Res Pt I, 49, 751-785,  
1311 2002.

1312 Foubert, A. and Henriët, J.-P.: Nature and Significance of the Recent Carbonate Mound Record, Lecture Notes in  
1313 Earth Sciences, 126, Springer-Verlag, Berlin, 298 pp., 2009.

1314 Frank, N., Freiwald, A., Correa, M.L., Wienberg, C., Eisele, M., Hebbeln, D., Van Rooij, D., Henriët, J.P., Colin, C.,  
1315 van Weering, T., de Haas, H., Buhl-Mortensen, P., Roberts, J.M., De Mol, B., Douville, E., Blamart, D., and  
1316 Hatte, C.: Northeastern Atlantic cold-water coral reefs and climate, Geology, 39, 743-746, 2011.

1317 Frank, N., Paterne, M., Ayliffe, L., van Weering, T., Henriët, J.-P., and Blamart, D.: Eastern North Atlantic deep-sea  
1318 corals: tracing upper intermediate water  $\Delta^{14}\text{C}$  during the Holocene, Earth Planet Sc Lett, 219, 297-309, 2004.

1319 Frank, N., Ricard, E., Lutringer-Paquet, A., van der Land, C., Colin, C., Blamart, D., Foubert, A., Van Rooij, D.,  
1320 Henriët, J.-P., de Haas, H., and van Weering, T.: The Holocene occurrence of cold water corals in the NE  
1321 Atlantic: Implications for coral carbonate mound evolution, Mar Geol, 266, 129-142, 2009.

1322 [Freiwald, A., Beuck, L., Rüggeberg, A., Taviani, M., Hebbeln, D: The white coral community in the central](#)  
1323 [Mediterranean Sea revealed by ROV surveys. Oceanography, 22, 58-74, 2009.](#)

1324 Freiwald, A., Fosså, J.H., Grehan, A., Koslow, T., and Roberts, J.M.: Cold-water coral Reefs, UNEP\_WCMC,  
1325 Cambridge, UK, 2004.

1326 Gasse, F.: Hydrological changes in the African tropics since the Last Glacial Maximum, Quaternary Sci Rev, 19,  
1327 189-211, 2000.

1328 Gasse, F. and Roberts, C.N.: Late Quaternary hydrologic changes in the arid and semiarid belt of northern Africa, in:  
1329 The Hadley Circulation: Present, Past and Future, edited by: Diaz, H.F. and Bradley, R.S., Kluwer Academic  
1330 Publishers, 313-345, 2005.

1331 Gilbert, E.R., Camargo, M.G. and Sandrini-Neto, L.: rysgran: Grain size analysis, textural classifications and  
1332 distribution of unconsolidated sediments, R package version 2.1.0, [https://CRAN.R-](https://CRAN.R-project.org/package=rysgran)  
1333 [project.org/package=rysgran](https://CRAN.R-project.org/package=rysgran), 2015.

Formatted: Font: Not Bold, English (U.K.)

Formatted: Indent: Left: 0 cm, Hanging: 1,83 ch

1334 Goldstein S.T.: Foraminifera: A biological overview, in: Modern Foraminifera, edited by: Sen Gupta, B.K., 37– 55,  
1335 Kluwer Acad., Norwell, Mass., 1999.

1336 Gooday, A.J.: The Biology of Deep-Sea Foraminifera: A Review of Some Advances and Their Applications in  
1337 Paleooceanography, *Palaios*, 9, 14-31, 1993.

1338

1339 Gregory, B.R.B., Patterson, T.R., Reinhardt, E.G., Galloway, J.M., and Roe, H.R.: An evaluation of methodologies  
1340 for calibrating Itrax X-ray fluorescence counts with ICP-MS concentration data for discrete sediment samples,  
1341 *Chem Geol*, 525, 12-27, 2019.

1342 Guieu, C., Thomas, A.J.: Saharan Aerosols: From the Soil to the Ocean. In: Guerzoni, S., Chester, R. (Eds.) *The*  
1343 *Impact of Desert Dust Across the Mediterranean*. Springer Netherlands: Dordrecht, 408 pp, 1996.

1344 Hanz, U., Wienberg, C., Hebbeln, D., Duineveld, G., Lavaley, M., Juva, K., Dullo, W.-C., Freiwald, A.,  
1345 Tamborrino, L., Reichart, G.-J., Flögel, S., and Mienis, F.: Environmental factors influencing cold-water coral  
1346 ecosystems in the oxygen minimum zones on the Angolan and Namibian margins, *Biogeosciences*, 1-37, 2019.

1347 Hebbeln, D.: Highly variable submarine landscapes in the Alborán Sea created by cold-water corals, in:  
1348 *Mediterranean Cold-Water Corals: Past, Present and Future*, published by: Orejas, C. and Jiménez, C., Springer  
1349 series: Coral Reefs of the World 9, Springer International Publishing, 61-65, 2019.

1350 Hebbeln, D., Van Rooij, D., and Wienberg, C.: Good neighbours shaped by vigorous currents: Cold-water coral  
1351 mounds and contourites in the North Atlantic, *Mar Geol*, 378, 171-185, 2016.

1352 ~~Hebbeln, D., Wienberg, C., Dullo, W.C., Freiwald, A., Mienis, F., Orejas, C., Titschack, J.: Cold-water coral reefs~~  
1353 ~~thriving under hypoxia. *Coral Reefs*, 39, 853-859, 2020.~~

1354 Heburn, G.W. and La Violette, P.E.: Variations in the structure of the anticyclonic gyres found in the Alboran Sea, *J*  
1355 *Geophys Res*, 95, 1990.

1356 Holbourn, A., Kuhnt, W., James, N.: Late Pleistocene bryozoan reef mounds of the Great Australian Bight:  
1357 Isotope stratigraphy and benthic foraminiferal record, *Paleoceanography*, 17, 2002.

1358 Huvenne, V.A.I., De Haas, H., Dekindt, K., Henriot, J-P., Kozachenko, M., Olu-Le Roy, K., and Wheeler, A.J.: The  
1359 seabed appearance of different coral bank provinces in the Porcupine Seabight, NE Atlantic: results from  
1360 sidescan sonar and ROV seabed mapping, in: *Cold-water Corals and Ecosystems*, edited by: Freiwald, A. and  
1361 Roberts, J.M., Springer-Verlag, Berlin, Heidelberg, 536-569, 2005.

1362 Huvenne, V.A.I., Masson, D.G., and Wheeler, A.J.: Sediment dynamics of a sandy contourite: the sedimentary  
1363 context of the Darwin cold-water coral mounds, Northern Rockall Trough, *Int J Earth Sci*98, 865-884, 2009.

1364 Jaffey, A.H., Flynn, K.F., Glendenin, L.E., Bentley, W.C., and Essling, A.M.: Precision measurements of half-lives  
1365 and specific activities of <sup>235</sup>U and <sup>238</sup>U, *Phys Rev*, 4, 5, 1889-1906, 1971.

1366 James, N.P., Feary, D.A., Surlyk, F., Toni Simo, J.A., Betzler, C., Holbourn, A.E., Li, Q., Matsuda, H., Machiyama,  
1367 H., Brooks, G.R., Andres, M.S., Hine, A.C., and Malone, M.J.: Quaternary bryozoan reef mounds in cool-water,  
1368 upper slope environments: Great Australian Bight, *Geology*, 28, 2000.

1369 ~~Johnson, T.C.: Sedimentary processes and signals of past climate change in the large lakes of East African Rift~~  
1370 ~~Valley, in: *Limnology, Climatology and Paleoclimatology of the East African Lakes*, edited by: Johnson, T.C.~~  
1371 ~~and Odada, E.O., The Gordon and Breach, Amsterdam, 367-412, 1996.~~

1372 Jorissen, F.J.: The distribution of benthic foraminifera in the Adriatic Sea, *Marine Micropaleontology*, 12, 21-48,  
1373 1987.

1374 [Jorissen, F.J.: Benthic foraminiferal successions across Late Quaternary Mediterranean sapropels, \*Marine Geology\*,  
1375 \*153\*, 1-4, 91-101, 1999.](#)

1376 Kano, A., Ferdelman, T.G., Williams, T., Henriot, J.-P., Ishikawa, T., Kawagoe, N., Takashima, C., Kakizaki, Y.,  
1377 Abe, K., Sakai, S., Browning, E.L., and Li, X.: Age constraints on the origin and growth history of a deep-water  
1378 coral mound in the northeast Atlantic drilled during Integrated Ocean Drilling Program Expedition 307,  
1379 *Geology*, 35, 2007.

1380 Katz, E.J.: The Levantine Intermediate Water between the Strait of Sicily and the Strait of Gibraltar, *Deep-Sea Res*,  
1381 19, 507-520, 1972.

1382 Kenyon, N.H., Akhmetzhanov, A.M., Wheeler, A.J., van Weering, T.C.E., de Haas, H., and Ivanov, M.K.: Giant  
1383 carbonate mud mounds in the southern Rockall Trough, *Mar Geol*, 195, 5-30, 2003.

1384 [Keller, N.B., Os'kina, N.S.: Habitat temperature ranges of azooxantellate scleraetianian corals in the world ocean,  
1385 \*Oceanology\*, 48, 77-84, 2008.](#)

1386 Knippertz, P., Christoph, M., and Speth, P.: Long-term precipitation variability in Morocco and the link to the large-  
1387 scale circulation in recent and future climates, *Meteorol Atmos Phys*, 83, 67-88, 2003.

1388 Koho, K.A., García, R., de Stigter, H.C., Epping, E., Koning, E., Kouwenhoven, T.J., and van der Zwaan, G.J.:  
1389 Sedimentary labile organic carbon and pore water redox control on species distribution of benthic foraminifera:  
1390 A case study from Lisbon–Setúbal Canyon (southern Portugal), *Prog Oceanogr*, 79, 55-82, 2008.

1391 [Krengel, T.: 550,000 years of marine climate variability in the western Mediterranean Sea revealed by cold-water  
1392 corals, PhD thesis, Heidelberg University \(Germany\), 189 pp., 2020.](#)

1393 Lavaysse, C., Flamant, C., Janicot, S., Parker, D.J., Lafore, J.-P., Sultan, B., and Pelon, J.: Seasonal evolution of the  
1394 West African heat low: a climatological perspective, *Clim Dyn*, 33, 313-330, 2009.

1395 La Violette, P.E.: The Advection of Submesoscale Thermal Features in the Alboran Sea Gyres, *J Phys Oceanogr*, 14,  
1396 550-565, 1983.

1397 Lafuente, J.G., Camno, N., Vargas, M., Rubín, J.P., and Hernández-Guerra, A.: Evolution of the Alboran Sea  
1398 hydrographic structures during July 1993, *Deep-Sea Res Pt I*, 45, 39-65, 1998.

1399 Lanoix, R.: *Projet Alboran: étude hydrologique et dynamique de la mer d'Alboran*, Technical Report 66, NATO,  
1400 Brussels, Belgium, 1974.

1401 Linke, P. and Lutze, G.F.: Microhabitat preferences of benthic foraminifera—a static concept or a dynamic  
1402 adaptation to optimize food acquisition?, *Mar Micropaleontol*, 20, 215-234, 1993.

1403 Lionello, P., Trigo, I.F., Gil, V., Liberato, M.L.R., Nissen, K.M., Pinto, J.G., Raible, C.C., Reale, M., Tanzarella, A.,  
1404 Trigo, R.M., Ulbrich, S., and Ulbrich U.: Objective climatology of cyclones in the Mediterranean region: a  
1405 consensus view among methods with different system identification and tracking criteria, *Tellus A*, 68, 1,  
1406 29391, 2016.

1407 Lisiecki, L.E. and Raymo, M.E.: A Pliocene-Pleistocene stack of 57 globally distributed benthic  $\delta^{18}\text{O}$  records,  
1408 *Paleoceanography*, 20, PA1003, 2005.

Formatted: Font: Not Bold, English (U.K.)

1409 Lo Iacono, C., Gràcia, E., Ranero, C.R., Emelianov, M., Huvenne, V.A.I., Bartolomé, R., Booth-Rea, G., Prades, J.,  
 1410 Ambroso, S., Dominguez, C., Grinyó, J., Rubio, E., and Torrent, J.: The West Melilla cold water coral mounds,  
 1411 Eastern Alboran Sea: Morphological characterization and environmental context, *Deep-Sea Res Pt II*, 99, 316-  
 1412 326, 2014.

1413 López Correa, M., Montagna, P., Joseph, N., Rüggeberg, A., Fietzke, J., Flögel, S., Dorschel, B., Goldstein, S.L.,  
 1414 Wheeler, A., and Freiwald, A.: Preboreal onset of cold-water coral growth beyond the Arctic Circle revealed by  
 1415 coupled radiocarbon and U-series dating and neodymium isotopes, *Quaternary Sci Rev*, 34, 24-43, 2012.

1416 Löwemark, L., Chen, H.F., Yang, T.N., Kylander, M., Yu, E.F., Hsu, Y.W., Lee, T.Q., Song, S.R., Jarvis, S.:  
 1417 Normalizing XRF-scanner data: A cautionary note on the interpretation of high-resolution records from organic-  
 1418 rich lakes. *Journal of Asian Earth Sciences*, 40, 1250-56, 2011.

1419 Lutze, G.F. and Coulbourn, W.T.: Recent benthic foraminifera from the continental margin of Northwest Africa:  
 1420 community structure and distribution, *Mar Micropaleontol*, 8, 361-401, 1984.

1421 Mackensen, A., Schmiedl, G., Harloff, J., and Giese, M.: Deep-sea foraminifera in the South Atlantic Ocean:  
 1422 Ecology and assemblage generation, *Micropaleontology*, 41, 342-358, 1995.

1423 Margreth, S., Rüggeberg, A., and Spezzaferri, S.: Benthic foraminifera as bioindicator for cold-water coral reef  
 1424 ecosystems along the Irish margin, *Deep-Sea Res Pt I*, 56, 2216-2234, 2009.

1425 Martínez-Ruiz, F., Kastner, M., Gallego-Torres, D., Rodrigo-Gámiz, M., Nieto-Moreno, V., Ortega-Huertas, M.:  
 1426 Paleoclimate and paleoceanography over the past 20,000 yr in the Mediterranean Sea Basins as indicated by  
 1427 sediment elemental proxies. *Quaternary Science Reviews*, 107, 25-46, 2015.

1428 Martins, V., Jouanneau, J.-M., Weber, O., Rocha, F.; Tracing the late Holocene evolution of the NW Iberian  
 1429 upwelling system, *Marine Micropaleontology*, 59, 1, 35-55, 2006.

1430 Martorelli, E., Petroni, G., Chiocci, F.L., and the Pantelleria Scientific Party: Contourites offshore Pantelleria Island  
 1431 (Sicily Channel, Mediterranean Sea): depositional, erosional and biogenic elements, *Geo-Marine Lett.* 31, 481–  
 1432 493, 2011

1433 Martrat, B., Grimalt, J.O., Lopez-Martinez, C., Cacho, I., Sierro, F.J., Flores, J.A., Zahn, R., Canals, M., Curtis, J.H.,  
 1434 and Hodell, D.A.: Abrupt temperature changes in the Western Mediterranean over the past 250,000 years,  
 1435 *Science*, 306, 1762-1765, 2004.

1436 Masqué, P., Fabres, J., Canals, M., Sanchez-Cabeza, J.A., Sanchez-Vidal, A., Cacho, I., Calafat, A.M., and Bruach,  
 1437 J.M: Accumulation rates of major constituents of hemipelagic sediments in the deep Alboran Sea: a centennial  
 1438 perspective of sedimentary dynamics, *Mar Geol*, 193, 207-33, 2003.

1439 Mastrototaro F., D'Onghia G., Corriero G., Matarrese A., Maiorano P., Panetta P., Gherardi M., Longo C., Rosso A.,  
 1440 Sciuto F., Sanfilippo R., Gravili C., Boero F, Taviani M., and Tursi A.: Biodiversity of the white coral bank off  
 1441 Cape Santa Maria di Leuca (Mediterranean Sea): An update, *Deep-Sea Res Pt II*, 57, 5-6, 412-430, 2010. doi  
 1442 10.1016/j.dsr2.2009.08.021.

1443 Matos, L., Mienis, F., Wienberg, C., Frank, N., Kwiatkowski, C., Groeneveld, J., Thil, F., Abrantes, F., Cunha, M.R.,  
 1444 and Hebbeln, D.: Interglacial occurrence of cold-water corals off the Cape Lookout (NW Atlantic): First  
 1445 evidence of the Gulf Stream influence, *Deep-Sea Res Pt I*, 105, 158-170, 2015.

**Formatted:** Font: Not Bold

**Formatted:** Indent: Left: 0 cm,  
Hanging: 1,42 ch

**Formatted:** Font: Not Bold, English  
(U.S.)

**Formatted:** Font: Not Bold, English  
(U.S.)

- 1446 Matos, L., Wienberg, C., Titschack, J., Schmiedl, G., Frank, N., Abrantes, F., Cunha, M.R., and Hebbeln, D.: Coral  
 1447 mound development at the Campeche cold-water coral province, southern Gulf of Mexico: Implications of  
 1448 Antarctic Intermediate Water increased influence during interglacials, *Mar Geol*, 392, 53-65, 2017.
- 1449 McCave, I.N. and Hall, I.R.: Size sorting in marine muds: Processes, pitfalls, and prospects for paleoflow-speed  
 1450 proxies, *Geochem Geophys Geosy*, 7, 2006.
- 1451 McCave, I.N., Manighetti, B., and Robinson, S.G.: Sortable silt and fine sediment size/composition slicing:  
 1452 Parameters for palaeocurrent speed and palaeoceanography, *Paleoceanography*, 10, 593-610, 1995.
- 1453 ~~McCave, I.N., Thorneley, D.J.R., and Hall, I.R.: Relation of sortable silt grain size to deep-sea current speeds:  
 1454 Calibration of the 'Mud Current Meter', *Deep Sea Res Pt I*, 127, 1-12, 2017.~~
- 1455 ~~Mienis, F., Duineveld, G.C.A., Davies, A.J., Ross, S.W., Seim, H., Bane, J., and van Weering, T.C.E.: The influence  
 1456 of near bed hydrodynamic conditions on cold-water corals in the Viosca Knoll area, Gulf of Mexico, *Deep Sea  
 1457 Res Pt I*, 60, 32-45, 2012.~~
- 1458 Mienis, F., de Stigter, H.C., White, M., Duineveld, G., de Haas, H., and van Weering, T.C.E.: Hydrodynamic  
 1459 controls on cold-water coral growth and carbonate-mound development at the SW and SE Rockall Trough  
 1460 Margin, NE Atlantic Ocean, *Deep-Sea Res Pt I*, 54, 1655-1674, 2007.
- 1461 Mienis, F., van der Land, C., de Stigter, H.C., van de Vorstenbosch, M., de Haas, H., Richter, T., van Weering,  
 1462 T.C.E.: Sediment accumulation on a cold-water carbonate mound at the Southwest Rockall Trough margin, *Mar  
 1463 Geol* 265, 40-50, 2009.
- 1464 Milker, Y., Schmiedl, G., Betzler, C., Römer, M., Jaramillo-Vogel, D., and Siccha, M.: Distribution of recent benthic  
 1465 foraminifera in shelf carbonate environments of the Western Mediterranean Sea, *Mar Micropaleontol*, 73, 207-  
 1466 225, 2009.
- 1467 Millot, C.: Circulation in the western Mediterranean Sea, *J Marine Syst*, 20, 423-442, 1999.
- 1468 Millot, C.: Another description of the Mediterranean Sea outflow, *Prog Oceanogr*, 82, 101-124, 2009.
- 1469 Millot, C.: Levantine Intermediate Water characteristics: an astounding general misunderstanding!, *Sci Mar*, 77, 217-  
 1470 232, 2013.
- 1471 Millot, C., Candela, J., Fuda, J.-L., and Tber, Y.: Large warming and salinification of the Mediterranean outflow due  
 1472 to changes in its composition, *Deep-Sea Res Pt I*, 53, 656-666, 2006.
- 1473 ~~Millot, C., Taupier-Letage, I.: Circulation in the Mediterranean Sea, in: *The Handbook of Environmental Chemistry:*  
 1474 *The Mediterranean Sea (HEC5, volume 5k)*, published by: Saliot, A., Springer-Verlag Berlin Heidelberg, 29-66,  
 1475 2005.~~
- 1476 Mohn, C., Rengstorf, A., White, M., Duineveld, G., Mienis, F., Soetaert, K., and Grehan, A.: Linking benthic  
 1477 hydrodynamics and cold-water coral occurrences: A high-resolution model study at three cold-water coral  
 1478 provinces in the NE Atlantic, *Prog Oceanogr*, 122, 92-104, 2014.
- 1479 Mojtahid, M., Jorissen, F., Lansard, B., Fontanier, C., Bombled, B., and Rabouille, C.: Spatial distribution of live  
 1480 benthic foraminifera in the Rhône prodelta: Faunal response to a continental-marine organic matter gradient,  
 1481 *Mar Micropaleontol*, 70, 177-200, 2009.
- 1482 Murray, J.W.: *Ecology and Applications of Benthic Foraminifera*, Cambridge University Press, 2006.

**Formatted:** Font: Not Bold, English (U.S.)

**Formatted:** Indent: Left: 0 cm, Hanging: 1,83 ch

**Formatted:** Font: Not Bold, English (U.S.)

**Formatted:** English (U.S.)

1483 Negri, M.P. and Corselli, C.: Bathyal *Mollusca* from the cold-water coral biotope of Santa Maria di Leuca (Apulian  
1484 margin, southern Italy), *Zootaxa*, 4186, 2016.

1485 Olivet, J.L., Auzende, J.M., and Bonnin, J.: Structure et évolution tectonique du bassin d'Alboran, *B Soc Geol Fr*, 7,  
1486 491-495, 1973.

1487 [Orejas, C., Wienberg, C., Titschack, J., Tamborrino, L., Freiwald, A., Hebbeln, D.: \*Madrepora oculata\* forms large  
1488 frameworks in hypoxic waters off Angola \(SE Atlantic\). \*Scientific reports\*, 11, 15170, 2021.](#)

1489 Osborne, A.H., Vance, D., Rohling, E.J., Barton, N., Rogerson, M., and Fello, N.: A humid corridor across the  
1490 Sahara for the migration of early modern humans out of Africa 120,000 years ago, *PNAS* 105, 16444-16447,  
1491 2008.

1492 Paillard, D., Labeyrie, L., Yiou, P.: Macintosh Program performs time Series Analysis, *EOS Trans. AGU*, 77.  
1493 <https://agupubs.onlinelibrary.wiley.com/doi/abs/10.1029/96EO00259><http://www.agu.org/eos/elec/96097e.html>,  
1494 1996.

1495 Pasquier, V., Toucanne, S., Sansjofre, P., Dixit, Y., Revillon, S., Mokeddem, Z., and Rabineau, M.: Organic matter  
1496 isotopes reveal enhanced rainfall activity in Northwestern Mediterranean borderland during warm substages of  
1497 the last 200 ky, *Quaternary Sci Rev*, 205, 182-192, 2018

1498 Pérez-Folgado, M., Sierro, F.J., Flores, J.A., Grimalt, J.O., and Zahn, R.: Paleoclimatic variations in foraminifer  
1499 assemblages from the Alboran Sea (Western Mediterranean) during the last 150 ka in ODP Site 977, *Mar Geol*,  
1500 212, 113-131, 2004.

1501 Phleger, F.B. and Soutar, A.: Production of Benthic Foraminifera in Three East Pacific Oxygen Minima,  
1502 *Micropaleontology*, 19, 110-115, 1973.

1503 Pomar, L., Morsilli, M., Hallock, P., and Bádenas, B.: Internal waves, and under-explored source of turbulence  
1504 events in the sedimentary record, *Earth Sci Rev*, 111, 56-81, 2012.

1505 R Core Team.: R: A language and environment for statistical computing, R Foundation for Statistical Computing,  
1506 Vienna, Austria, URL <https://www.R-project.org/>, 2018

1507 Rabineau, M., Berné, S., Olivet, J.-L., Aslanian, D., Guillocheau, F., and Joseph, P.: Paleo sea levels reconsidered  
1508 from direct observation of paleoshoreline position during Glacial Maxima (for the last 500,000 yr), *Earth Planet  
1509 Sc Lett*, 252, 119-137, 2006.

1510 Rachid, J., Hssaida, T., Hamoumi, N., Terhaz, L., Spezzaferri, S., Frank, N., and Daghor, L.: Palynological study of  
1511 carbonated mounds during the Holocene along the Atlantic and Mediterranean Moroccan margins, *Rev  
1512 Palaeobot and Palyno*, 278, 104213, 2020

1513 Raddatz, J., Rüggeberg, A., Flögel, S., Hathorne, E.D., Liebetrau, V., Eisenhauer, A., and Dullo, W.-C.: The  
1514 influence of seawater pH on U/Ca ratios in the scleractinian cold-water coral *Lophelia pertusa*, *Biogeosciences*,  
1515 7, 1863-1871, 2014.

1516 Ramsey, C.: OxCal 4.2.4, Electronic document, URL <https://c14.arch.ox.ac.uk/oxcal.html>, 2017.

1517 Reimer, P.J., Bard, E., Bayliss, A., Beck, J.W., Blackwell, P.G., Ramsey, C.B., Buck, C.E., Cheng, H., Edwards,  
1518 R.L., Friedrich, M., Grootes, P.M., Guilderson, T.P., Haflidason, H., Hajdas, I., Hatté, C., Heaton, T.J.,  
1519 Hoffmann, D.L., Hogg, A.G., Hughen, K.A., Kaiser, K.F., Kromer, B., Manning, S.W., Niu, M., Reimer, R.W.,

Formatted: English (U.K.)

Formatted: Font: Italic

Formatted: English (U.K.)

1520 Richards, D.A., Scott, E.M., Southon, J.R., Staff, R.A., Turney, C.S.M., and van der Plicht, J.: IntCal13 and  
1521 Marine13 Radiocarbon Age Calibration Curves 0–50,000 Years cal BP, *Radiocarbon*, 55, 1869-1887, 2013.

1522 [Remia, A., Taviani. Shallow-buried Pleistocene Madrepora-dominated coral mounds on a muddy continental slope,](#)  
1523 [Tuscan Archipelago, NE Tyrrhenian Sea, \*Facies\*, 50, 419- 425, 2005.](#)

1524 Roberts, J.M., Wheeler, A.J., and Freiwald, A.: Reefs of the Deep: The Biology and Geology of Cold-Water Coral  
1525 Ecosystems, *Science*, 312, 543-547, 2006.

1526 Roberts, J.M., Wheeler, A.J., Freiwald, A., and Cairns, S.: Cold-Water Corals, Cambridge University Press, 351 pp.,  
1527 2009.

1528 Rodrigo-Gámiz, M., Martínez-Ruiz, F., Jiménez-Espejo, F.J., Gallego-Torres, D., Nieto-Moreno, V., Romero, O.,  
1529 Ariztegui, D.: Impact of climate variability in the western Mediterranean during the last 20,000 years: oceanic  
1530 and atmospheric responses. *Quaternary Science Reviews*, 30, 2018-2034, 2011.

1531 ~~Rogerson, M., Dublyansky, Y., Hoffmann, D.L., Luetscher, M., Spötl, C., and Töchterle, P.: Enhanced~~  
1532 ~~Mediterranean water cycle explains increased humidity during MIS 3 in North Africa, *Clim Past Discussions*, 1-~~  
1533 ~~31, 2018.~~

1534 Rohling, E.J., Cane, T.R., Cooke, S., Sprovieri, M., Bouloubassi, I., Emeis, K.C., Schiebel, R., Kroon, D., Jorissen,  
1535 F.J., Lorre, A., and Kemp, A.E.S.: African monsoon variability during the previous interglacial maximum, *Earth*  
1536 *Planet Sc Lett*, 202, 61-75, 2002.

1537 Rüggeberg, A., Dullo, C., Dorschel, B., and Hebbeln, D.: Environmental changes and growth history of a cold-water  
1538 carbonate mound (Propeller Mound, Porcupine Seabight), *Int J Earth Sci*, 96, 57-72, 2007.

1539 [Sánchez-Guillamón, O., Rueda, J.L., Wienberg, C., Ercilla, G., Vázquez, J.T., Gómez-Ballesteros, M., Urra, J.,](#)  
1540 [Moya-Urbano, E., Estrada, F., Hebbeln, D.: Morphosedimentary, Structural and Benthic Characterization of](#)  
1541 [Carbonate Mound Fields on the Upper Continental Slope of the Northern Alboran Sea \(Western Mediterranean\),](#)  
1542 [Geosciences, 12, 111, 2022.](#)

1543 Schiebel, R. and Hemleben, C.: Planktic Foraminifers in the Modern Ocean, Springer-Verlag, Berlin, Heidelberg,  
1544 358 pp., 2017.

1545 [Schmiedl, G., Mackensen, A.: Late Quaternary paleoproductivity and deep water circulation in the eastern South](#)  
1546 [Atlantic Ocean: Evidence from benthic foraminifera. \*Palaeogeography, Palaeoclimatology, Palaeoecology\*, 130](#)  
1547 [\(1-4\), 43-80, 1997.](#)

1548 Schmiedl, G., De Bovée, F., Buscail, R., Charriere, B., Hemleben, C., Medernach, L., and Picon, P.: Trophic control  
1549 of benthic foraminiferal abundance and microhabitat in the bathyal Gulf of Lions, western Mediterranean Sea,  
1550 *Mar Micropaleontol*, 40, 167-188, 2000.

1551 Schmiedl, G., Kuhnt, T., Ehrmann, W., Emeis, K.-C., Hamann, Y., Kotthoff, U., Dulski, P., and Pross, J.: Climatic  
1552 forcing of eastern Mediterranean deep-water formation and benthic ecosystems during the past 22 000 years,  
1553 *Quaternary Sci Rev*, 29, 3006-3020, 2010.

1554 [Schmiedl, G., Mitschele, A., Beck, A., Emeis, K.-C., Hemleben, C., Schulz, H., Sperling, M., Weldeab, S.: Benthic](#)  
1555 [foraminiferal record of ecosystem variability in the eastern Mediterranean Sea during times of sapropel S<sub>6</sub> and](#)  
1556 [S<sub>6</sub> deposition, \*Palaeogeography, Palaeoclimatology, Palaeoecology\*, 190, 139-164, 2003.](#)

Formatted: English (U.K.)

Formatted: English (U.K.)

Formatted: English (U.K.)

Formatted: English (U.S.)

Formatted: Subscript

Formatted: Subscript



1557 Scholz, J. and Hillmer, G.: Reef-Bryozoans and Bryozoan-Microreefs: Control Factor Evidence from the Philippines  
1558 and other Regions, *Facies*, 32, 109-144, 1995.

1559 ~~Shanahan, T.M., McKay, N.P., Hughen, K.A., Overpeck, J.T., Otto-Bliesner, B., Heil, C.W., Scholz, C.A., and Peck,~~  
1560 ~~J.: The time transgressive termination of the African Humid Period, *Nat Geosci*, 8, 140-144, 2015.~~

1561 Siani, G., Paterne, M., Arnold, M., Bard, E., Métivier, B., Tisnérat-Laborde, N., and Bassinot, F.: Radiocarbon  
1562 reservoir ages in the Mediterranean Sea and Black Sea, *Radiocarbon*, 42, 2, 271-280, 2000.

1563 Sierro, F.J., Hodell, D.A., Curtis, J.H., Flores, J.A., Reguera, I., Colmenero-Hidalgo, E., Bárcena, M.A., Grimalt,  
1564 J.O., Cacho, I., Frigola, J., and Canals, M.: Impact of iceberg melting on Mediterranean thermohaline circulation  
1565 during Heinrich events, *Paleoceanography*, 20, 2005.

1566 Snousi, M.: Review of Certain Basic Elements for the Assessment of Environmental Flows in the Lower Moulouya,  
1567 IUCN International Union for Conservation of Nature, Gland, Switzerland, 2004. Available online:  
1568 <http://cmsdata.iucn.org/downloads/morocco.pdf> (accessed on 20 August 2012).

1569 Sparnocchia, S., Picco, P., Manzella, G., Ribotti, A., Copello, S., and Brasey, P.: Intermediate water formation in the  
1570 Ligurian Sea, *Oceanol Acta*, 18, 151-162, 1995.

1571 Spezzaferri, S., Rüggeberg, A., Stalder, C., and Margreth, S.: Benthic foraminiferal assemblages from cold-water  
1572 coral ecosystems, in: Atlas of Benthic Foraminifera From Cold-Water Coral Reefs, edited by: Spezzaferri, S.,  
1573 Rüggeberg, A., and Stalder, C., Special Publication/Cushman Foundation For Foraminiferal Research, 20-48,  
1574 2014.

1575 Spötl C. and Vennemann T.W.: Continuous-flow IRMS analysis of carbonate minerals, *Rapid Commun Mass Sp*,  
1576 17, 1004-1006, 2003.

1577 Stalder, C., El Kateb, A., Vertino, A., Rüggeberg, A., Camozzi, O., Pirkenseer, C.M., Spangenberg, J.E., Hajdas, I.,  
1578 Van Rooij, D., and Spezzaferri, S.: Large-scale paleoceanographic variations in the western Mediterranean Sea  
1579 during the last 34,000 years: From enhanced cold-water coral growth to declining mounds, *Mar Micropaleontol*,  
1580 143, 46-62, 2018.

1581 Stalder, C., Vertino, A., Rosso, A., Rüggeberg, A., Pirkenseer, C., Spangenberg, J.E., Spezzaferri, S., Camozzi, O.,  
1582 Rappo, S., and Hajdas, I.: Microfossils, a Key to Unravel Cold-Water Carbonate Mound Evolution through  
1583 Time: Evidence from the Eastern Alboran Sea, *PLoS One*, 10, e0140223, 2015.

1584 Suhr, S.B., Pond, D.W., Gooday, A.J., and Smith, C.R.: Selective feeding by benthic foraminifera on phytodetritus  
1585 on the western Antarctic Peninsula shelf: Evidence from fatty acid biomarker analysis, *Mar Ecol Prog Ser*, 262,  
1586 153-162, 2003.

1587 Sun, X., Corliss, B.H., Brown, C.W., and Showers, W.J.: The effect of primary productivity and seasonality on the  
1588 distribution of deep-sea benthic foraminifera in the North Atlantic, *Deep-Sea Res Pt I*, 53, 28-47, 2006.

1589 Sval, H.A., Stocker, M., and Suter, M.: MICADAS: A new compact radiocarbon AMS system, *Nucl Instrum Meth*  
1590 B, 259, 7-13, 2007.

1591 ~~Talbot, M.R. and Livingstone, D.A.: Hydrogen index and carbon isotopes of lacustrine organic matter as lake level~~  
1592 ~~indicators, *Palaeogeogr Palaeoclimatol*, 70, 121-137, 1989.~~

1593 ~~Tamborino, L., Wienberg, C., Tjitschack, J., Wintersteller, P., Mienis, F., Schröder-Ritzrau, A., Freiwald, A., Orejas,~~  
1594 ~~C., Dullo, W.C., Haberkern, J., Hebbeln, D.: Mid Holocene extinction of cold water corals on the Namibian~~

Formatted: English (U.K.)

1595 [shelf steered by the Benguela oxygen minimum zone. \*Geology\*, 47, 12, 1185–1188, 2019.](#) Taviani, M., Angeletti,  
1596 [L., Foglini, F., Corselli, C., Nasto, I., Pons-Branchu, E., Montagna, P.: U/Th dating records of cold-water coral](#)  
1597 [colonization in submarine canyons and adjacent sectors of the southern Adriatic Sea since the Last Glacial](#)  
1598 [Maximum, \*Prog. Oceanogr.\* 175, 300-308, 2019.](#)

1599 Tekken, V. and Kropp, J.P.: Climate-driven or human-induced; indicating severe water scarcity in the Moulouya  
1600 River basin (Morocco), *Water*, 4, 959-982, 2012.

1601 Terhzaz, L., Hamoumi, N., Spezzaferri, S., El Mostapha L., and Henriot, J.P.: Carbonate mounds of the Moroccan  
1602 Mediterranean margin: Facies and environmental controls, *C R Geosci*, 350, 212–221. 2018.

1603 Titschak, J., Thierens, M., Dorschel, B., Schulbert, C., Freiwald, A., Kano, A., Takashima, C., Kawagoe, N., Li, X.,  
1604 and IODP Expedition 307 scientific party: Carbonate budget of a cold-water coral mound (Challenger Mound,  
1605 IODP Exp. 307), *Mar Geol*, 259, 36-46, 2009.

1606 Toucanne, S., Jouet, G., Ducassou, E., Bassetti, M.-A., Dennielou, B., Angue Minto'o, C.M., Lahmi, M., Touyet, N.,  
1607 Charlier, K., Lericolais, G., and Mulder, T.: A 130,000-year record of Levantine Intermediate Water flow  
1608 variability in the Corsica Trough, western Mediterranean Sea, *Quaternary Sci Rev*, 33, 55-73, 2012.

1609 Tüenter, E., Weber, S.L., Hilgen, F.J., and Lourens, L.J.: The response of the African summer monsoon to remote  
1610 and local forcing due to precession and obliquity, *Global Planet. Change*, 36, 219-235, 2003.

1611 Van Krevelen, D.W.: *Coal: typology–physics–chemistry–constitution*, 3rd edition, Elsevier Science Publishers,  
1612 1993.

1613 Van Rooij, D., Hebbeln, D., Comas, M., Vandorpe, T., Delivet, S., and the shipboard scientific party,:  
1614 EUROFLEETS Cruise Summary Report, The Mediterranean-Atlantic Gateway Code: The Late Pleistocene  
1615 Carbonate Mound Record, 2013.

1616

1617 Viúdez, Á. and Tintoré, J.: Time and space variability in the Eastern Alboran Sea from March to May 1990, *J*  
1618 *Geophys Res*, 100, 1995.

1619 Wang, H., Lo Iacono, C., Wienberg, C., Titschack, J., and Hebbeln, D.: Cold-water coral mounds in the southern  
1620 Alboran Sea (western Mediterranean Sea): Internal waves as an important driver for mound formation since the  
1621 last deglaciation, *Mar Geol*, 412, 1-18, 2019.

1622 [Wang, H., Titschack, J., Wienberg, C., Korpanty, C., Hebbeln, D.: The importance of ecological accommodation](#)  
1623 [space and sediment supply for cold-water coral mound formation, a case study from the Western Mediterranean](#)  
1624 [Sea. \*Frontiers in Marine Science\*, 8, 760909, 2021.](#)

1625 Wefing, A.-M., Arps, J., Blaser, P., Wienberg, C., Hebbeln, D., and Frank, N.: High precision U-series dating of  
1626 scleractinian cold-water corals using an automated chromatographic U and Th extraction, *Chem Geol*, 475, 140-  
1627 148, 2017.

1628 ~~Wehrmann, L.M., Knab, N.J., Pirlet, H., Unnithan, V., Wild, C., and Ferdeman, T.G.: Carbon mineralization and~~  
1629 ~~carbonate preservation in modern cold water coral reef sediments on the Norwegian shelf, *Biogeosciences*, 6,~~  
1630 ~~663–680, 2009.~~

1631 White, M.: Benthic dynamics at the carbonate mound regions of the Porcupine Sea Bight continental margin, *Int J*  
1632 *Earth Sci*96, 1-9, 2007.

Formatted: English (U.K.)

1633 White, M., Mohn, C., De Stigter, H.C., and Mottram, G.: Deep-water coral development as a function of  
1634 hydrodynamics and surface productivity around the submarine banks of the Rockall Trough, NE Atlantic, in:  
1635 Cold-water Corals and Ecosystems, edited by: Freiwald, A. and Roberts, J.M., Springer-Verlag, Berlin,  
1636 Heidelberg, 503-514 pp., 2005.

1637 Wickham, H.: ggplot2: Elegant Graphics for Data Analysis, Springer-Verlag, New York, 2016.

1638 Wienberg, C. A deglacial cold-water coral boom in the Alboran Sea: From coral mounds and species dominance, in:  
1639 Mediterranean cold-water corals: past, present and future, edited by: Orejas, C. and Jiménez, C., Springer, 57-  
1640 60, 2019.

1641 Wienberg, C. and Titschak, J.: Framework-forming scleractinian cold-water corals through space and time: a Late  
1642 Quaternary North Atlantic perspective, in: Marine Animal Forests, edited by: Rossi, S., Springer, Switzerland,  
1643 2016.

1644 Wienberg, C., Hebbeln, D., Fink, H.G., Mienis, F., Dorschel, B., Vertino, A., Correa, M.L., and Freiwald, A.:  
1645 Scleractinian cold-water corals in the Gulf of Cádiz—First clues about their spatial and temporal distribution,  
1646 Deep-Sea Res Pt I, 56, 1873-1893, 2009.

1647 Wienberg, C., Titschack, J., Frank, N., De Pol-Holz, R., Fietzke, J., Eisele, M.H., Kremer, A., Hebbeln, D.: Deglacial  
1648 upslope shift of NE Atlantic intermediate waters controlled slope erosion and cold-water coral mound  
1649 formation (Porcupine Seabight, Irish margin). Quaternary Science Reviews, 237, 106310, 2020.

1650 Wienberg, C., Titschack, J., Freiwald, A., Frank, N., Lundälv, T., Taviani, M., Beuck, L., Schröder-Ritzrau, A.,  
1651 Krengel, T., Hebbeln, D.: The giant Mauritanian cold-water coral mound province: Oxygen control on coral  
1652 mound formation, Quaternary Sci Rev, 185, 135-152, 2018.

1653 Wilson, J.B.: 'Patch' development of the deep-water coral *Lophelia Pertusa* (L.) on Rockall Bank, J Mar Biol Assoc  
1654 UK, 59, 1979.

1655 Winston, J.E.: Feeding in marine bryozoans, in Biology of Bryozoans, edited by: Woollacott, R.M. and Zimmer,  
1656 R.L., 233–271 pp., Academic, San Diego, Calif., 1977.

1657 Winston, J. E.: Feeding behaviour of modern bryozoans, in Lophophorates: Notes for a Short Course, Stud. Geol.,  
1658 vol. 5, edited by: Broadhead, T.W., 1–21 pp., Univ. of Tenn., Knoxville, 1981.